Study of the nonlinear behavior of large bridge supports under earthquake solicitations

Auteur : Flamigni, Filippo
Promoteur(s) : Gens, Frédéric
Faculté : Faculté des Sciences appliquées
Diplôme : Master en ingénieur civil des constructions, à finalité spécialisée en "civil engineering"
Année académique : 2022-2023
URI/URL : http://hdl.handle.net/2268.2/17812

UNIVERSITÉ DE LIÈGE

FACULTÉ DES SCIENCES APPLIQUÉES
Master's thesis completed in order to obtain the degree of
Master of Science in Civil Engineering

Study of the nonlinear behavior of large bridge supports under earthquake solicitations

Supervisors:
GENS Frédéric
SILVESTRI Stefano

Co-supervisors:
DE VILLE DE GOYET Vincent
DUCHÊNE Yves
FLOCK Julian

Presented by:
FLAMIGNI Filippo

Members of the jury:
COLLIN Frédéric
DEGÉE Hervé
DE VILLE DE GOYET Vincent
GENS Frédéric

LIÈGE
Academic year 2022 - 2023

Contents

Abstract

For very large bridges it is important to efficiently manage displacements and deformation during earthquakes and under the passage of vehicles to avoid damage and collapse of the structure.
Classic solutions consist in implementing spring type shock absorbers, which convert the kinetic energy into heat energy, helping in dissipating it. A very effective and rather simple solution which is often adopted for large bridges and other sensitive structures is to implement pendular bearings, characterized by a curved geometry: they have the dual role of vertical support and of horizontal elastic support, the stiffness of which is proportional to the vertical reaction divided by the radius of curvature (called "pendulum effect of the support").
Between the moving parts of the support device, the sliding surfaces may have some roughness: in this case, the frictional force must be defeated before any displacement can take place. Whenever a force which would cause the structure to undergo a horizontal movement is applied:

- the deck is horizontally stationary if the horizontal force is smaller than the frictional force;
- the deck moves if the horizontal force is greater than the frictional force;
- if there is movement, the deck will undergo both horizontal and vertical displacement.

The behaviour is therefore, by definition, nonlinear.
During the study of the Third Bosphorus Bridge in Turkey all phenomena were considered for the passage of a train; for the earthquake, on the other hand, only the pendulum effect was taken into account, while friction has been neglected.
The present Master Thesis consists of studying and modelling the entire behavior, with both pendulum effect and friction, under earthquake solicitations, analyzing a real case, specifically the Third Bosphorus Bridge, and evaluating the dynamic response in time.

1 Introduction

The study of the behaviour of structures subjected to variable dynamic forces, such as those resulting from a seismic event, is an important but complicated aspect of Civil Engineering. Whereas the basic design is performed considering static actions, limiting displacements and imposing no motion of the structure, the process is indeed rather different in seismic areas, as the consequences of possible dynamic effects must be predicted and accounted for; the problem becomes even more challenging when any frictional behaviour is added in the analysis, since it is modelled with a spring which has a nonlinear constitutive law.

An example of such a dynamic analysis is the study of the behaviour of storage racks in seismic areas (as developed by Denoël V., Degée H., 2007): given their very light weight, considerable height and large live load of the supported goods, the ground shaking caused by an earthquake may lead to sliding and falling of pallets, or on the other hand the friction between pallet and rack could be sufficient to only have some or no movement. Therefore, the modelling of friction in this kind of structures is very important in order to have a good design.

For this type of problem, the basic concept relies on the definition of a "mathematical deck": the behaviour is obtained through the solution of two uncoupled sets of equations (one for the structure and the other for the pallets), then equilibrium and compatibility are imposed at the contact points with an iterative procedure; the same concept can be applied to study the behaviour of bridges subjected to variable loads caused by vehicle traffic (Yang F., 1996), but in the case of storage racks, instead of a moving mass on the structure with no imposed speed, the pallets are initially stationary and a stick-slip model is used to determine the horizontal behaviour through a dynamic computation.

Equally interesting is the dynamic behaviour of bridges subjected to variable forces caused by an earthquake event: given the very large mass of such structures and their relatively high flexibility, the design in seismic areas must be performed accurately and both displacements and internal stresses managed as much as possible in order to prevent damages and collapse. An effective solution is the implementation of pendular bearings on the supports, which have a curved geometry causing any horizontal movement to be accompanied by a vertical displacement and an elastic recalling force opposite to the direction of motion, effectively incrementing the stiffness of the struc-

ture compared to an ideal non curved roller, which actually would have no stiffness at all.

The behaviour of this type of supports is linear, but the surfaces in contact have a certain roughness, therefore some friction depending on the vertical reaction force will cause the problem to be nonlinear: in this case only the structure is studied, with no additional moving masses, but it still must be solved with a stick-slip model as for the storage racks above. In addition, any displacement may cause the vertical reaction on each support to change, modifying both the response of the pendular bearing and the friction resistance.

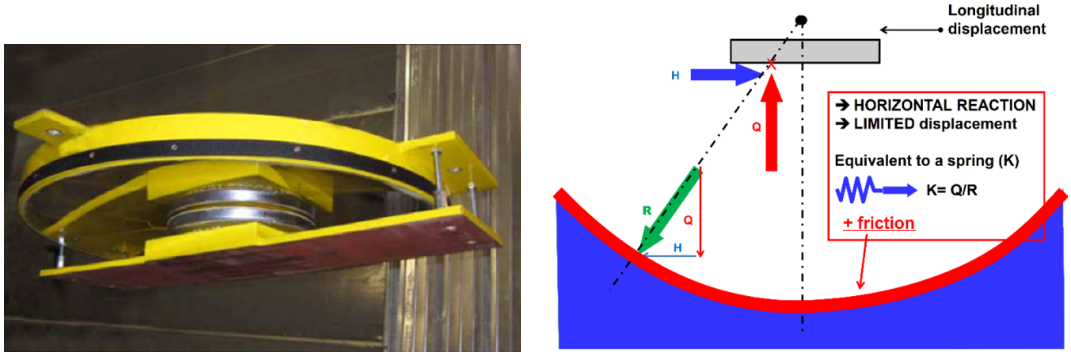

(a) Pendular bearing (b) Functioning of a pendular bearing

Figure 1: Illustration of geometry and operation of pendular bearings

Since a dynamic nonlinear seismic analysis can be very laborious and lead to multiple numerical problems, especially for large and complex structures, the effect of friction is sometimes neglected or only partially accounted for, designing on the safe side but obtaining results which can be unrealistic.

The object of this work is therefore to analyze the horizontal behaviour of bridges under seismic action with and without pendular bearings and friction between the contacting surfaces, in order to evaluate their effect on the evolution of displacements. The work will be developed in several stages:

- First, the problem at hand will be studied with the application of a variable horizontal force on a simple theoretical structure. The response will be determined both statically and dynamically, first considering an ideal freely moving roller as a support, then adding pendulum effect and friction and comparing the results. The same model will be built both analytically and with the use of the software FineLg, comparing the outputs of the two as well.

- Afterwards, a seismic analysis will be carried out by substituting the sinusoidal force used previously with a ground acceleration, performing the calculations dynamically and comparing the differences between the various boundary conditions.

- Finally, having performed a preliminary analysis, the same accelerogram will be applied on a real structure, specifically the Third Bridge over the Bosphorus, using FineLg. Such model does not account for friction, therefore a simplified version of it will be calibrated and used to assess the effects of frictional supports.

For most of this work, the various configurations of supports will be compared and whenever a case without neither pendular bearing nor friction effect is considered it will refer to a scenario where the supports are assumed to be ideal rollers, able to move horizontally and with no stiffness of their own; moreover, both friction and pendulum effect will be considered simply as additional characteristics added to such ideal rollers.
Therefore, the results obtained will ultimately be compared among themselves and to the ideal case of freely moving supports and not to an alternative type of bearing, which would otherwise be implemented in a real situation.

2 Study of a simple structure

As a preliminary step of the study of the problem, a simple structure was analyzed to assess the effect of a pendulum support and of the friction. The geometry is reported in Figure 2.

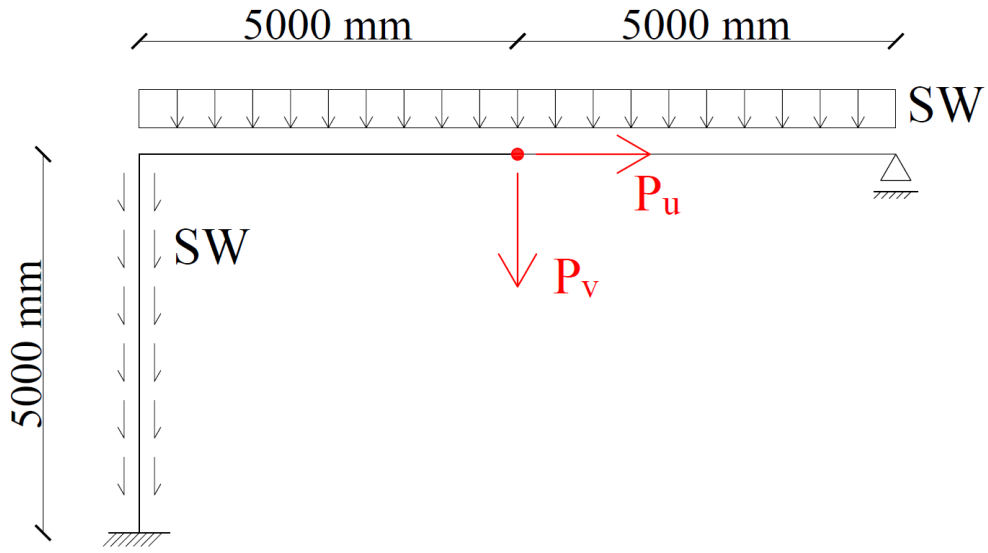

Figure 2: Geometry of the structure

The vertical punctual load P_v is constant, equal to $-10kN$, while the horizontal force P_u varies between $-5kN$ and $5kN$, both applied in the midpoint of the beam; both elements were chosen to be IPE 140 profiles, therefore with a self weight $SW = 0.13kN/m$. Three different scenarios have been considered, displayed in Figure 3.

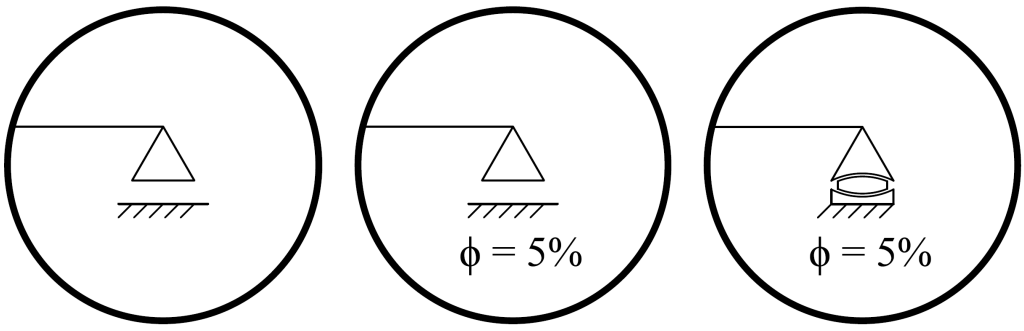

(a) First scenario: ideal roller

(b) Second scenario: roller with friction

(c) Third scenario: frictional pendular bearing

Figure 3: The three analyzed scenarios for the various calculations

Firstly, the right support was considered to be an ideal roller, without any pendulum effect, to which friction with a coefficient $\phi = 5\%$ was subsequently added; therefore, for a horizontal action smaller than 5% of the vertical reaction R_v at the support, the roller behaves as a fixed hinge, while for larger forces it moves with a constant reaction provided by the friction and directed in the opposite direction with respect to the motion. This kind of behaviour can be modelled as a nonlinear spring, with an almost infinite initial stiffness and a horizontal plateau after reaching the elastic limit (see Figure 4, left picture).
Subsequently, the effect of a pendulum bearing was included in the model as well: it has the dual role of vertical support and horizontal elastic support, which can be modelled as a spring with a stiffness equal to the ratio between the vertical applied force and the radius of curvature r (known as "pendulum effect"). Such spring would be linear considering a constant value of vertical force on the support (see Figure 4, right picture), but in fact the force does change with displacements and so does the stiffness of the spring.

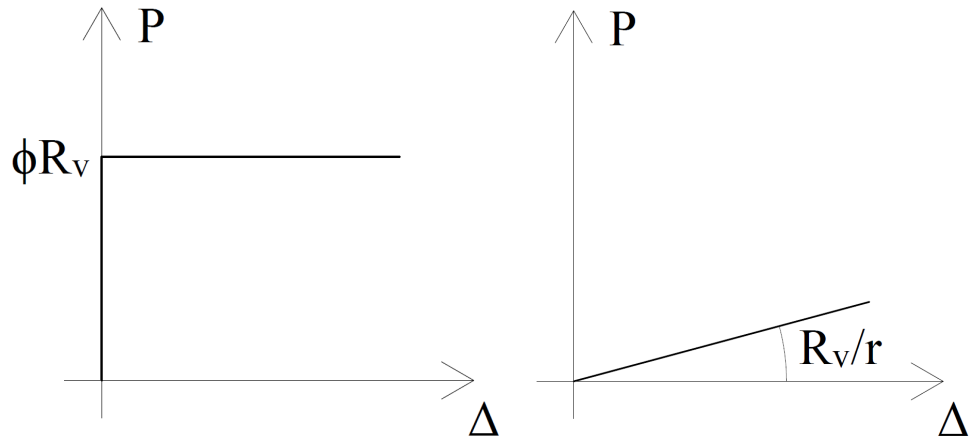

(a) Friction modelling spring

(b) Pendulum support modelling spring (considering constant stiffness)

Figure 4: Constitutive laws of the springs used on the moving support

To model friction and pendulum effect together, therefore, two springs in parallel are used (see Figure 5). When a horizontal force is applied, no movement occurs until the friction force has been overcome; after that, the support sees displacements both horizontally and vertically, moving along the surface of the pendulum, and a recalling force proportional to the stiffness of the pendular bearing and to the entity of the dis-

placement is applied on the roller, opposite to the direction of motion, contrasting it. The increase of force after reaching the elastic limit is known as hardening, in this case considered kinematic hardening, meaning that when the spring is unloaded and pushed in the opposite direction it experiences a vertical drop equal to twice the elastic limit.

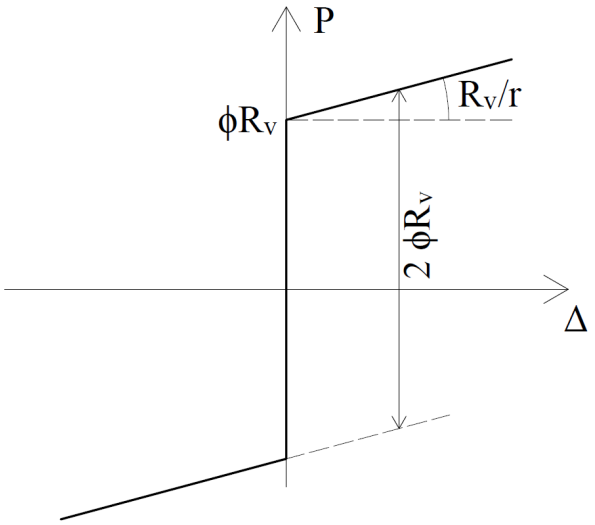

Figure 5: Constitutive law of the resulting spring with kinematic hardening

The structure defined in such way was therefore solved statically and dynamically, both analytically and using the software FineLg, comparing the results.

2.1 Static analysis

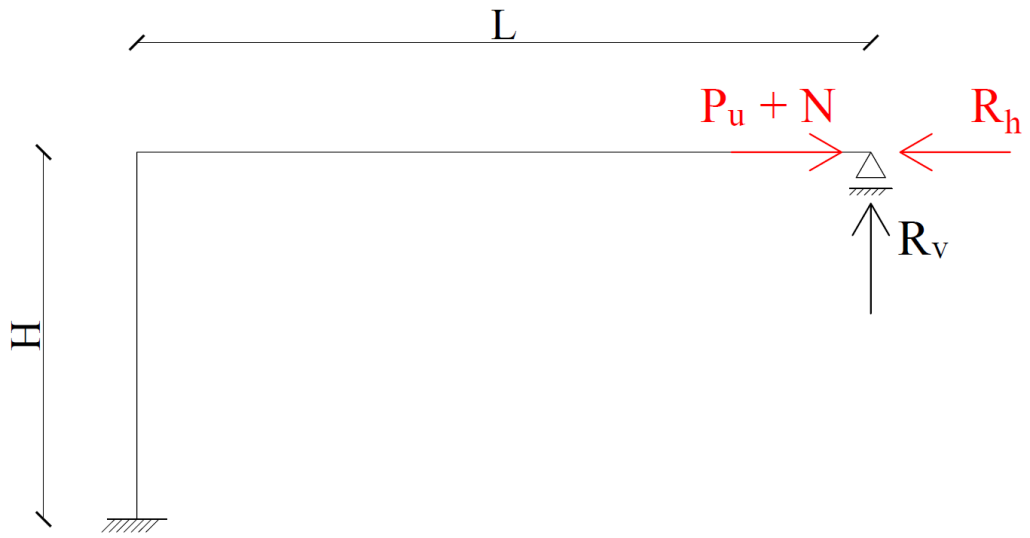

Figure 6: Forces considered for the static analysis

Firstly, the horizontal displacements of the roller were evaluated according to the static response of the structure, applying all the loads as illustrated in Figure 6 and determining the movement after the structure has settled in the new equilibrium configuration, therefore without considering any dynamic effects. The structure is solved statically by ensuring the equilibrium of the forces at all times: the action on the structure is obtained by summing up the external applied force and the axial force N in the beam (caused by vertical loads only and calculated as if there was no movement), while the horizontal reaction at the support R_h is given entirely by the friction and is proportional to the vertical reaction R_v through the friction coefficient ϕ.
Equating the two horizontal forces for all the given values of P_u, the displacement x (considered positive towards the right) can be easily obtained. From the static analysis:

- $N = \frac{(6 \cdot SW \cdot L + 9P_v)L^2}{(32L+24H)H} - \frac{6EJ}{H^3}(1 + \frac{3H-2L}{4L+3H})x = A - Bx$
- $R_v = \frac{SW \cdot L + P_v}{2} - \frac{(2SW \cdot L + 3P_v)L}{16L+12H} + \frac{18EJ}{(4L+3H)LH}x = \alpha + \beta x$
- $R_h = min(P_u + N \; ; \; \phi R_v)$
- $E = 210000MPa$ (steel) and $J = 5410000mm^4$ (IPE 140)

The displacements have been calculated by first applying the vertical loads and then gradually increasing, both in positive and negative directions, the horizontal force. The

analytical results are reported in Figure 7 and compared to the ones obtained using the software, considering the friction-less case as well, for which simply $\phi = 0$.

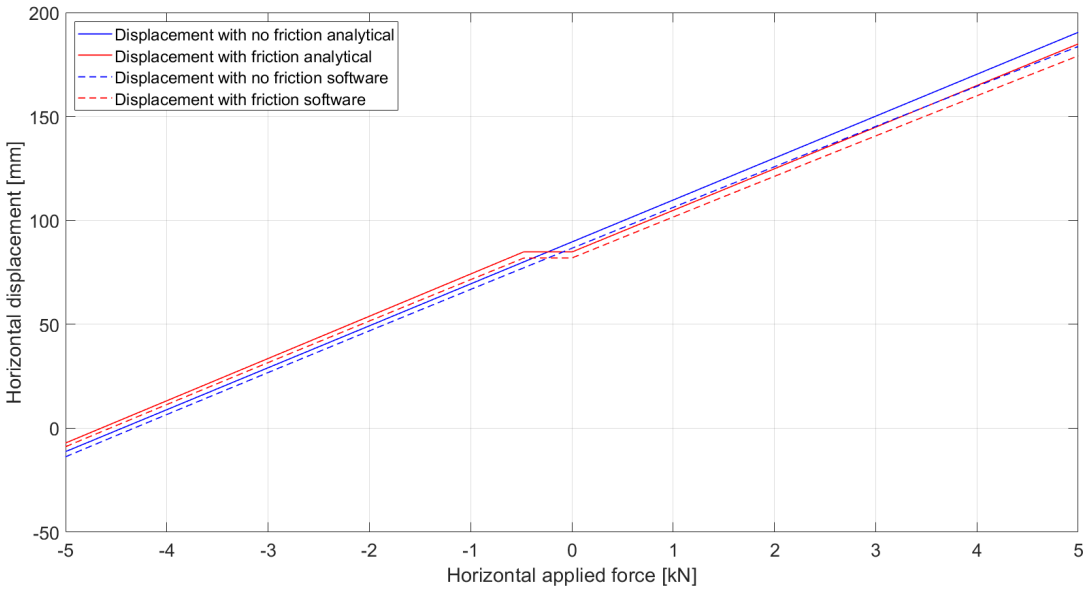

Figure 7: Displacements calculated for the static analysis

As expected, the maximum absolute displacements in the case with friction are slightly smaller than those considering a pure roller, since a certain amount of horizontal reaction contrasting such movement can be provided; also, when the horizontal applied force inverts itself and becomes negative, while the roller smoothly transitions to negative displacements, the case with friction sees the support being stationary for a certain period of time; this is expected as well, since the structure is initially in equilibrium with a positive displacement and in order to generate any movement in the opposite direction the friction has to be overcome first.
Furthermore, the variation of the reactions at the support are shown in Figure 8.

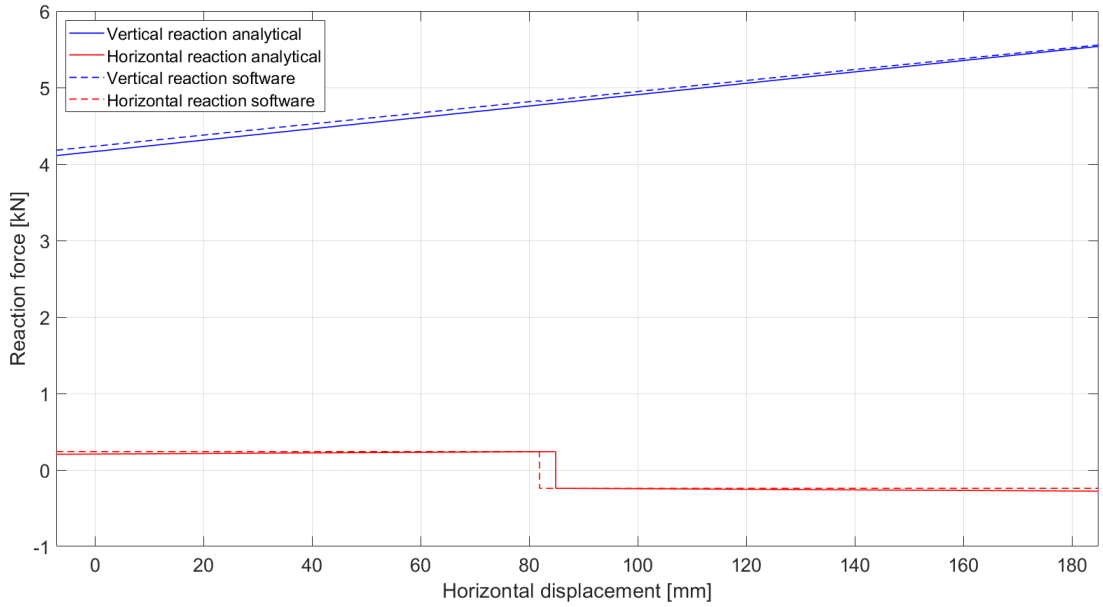

Figure 8: Vertical and horizontal reactions at the support

Any movement towards the right increases the downward push on the roller and the friction that can be mobilized, while the opposite happens for displacements towards the left (for which the horizontal reaction also changes sign in order to contrast the movement).

Following these results, the same analysis considering both friction and pendulum support was carried out (see Figure 9). Real such supports have radii of curvature ranging from $2m$ to $10m$, but the structure studied is so much smaller compared to the large bridges for which these supports are used that their effect would be close to negligible; hence, the pendulum was added in the model with a radius of curvature of $0.1m$, scaled down from the realistic values to account for the much smaller loads acting on the structure and to be able to see an effect.

The variation of vertical reaction and therefore of stiffness of the pendulum modelling spring can be accounted for in the analytical solution, while on FineLg, where this is not possible, a constant value of $45kN/m$ for the hardening past the elastic limit is considered.

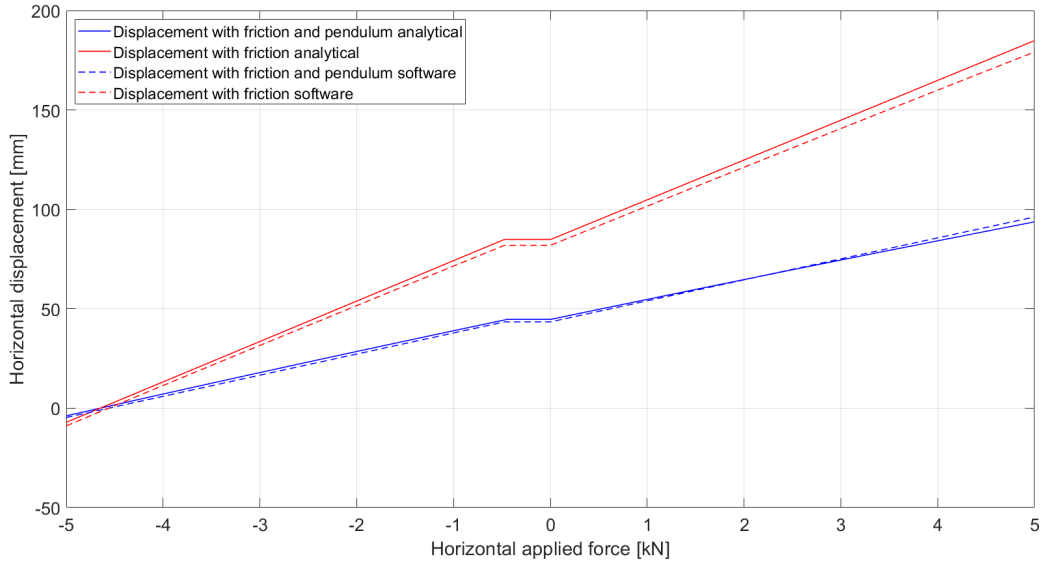

(a) Displacement as a function of the horizontal force

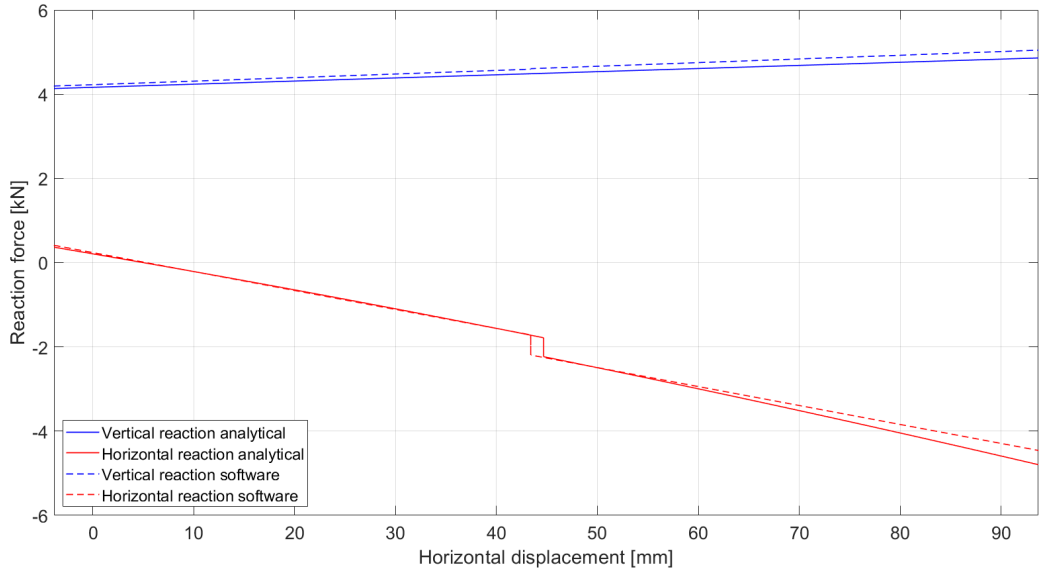

(b) Support reactions as a function of the displacement

Figure 9: Displacement and support reactions at the moving support considering both friction and pendulum effect, compared to the previously obtained results

Evidently, the results obtained with the software are very close to those given by the analytical model, with small differences attributable to the geometry of the structure: given its slenderness and modest overall stiffness, the exact behaviour is slightly nonlinear under the external defined loads, fact which is not correctly matched using the analytical linear modelling. Moreover, there are small differences also in the mag-

nitude and variation of the horizontal reaction force at the support, imputable to the necessity of using a constant value for the elastic limit and the slope of the hardening phase of the spring modelling the friction on FineLg, in reality partially influenced by the entity and direction of the movement of the structure, which the analytical solution correctly accounts for.

2.2 Dynamic analysis

Afterwards, a dynamic analysis of the structure was carried out: the horizontal load $P_u(t)$ is applied varying with time in a sinusoidal fashion and by changing its frequency the dynamic effects on the structure are evaluated. To do so, the equation of motion was derived:

$$m\ddot{x} + kx + R_h = P_u(t) + N \tag{1}$$

At each time step, the horizontal force (which is the sum of the applied load and of the axial force in the beam) is dynamically balanced by the inertia force, the elastic recalling force and the friction R_h, the latter being oriented in the opposite direction with respect to the motion of the structure at all times; also, it has an intensity equal to the smallest between the horizontal force itself and the maximum possible friction force that can be mobilized, which is the elastic limit of the spring.
To solve the problem analytically, the structure was simplified as a 1 DOF (Degree Of Freedom) system with an active mass supported by a mass-less column of height H, fixed to the ground (see Figure 10), and the friction modelled using the hyperbolic tangent function, which for a small enough value of ε (see below) is able to approximate well the nonlinear constitutive law of the spring.

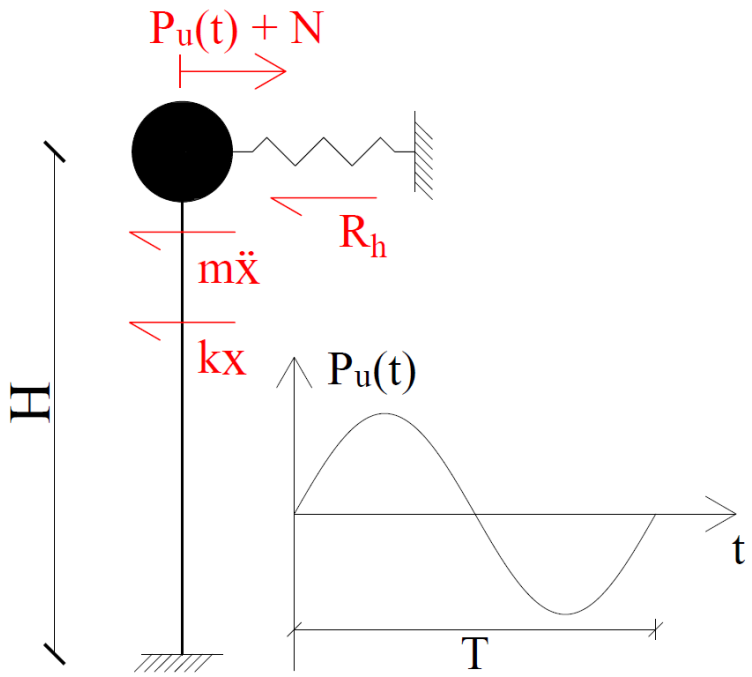

Figure 10: Simplified system considered for the dynamic analysis

At each time step i, the intensity of the friction force is determined as follows:

$$|R_h^i| = min\left(\left|R_h^{i-1} + \phi R_v^i \cdot tanh\left(\frac{x^i - x^{i-1}}{\varepsilon}\right)\right| \; ; \; |\phi R_v^i|\right) \tag{2}$$

Therefore, the friction force is modified in absolute value at each step until the elastic limit ϕR_v is reached, while its orientation is always opposite to the movement of the structure; moreover, the vertical reaction R_v at the support varies with the displacement, as shown before, factor which is included in the analytical solution but which cannot be accounted for in the FineLg model.

Performing the structural analysis, the defining parameters of the structure are obtained, specifically its mass, stiffness and natural period of vibration (always considering the linear case with no spring). Given the slight differences between the two models already pointed out in the static analysis, these parameters are not exactly the same for analytical and software solutions, which would cause the dynamic results to not match very neatly; therefore, in order to have more comparable outputs, a linear eigenmode analysis was performed using FineLg and the mass, stiffness and consequent natural period of vibration for the analytical model were taken equal to those corresponding to the first and most important mode of vibration.

The results are as follows:

- The modal stiffness of the structure relative to horizontal movement for the first and most important mode of vibration is equal to $k = 56.14 kN/m$;
- The modal mass for the first and most important mode of vibration, including the vertical force P_v, is equal to $m = 1660 kg$;
- The natural period of vibration is equal to $2\pi\sqrt{\frac{m}{k}} = 1.08 s$.

The dynamic behaviour was determined using the Newmark method with parameters $\alpha = 0.25$ and $\beta = 0.5$ for different periods T of the applied horizontal force.
On FineLg, a very small amount of structural damping was applied to the non-frictional case in order to stabilize the oscillations caused by the vertical loads before the application of the horizontal force, allowing the model to better match the analytical solution (for which the structure is initially still).
The results are shown in Figures 11 - 20, comparing analytical and software solutions.

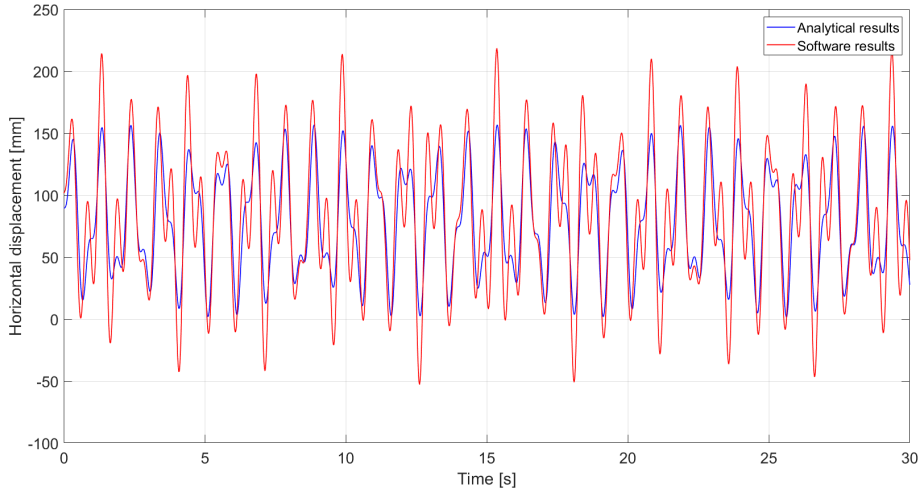

(a) Displacement variation

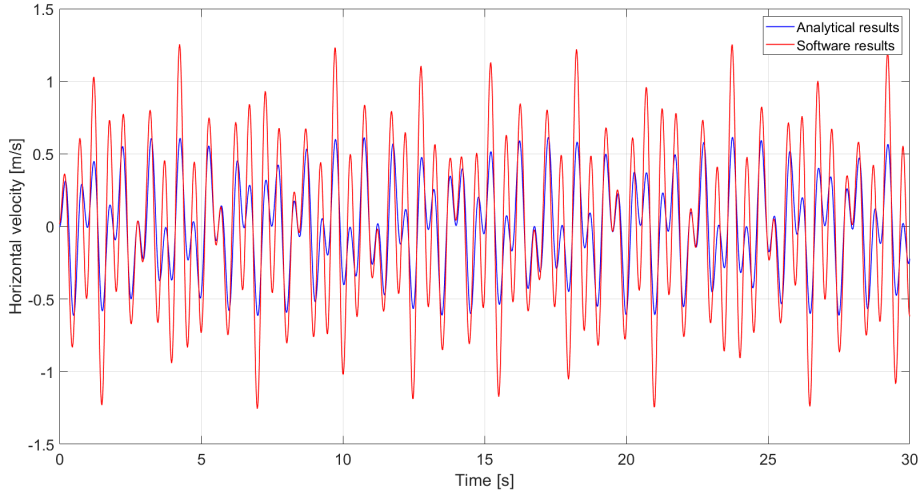

(b) Velocity variation

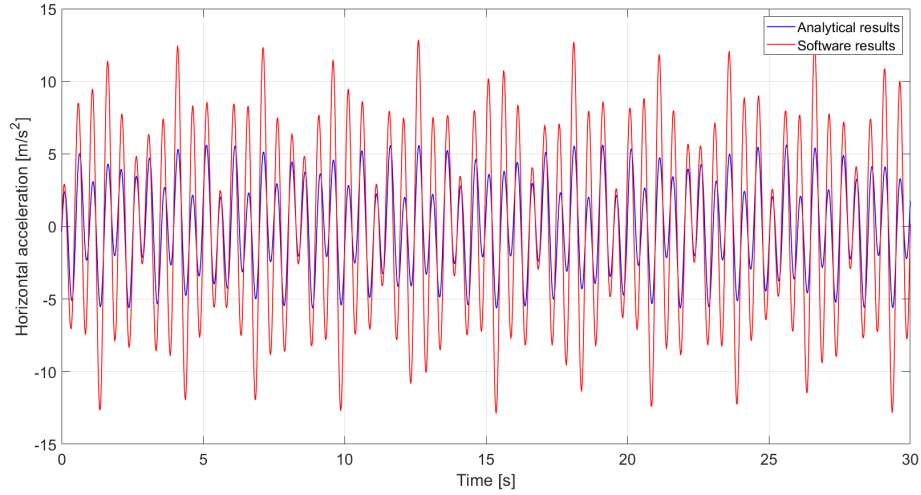

(c) Acceleration variation

Figure 11: Variation of displacement, velocity and acceleration at the moving support for a period of the applied force T = 0.5s - No friction

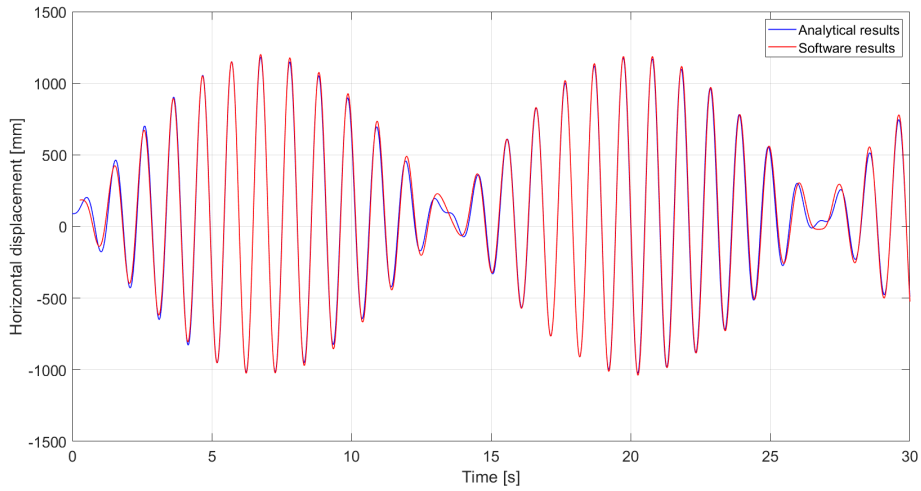

(a) Displacement variation

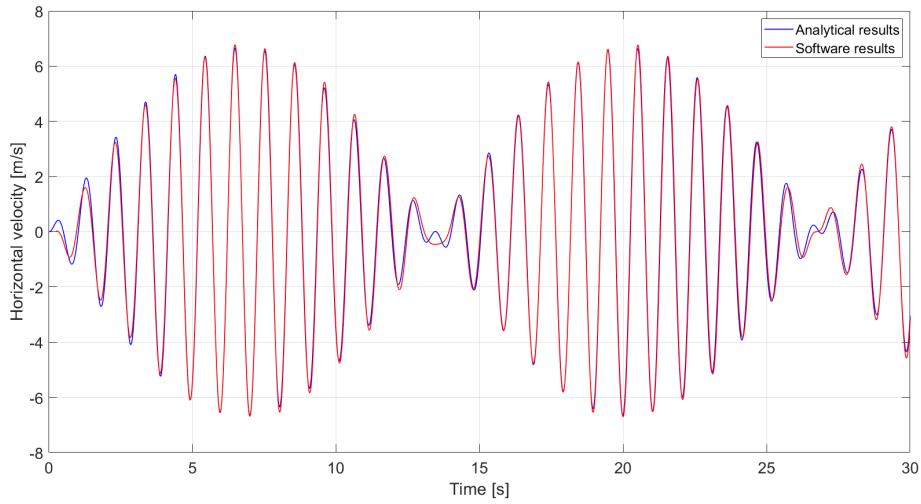

(b) Velocity variation

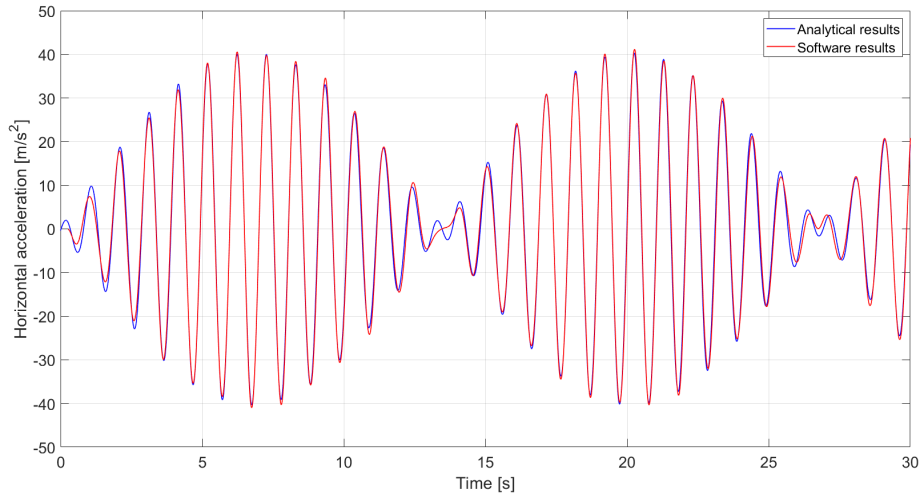

(c) Acceleration variation

Figure 12: Variation of displacement, velocity and acceleration at the moving support for a period of the applied force T = 1s - No friction

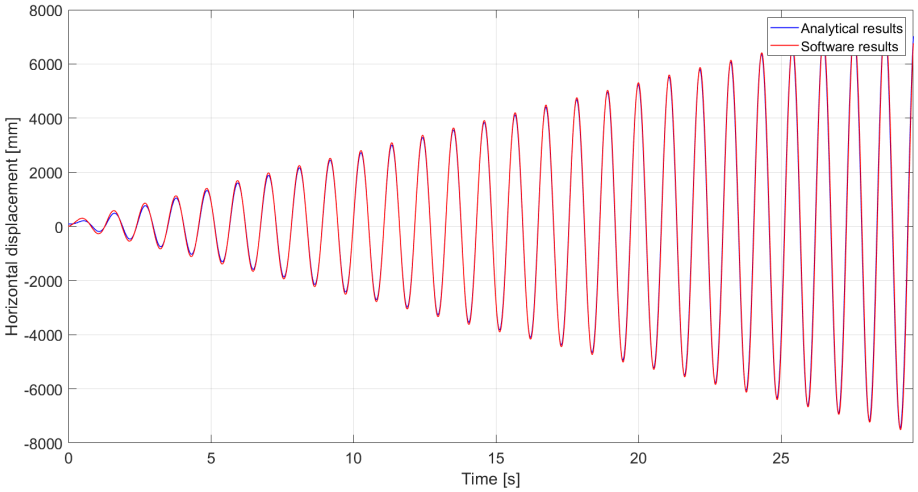

(a) Displacement variation

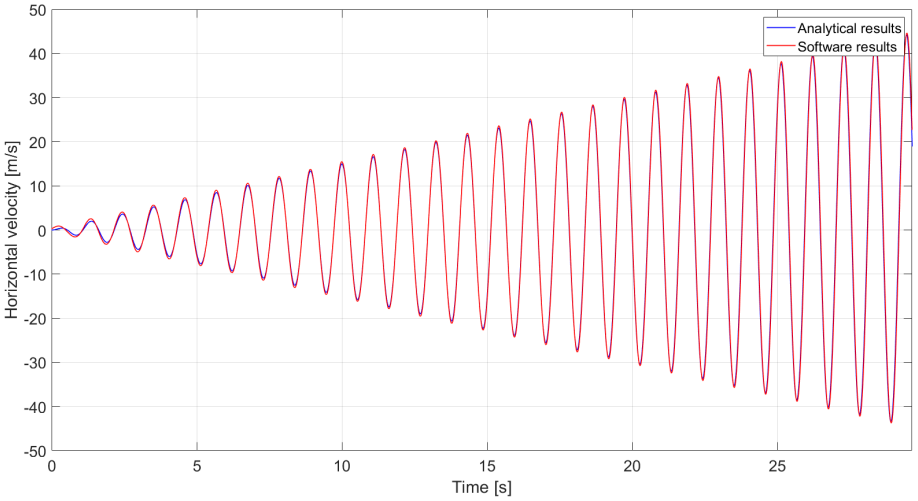

(b) Velocity variation

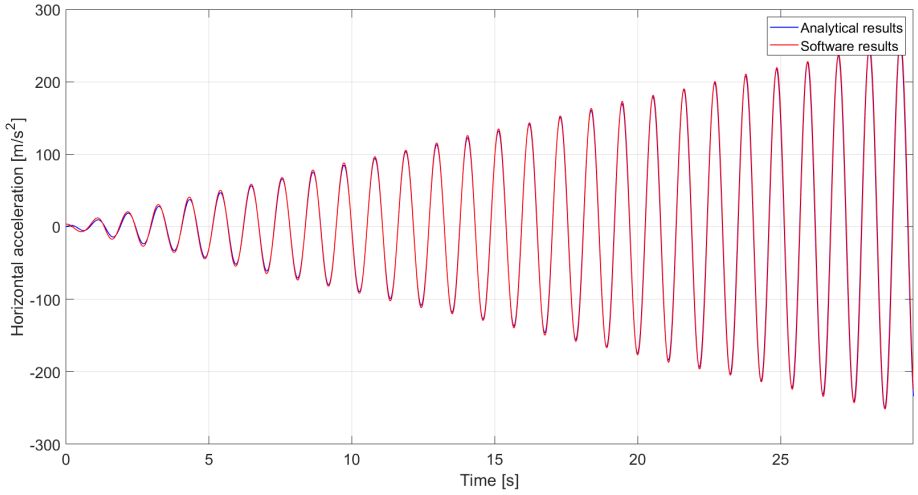

(c) Acceleration variation

Figure 13: Variation of displacement, velocity and acceleration at the moving support for a period of the applied force T = 1.08s - No friction

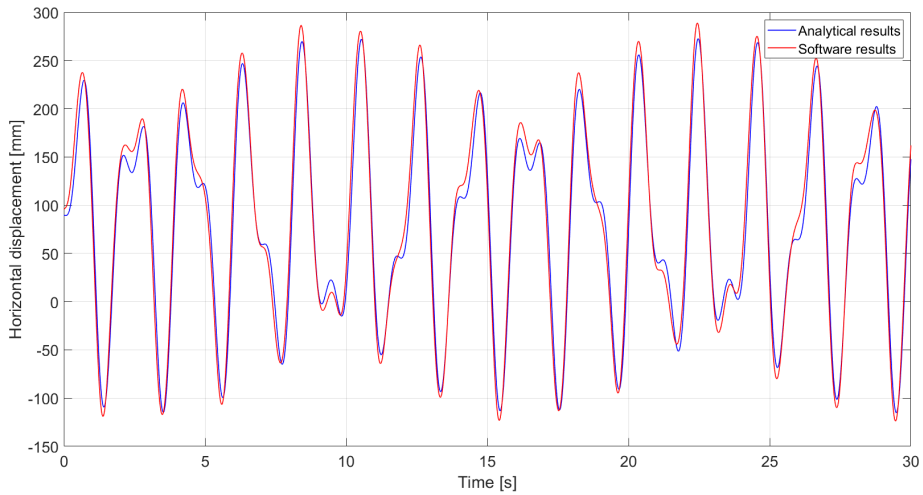

(a) Displacement variation

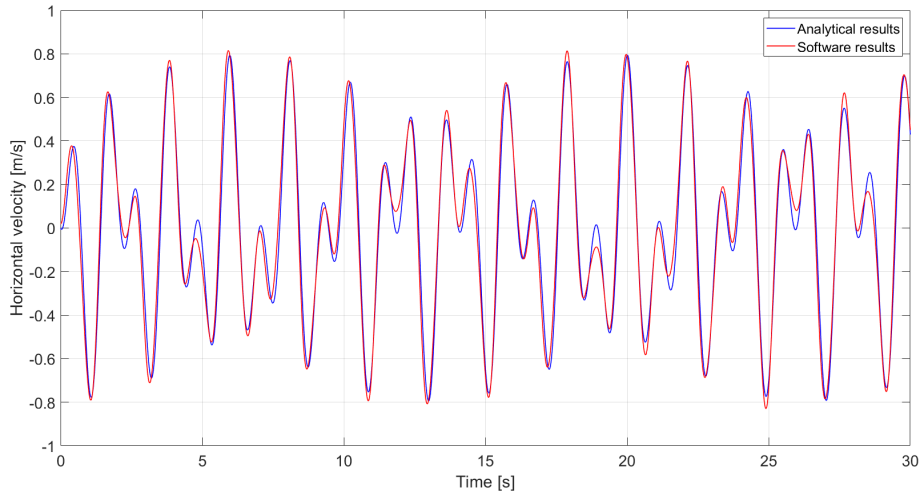

(b) Velocity variation

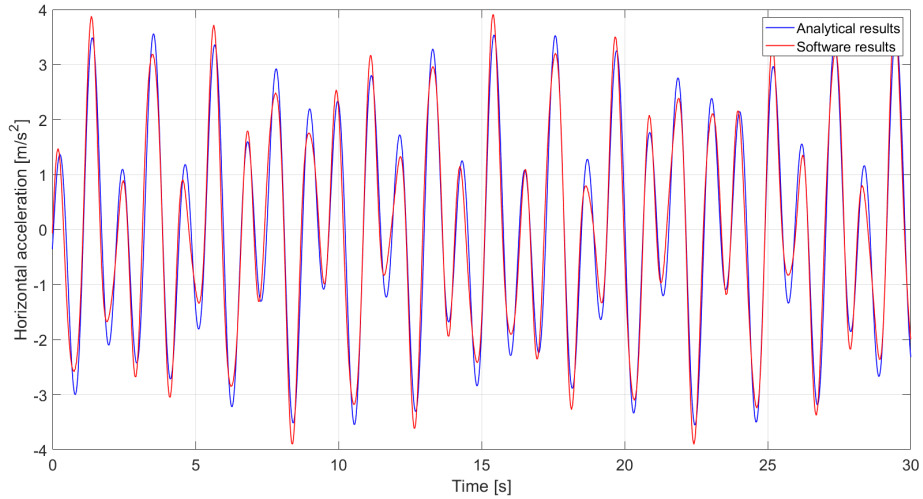

(c) Acceleration variation

Figure 14: Variation of displacement, velocity and acceleration at the moving support for a period of the applied force T = 2s - No friction

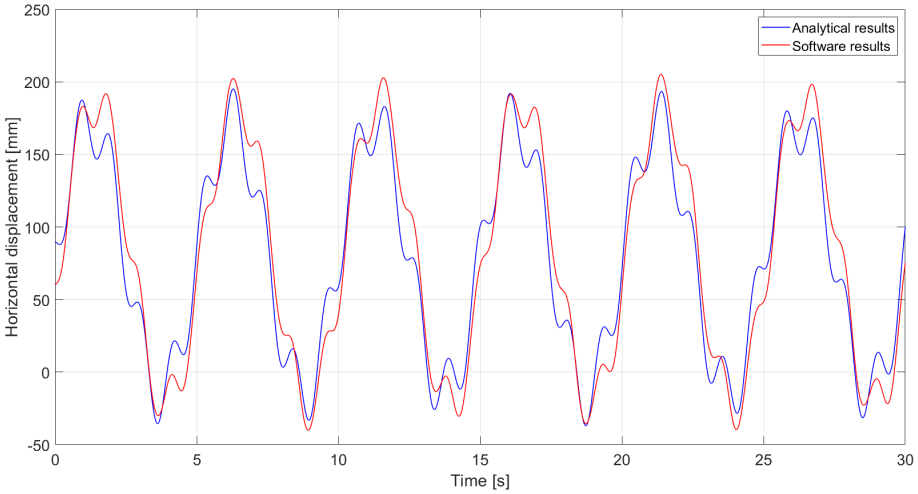

(a) Displacement variation

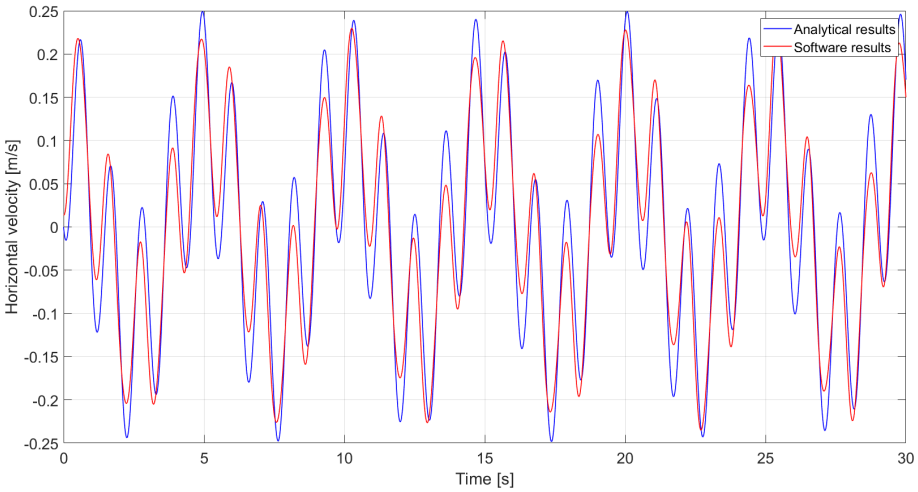

(b) Velocity variation

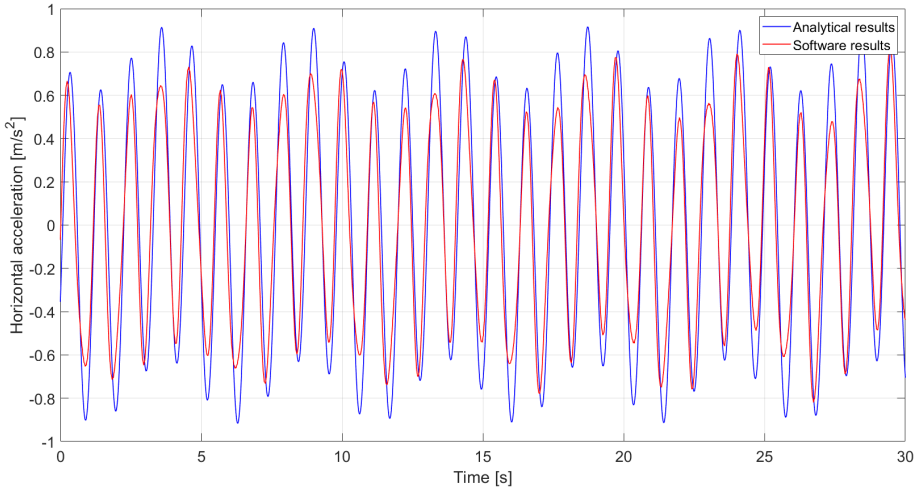

(c) Acceleration variation

Figure 15: Variation of displacement, velocity and acceleration at the moving support for a period of the applied force T = 5s - No friction

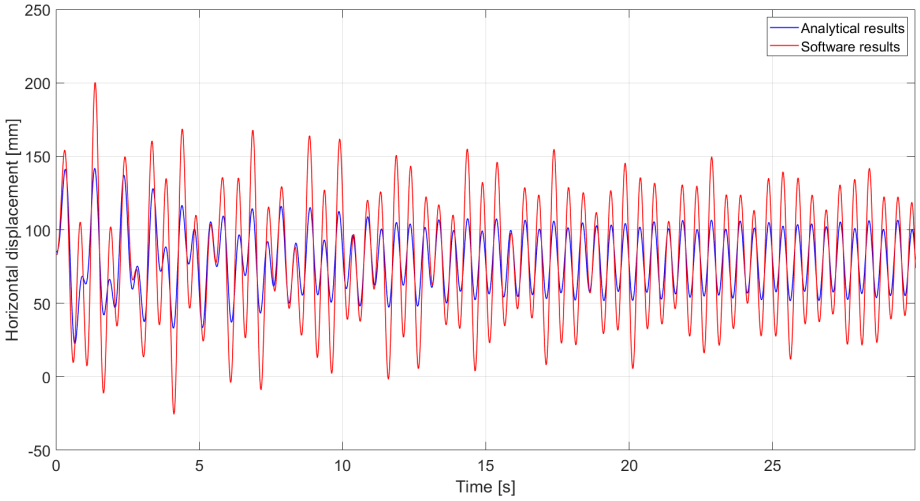

(a) Displacement variation

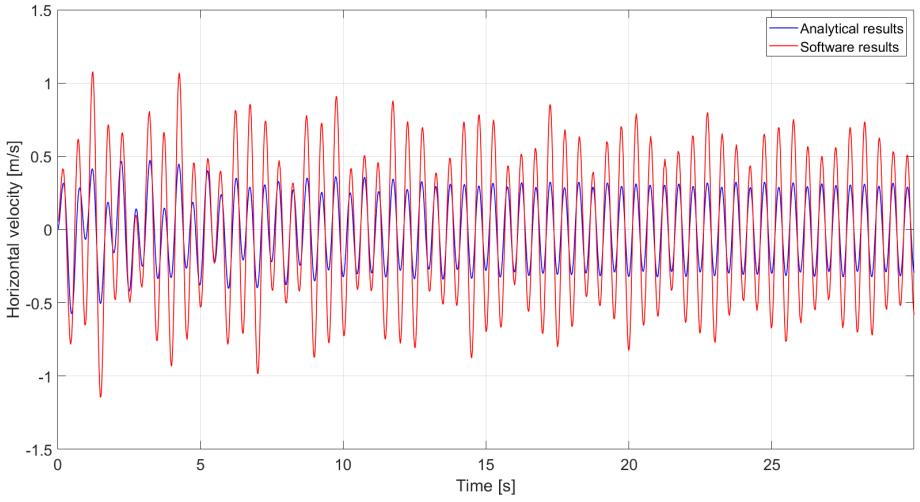

(b) Velocity variation

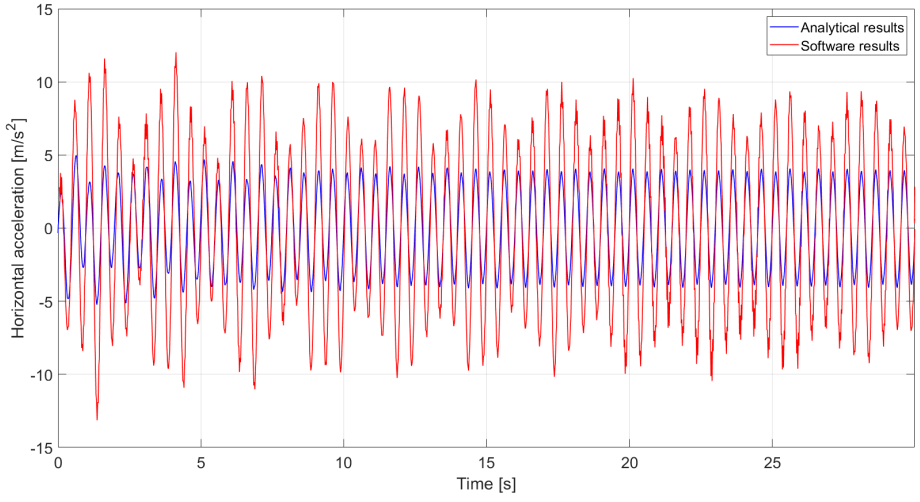

(c) Acceleration variation

Figure 16: Variation of displacement, velocity and acceleration at the moving support for a period of the applied force T = 0.5s - Friction only

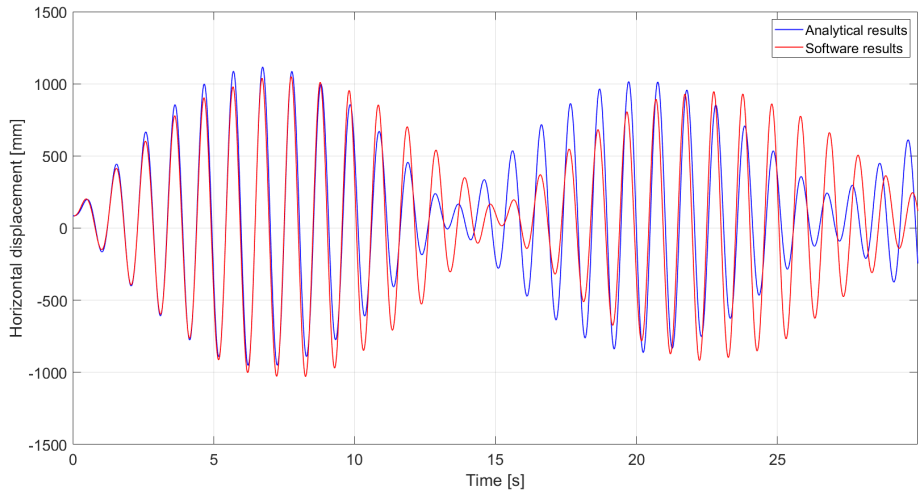

(a) Displacement variation

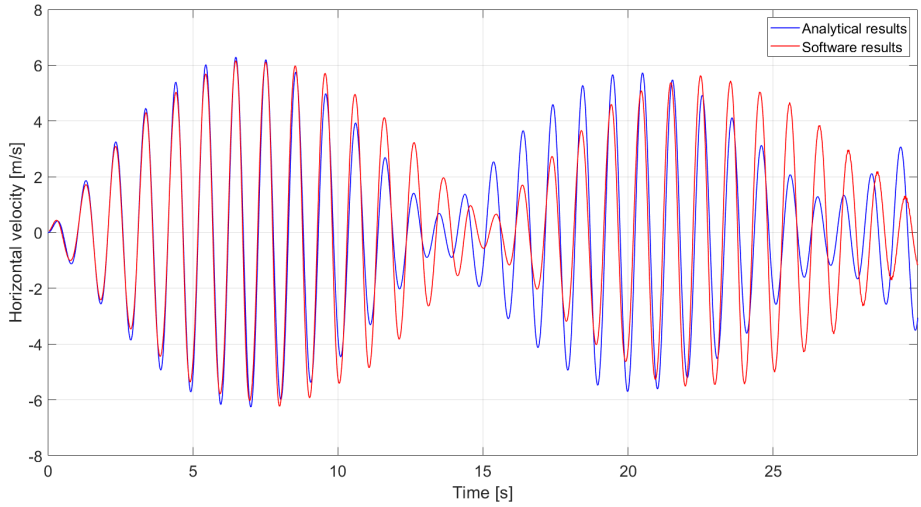

(b) Velocity variation

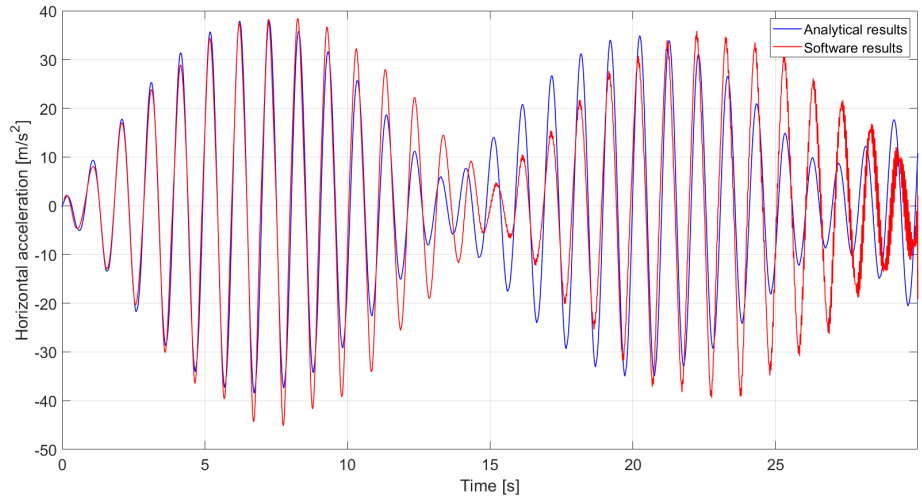

(c) Acceleration variation

Figure 17: Variation of displacement, velocity and acceleration at the moving support for a period of the applied force T = 1s - Friction only

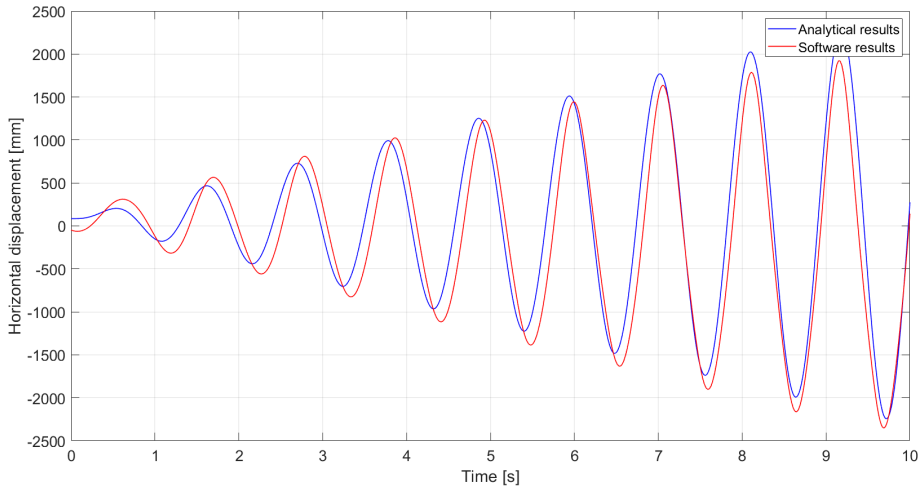

(a) Displacement variation

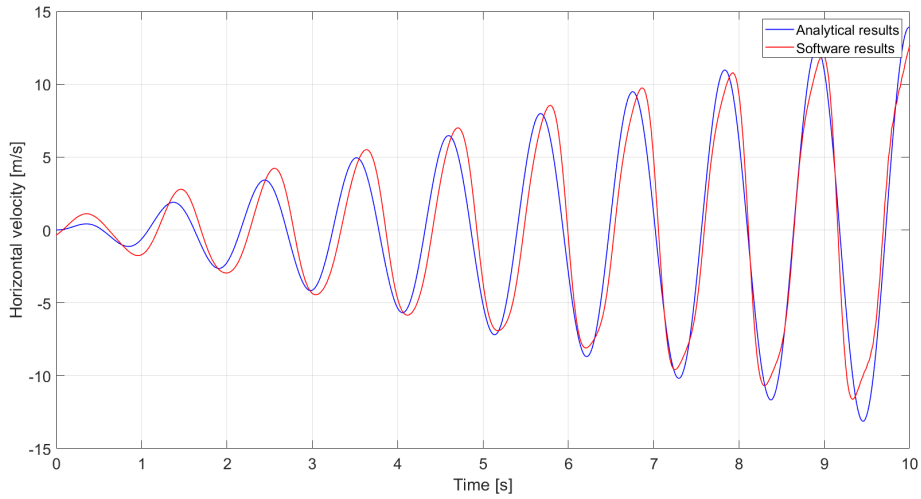

(b) Velocity variation

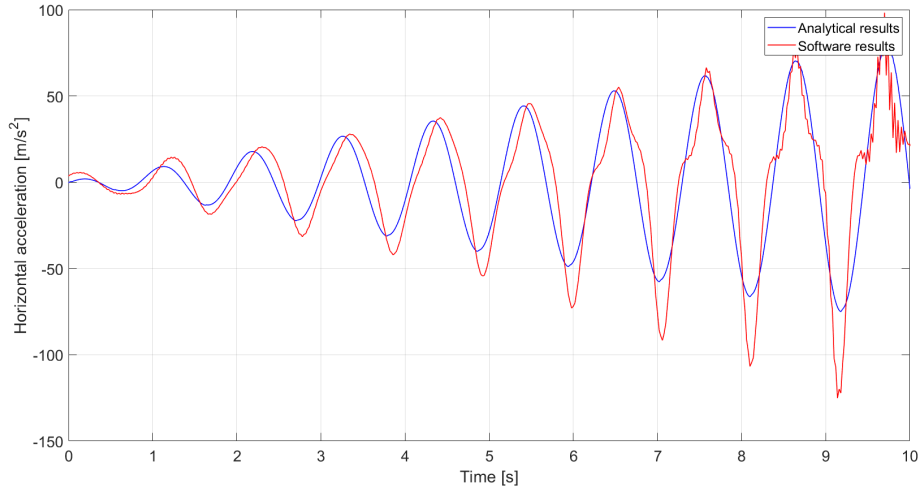

(c) Acceleration variation

Figure 18: Variation of displacement, velocity and acceleration at the moving support for a period of the applied force T = 1.08s - Friction only

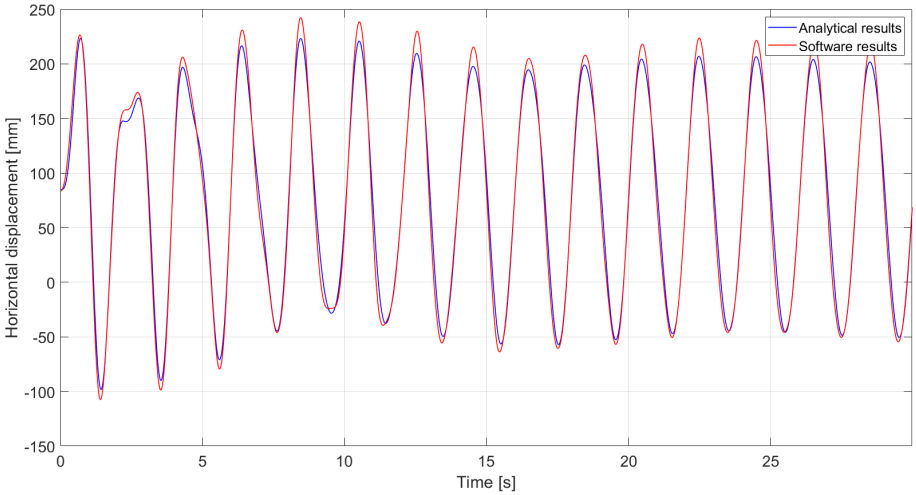

(a) Displacement variation

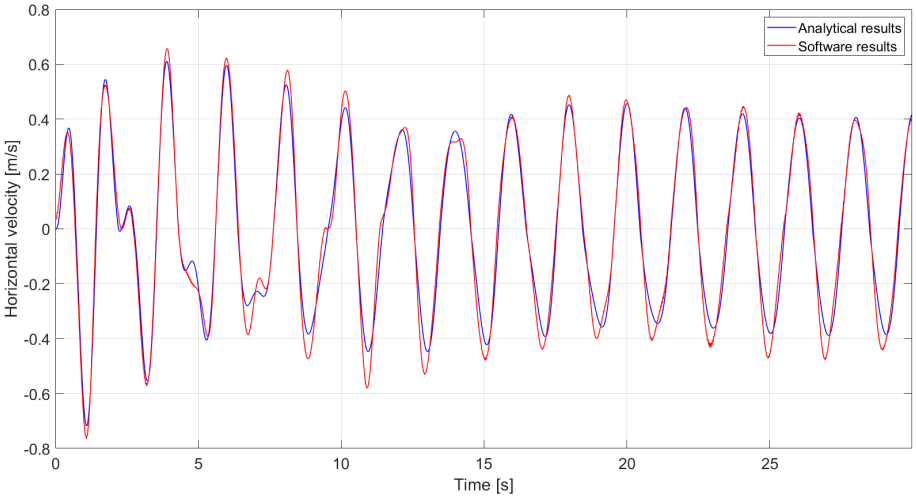

(b) Velocity variation

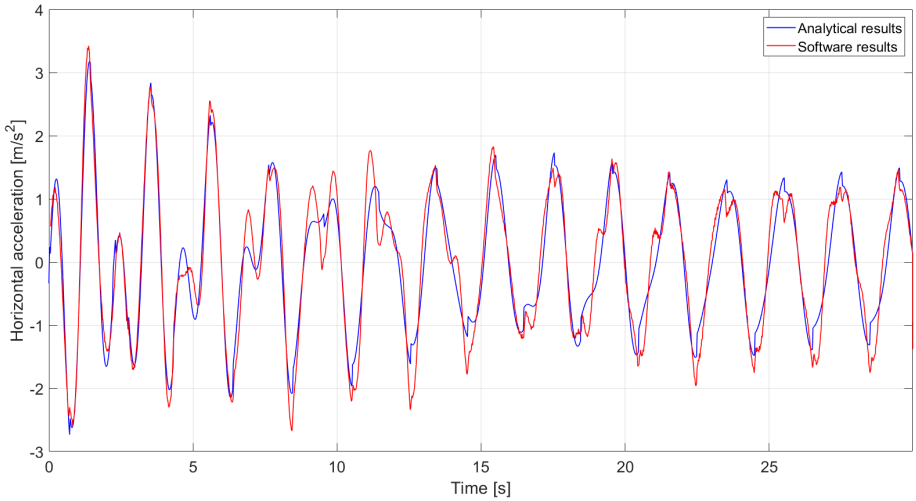

(c) Acceleration variation

Figure 19: Variation of displacement, velocity and acceleration at the moving support for a period of the applied force T = 2s - Friction only

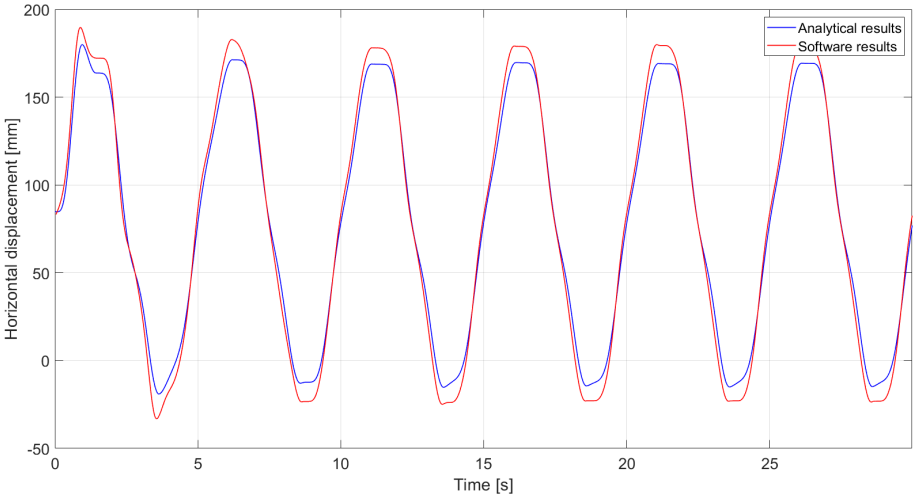

(a) Displacement variation

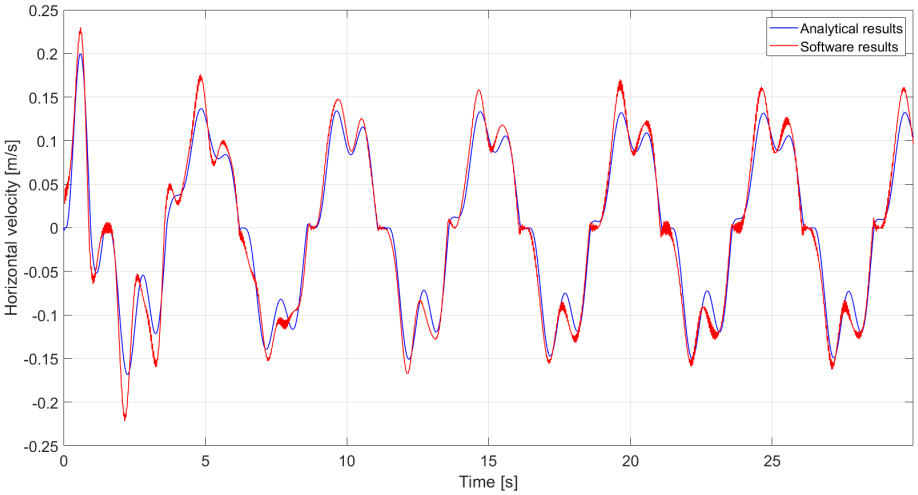

(b) Velocity variation

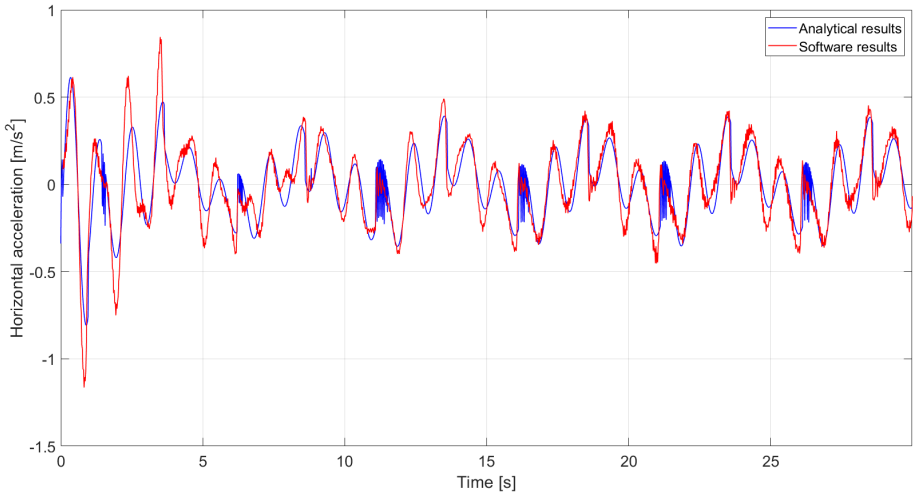

(c) Acceleration variation

Figure 20: Variation of displacement, velocity and acceleration at the moving support for a period of the applied force T = 5s - Friction only

A few key observations can be deducted from the results shown. First of all, in opposition with the frictional case, the behaviour of the structure when no friction is considered is characterized by more oscillations and by larger displacement, velocity and acceleration in absolute value, as is to be expected; when friction is accounted for, even with a coefficient as small as 5%, the curves describing the behaviour are noticeably smoother.
Secondly, the smaller the period of the force, the smaller the peak displacements tend to be, especially when friction is included in the analysis, since the structure is forced to change its motion much more frequently and is unable to develop its full movement, which results in the velocity and acceleration to be noticeably larger; conversely, the larger the period of the force, the closer the behaviour is to the static one, resulting in smaller velocity and acceleration and in larger peak displacements.
This is true except for when the force has a period close to the natural period of vibration of the structure: in this case, when the two periods are similar but not exactly the same, the oscillations in displacement, velocity and acceleration follow the frequency of the force as normal, but at the same time they display a macro-periodicity, as evident in Figures 12 and 17. Finally, when the period of the force matches the period of the structure, resonance settles in, which means that the oscillations increase with time without ever damping down, until failure. The natural period is of course the same also when friction is considered, since all it does is reducing the movements and it does not change the overall stiffness.
It is also observed that the software and analytical models differ more and more as time progresses for periods close to the natural period of vibration when friction is accounted for (Figures 17 and 18), but not in the linear case (Figures 12 and 13); this is due to the fact that for such frequencies the structure tends to accumulate energy instead of dissipating it, therefore the small differences in the modelling of the spring (namely its varying elastic limit, included in the analytical solution but not in FineLg, and the slightly different stiffness before reaching it) become more and more significant with time, hence the curves phasing out.
Furthermore, as shown also in the static case, the presence of friction causes the structure to display a stick-slip behaviour: whenever the movement is inverted, the displacement does not vary until the friction force reaches the same intensity in absolute value but with the opposite sign (see Figure 21); in the dynamic case, this translates also to velocity and acceleration being zero whenever peak displacements, both positive

and negative, are reached. Such behaviour is clearly visible for large periods of the applied force (see Figure 20), while in other cases, given the relatively small friction coefficient, the structure oscillates so quickly that the stick phase is not observed as much.

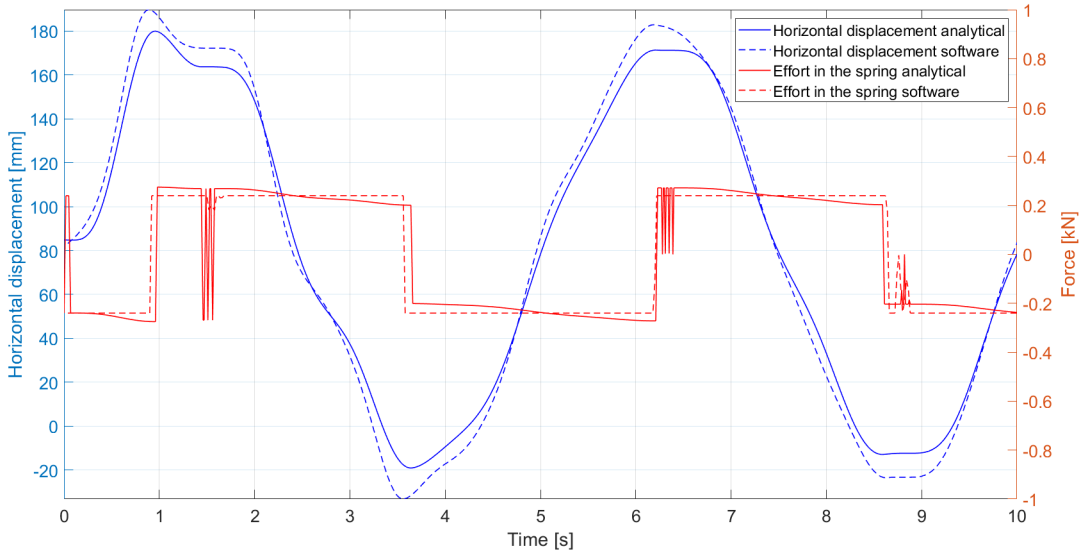

Figure 21: Evolution of the stress in the spring taking as example the force with period T = 5s

As previously stated, the Figure above displays how the analytical model is able to correctly capture the increase and decrease in absolute value of the maximum friction force depending on the displacement, whereas for the software a constant value of the elastic limit has to be used; the difference in the final results, however, is rather small. Given the presence of some differences in the analytical solution and software modelling, mainly small geometric non-linearities not considered analytically, variable elastic limit of the spring not included on FineLg and its relatively lower stiffness to ensure convergence of the calculation, the results obtained are not exactly the same; nevertheless, they are always in very good agreement.

Having thus performed the dynamic analysis analytically and compared it to the software resolution, both with and without friction, the pendulum effect was then included in the calculations as was done for the static analysis, considering the same radius of curvature of $r = 0.1m$ and the same constitutive law for the modelling spring (illustrated in Figure 5). The stiffness of the hardening stage, as the elastic limit itself,

depends on the vertical reaction at the support and therefore on the displacement; just as before, the software uses a constant stiffness of $45kN/m$, while to account for such phenomenon in the analytical model the equation of motion was modified. Specifically, the horizontal reaction force R_h is split into two components, the friction R_f and the pendulum effect R_p, and at each time step i:

$$|R_f^i| = min\left(\left|R_f^{i-1} + \phi R_v^i \cdot tanh\left(\frac{x^i - x^{i-1}}{\varepsilon}\right)\right| \; ; \; |\phi R_v^i|\right) \tag{3}$$

$$R_p^i = \frac{R_v^i}{r} \cdot x^i \tag{4}$$

$$R_h^i = R_f^i + R_p^i \tag{5}$$

The equation of motion is then solved as normal using the Newmark method and the results are reported in Figures 43 - 46 in the Appendix, comparing analytical and FineLg outputs as before; moreover, in order to have a better idea of the influence of pendular bearings on the case with friction only, an additional comparison of displacements is displayed in Figure 22, taking as example the scenario with the applied force with period $T = 5s$.

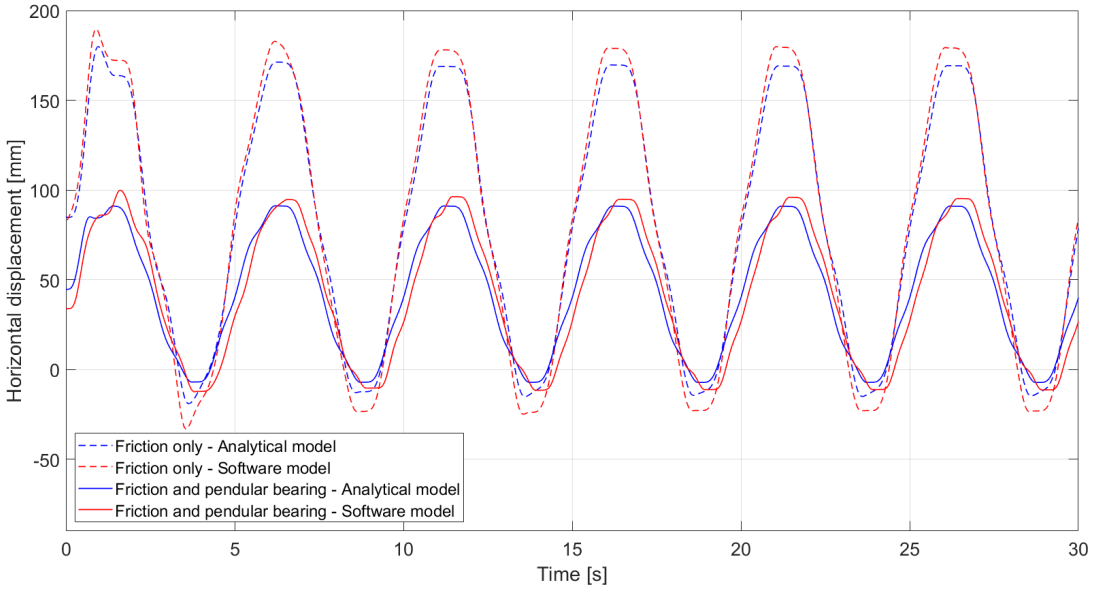

Figure 22: Comparison of the evolution of displacements taking as example the force with period T = 5s

The effect of the pendular bearing is substantial: for larger periods the displacement, velocity and acceleration curves are smoother and more controlled and their peaks much smaller in absolute value; moreover, since hardening increases the overall stiffness of the structure, its natural period of vibration is expected to be quite smaller than before, hence for $T = 1s$ the values of displacement, velocity and acceleration reached are much lower and the macro-periodicity has a noticeably larger frequency compared to the one displayed in the case with friction only.
The variation of the horizontal reaction with time has been computed too, as shown in Figure 23.

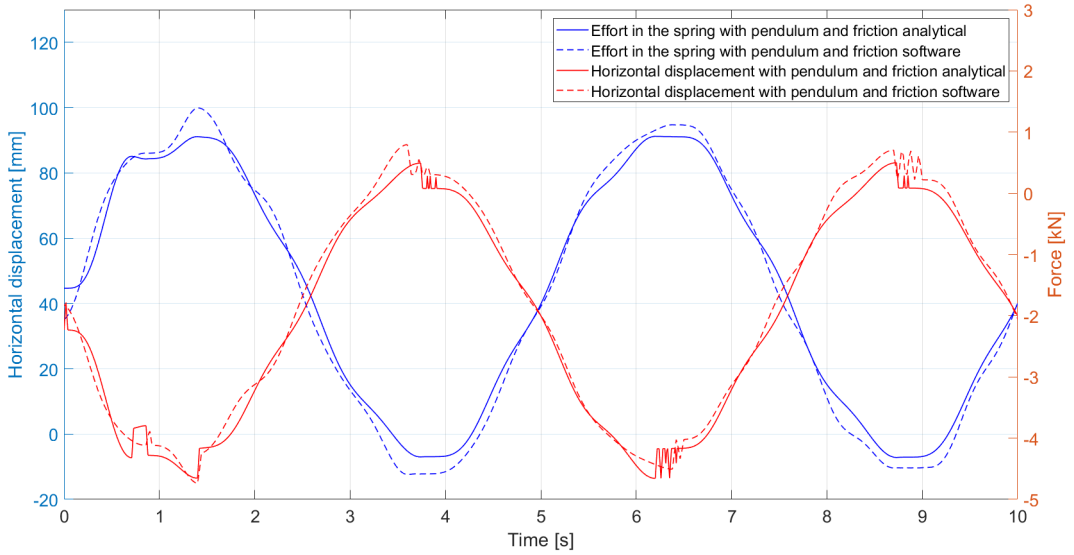

Figure 23: Evolution of the stress in the spring taking as example the force with period T = 5s

Again, after each peak in displacement there is a drop in the horizontal reaction caused by the inversion of friction, but its contribution is rather small compared to the pendulum effect, which is directly proportional to the displacement variation through a much larger coefficient and with no limit to its intensity, therefore it ends up being the most significant contribution to the behaviour of the structure. Moreover, even though only the analytical model accounts for varying elastic limit and stiffness of the hardening phase, the differences between the curves are still rather limited, making the simplification adopted on FineLg quite accurate.

2.3 Increased friction effect

Given that the dimensions and loads of this simple academic structure are very tiny compared to those of a massive bridge, the effect of only a 5% friction is rather small. To better see its influence on the structure, the static and dynamic calculations are performed again as before using the analytical model with an additional vertical downward force on the moving support of $20kN$ (not considered when determining the natural period, which is still $1.08s$), in order to increase the effect of the friction on the behaviour; as a comparison, the resulting reaction force is roughly six times the one obtained and considered earlier. The outputs are reported in the following graphs, compared to the previously obtained behaviour using the analytical model.

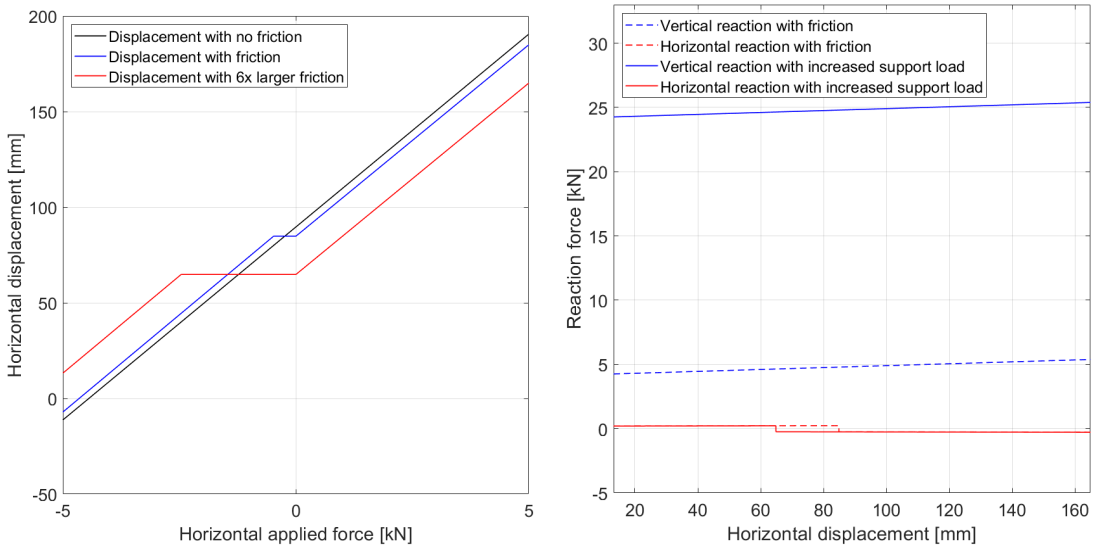

(a) Displacement as a function of the horizontal force

(b) Support reactions as a function of the displacement

Figure 24: Displacement and support reactions at the moving support with increased friction contribution, compared with the previous results

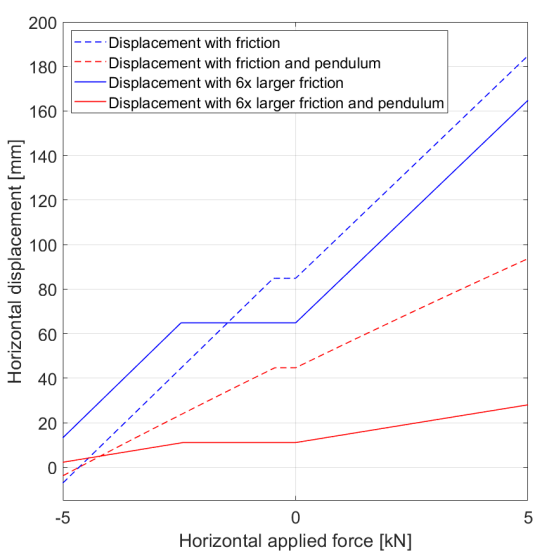

(a) Displacement as a function of the horizontal force

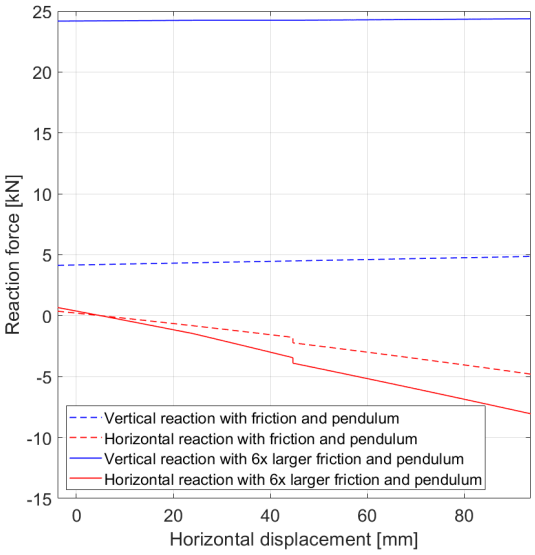

(b) Support reactions as a function of the displacement

Figure 25: Displacement and support reactions at the moving support with increased friction contribution and pendulum effect, compared with the previous results

As expected, an increase in the vertical force applied on the support causes a significant reduction in the initial displacement with no applied horizontal load and a substantial increase in the stick phase after the motion is reversed. The difference is even more pronounced when the pendulum effect is considered alongside a heightened friction force, since both are positively influenced by a larger vertical force on the roller: the stiffness of the structure is greatly increased and the displacement variation with the horizontal load is reduced to the point that it almost does not vary.
For the dynamic analysis, Figures 47 - 51 in the Appendix display the comparison for the friction only case: as clear from the graphs, the increase in friction not only has the effect of lowering the peak values of displacement, velocity and acceleration, but also of making the behaviour smoother, meaning that the amplitudes of macro-periodicity or oscillations, where previously present, are now greatly reduced. Moreover, the stick behaviour is more prevalent and long lasting: for $T = 5s$, for instance, the peak displacements are lower and the velocity lingers around a value of zero for a longer time, while for $T = 2s$, where the sticking phase was previously not present, the structure now remains stationary for a short while after each peak before reversing its motion.
In Figure 26, the force in the spring with time is compared as well.

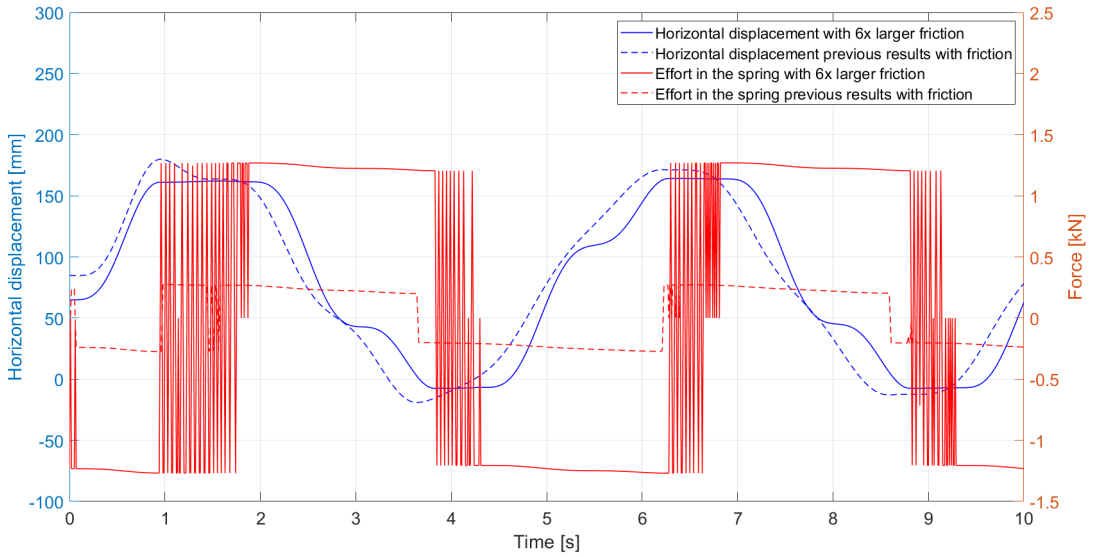

Figure 26: Evolution of the stress in the spring taking as example the force with period T = 5s, compared with the previous results

The displacements are generally speaking reduced due to the significant increase in the maximum friction force, or in the elastic limit of the spring used to model it; moreover, notice that in correspondence with each peak the stick phase is slightly prolonged, since the stronger friction force oscillates for a significant amount of time before changing sign.

Finally, the comparison considering both friction and pendular bearing is displayed in Figures 52 - 55 in the Appendix, where the results are shown to be very different: the longer stick phase and larger elastic limit of the spring cause the reaction force at the support to be significantly greater at all times, hence the displacement, velocity and acceleration curves reach more modest values. Only for $T = 0.5s$ the effect looks to be the opposite, the reason for that being that the structure with an increased pendulum effect has such a larger stiffness that the natural period of vibration is significantly lower than before; therefore, at such frequency of the applied load, the stiffer structure is closer to its natural period.

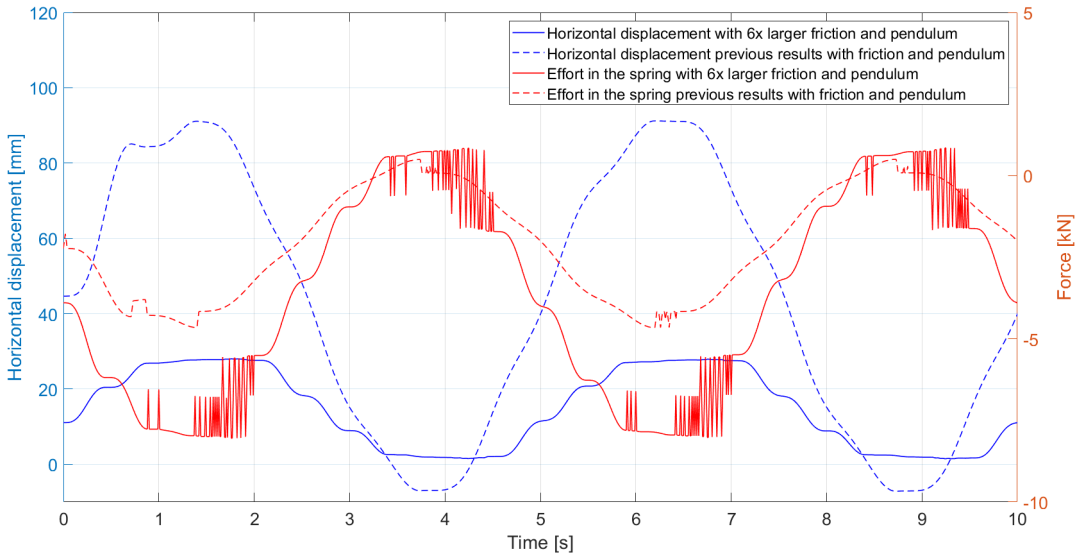

Figure 27: Evolution of the stress in the spring taking as example the force with period T = 5s, compared with the previous results

In Figure 27 the stress in the spring is compared to the previous results relative to lower friction and pendulum effect. Clearly, in this case the horizontal reaction is always much larger, and also its drop in absolute value after every peak in displacement, being caused by the inversion of the friction force, is bigger and more significant than it was previously; moreover, as was observed before, the duration of the stick phases is quite significantly increased in this analysis as well, due to the larger friction force oscillating for some time before switching sign.

2.4 Comparison of the results

In order to better visualize the problem, a comparison between the calculations performed so far was carried out to see the influence of the various parameters on the final output; in Figure 28, a graph displaying the variation of the maximum displacements in absolute value of the support depending on the period of the applied horizontal force for all the previous scenarios of friction and pendulum effect is reported, from which a few conclusions can be drawn.

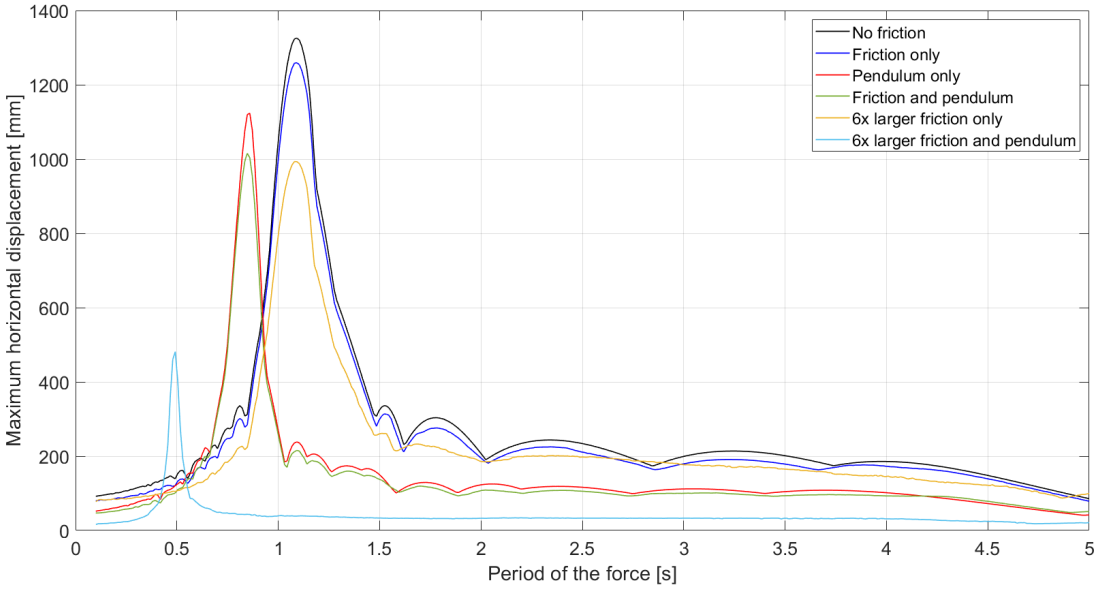

Figure 28: Variation of the maximum displacement undergone by the structure for different periods of the applied force

For small and large periods of the force, the maximum displacement is quite small and fairly constant, since the structure either hardly feels the effect of the external action or the latter acts so slowly that the behaviour is close to the static one; only for frequencies similar to the natural frequency of vibration there are dynamic effects developing, with an increase in the displacement and eventually reaching resonance. As previously calculated, this critical condition happens when the period of the force is $T = 1.08s$, hence the curves reaching a peak around such value; it is significant to note that for any amount of friction, even with the total displacements being reduced, still the natural frequency of vibration remains the same, since the stiffness is not altered. However, the behaviour starts to change once the pendulum effect is added: the recalling force, which was modelled as kinematic hardening of the friction spring, is

effectively an extra contribution to the stiffness, which causes the natural period of the structure to go down to $T = 0.84s$. This does not change if the friction is considered as well, for the same reasons as before, but if an increased vertical force is applied on the support the natural period of vibration predictably goes down even more, reaching a value $T = 0.47s$.

Therefore, compared to an ideal roller, the pendular bearing not only reduces the maximum displacement, but it also increases the frequency of the force required to reach resonance; moreover, the larger the reductions of the movement, the narrower the peak of the curve, which ensures that for periods not quite equal to the natural period of vibration the displacement is efficiently controlled and kept small, albeit greater than normal.

3 Seismic analysis

An interesting scenario for the analysis of the dynamic behaviour of structures, and for which pendular bearings are often implemented, is during a seismic event. In this section of the work, the evolution of displacements will be evaluated taking as input the accelerogram of an earthquake instead of a varying horizontal force, first applied on the simple structure considered before, in order to gain familiarity with the problem, and then on a real case, specifically the Third Bosphorus Bridge in Turkey.

3.1 Simple structure under seismic action

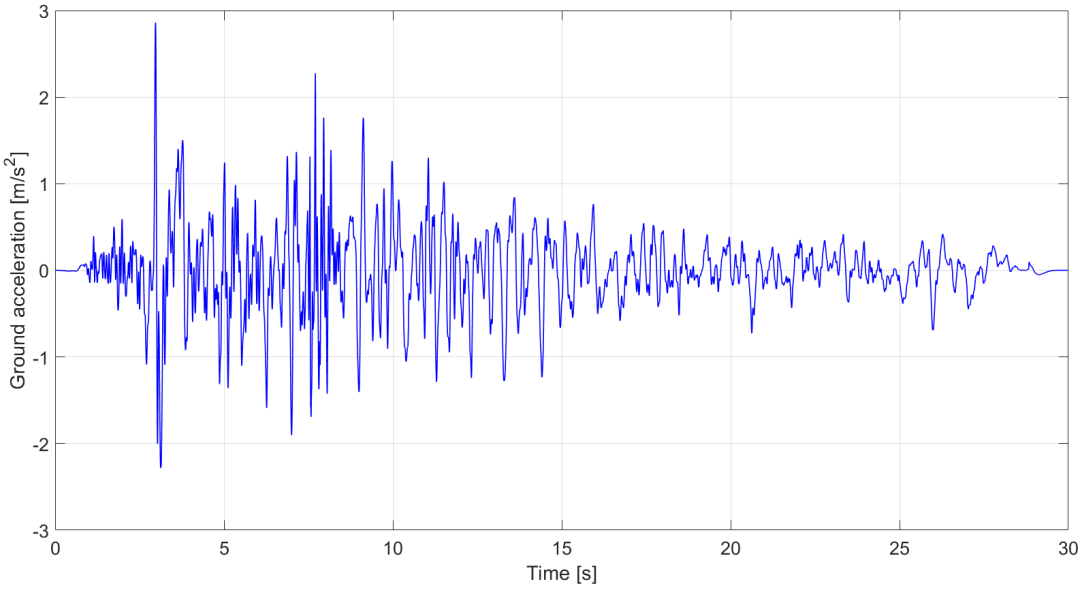

Figure 29: Ground acceleration for the considered seismic event

In Figure 29, the accelerogram for the considered earthquake is shown. In order to determine the behaviour of the structure, simplified as a 1 DOF system as before (see Figure 10), the ground acceleration $a_g(t)$ was converted at each time step into an equivalent force applied on the mass, starting from the equation of motion, as follows:

$$m(\ddot{x} + a_g(t)) + kx + R_h = N \tag{6}$$

$$m\ddot{x} + kx + R_h = N - m \cdot a_g(t) \tag{7}$$

The displacements in time were then calculated using the Newmark method with all the previously defined parameters for four different scenarios: free moving roller, frictional support, penduar bearing and both friction and pendulum effect. The results of such analysis are reported in Figure 30; specifically, since the structure has an initial displacement different from zero and related to the boundary conditions, the displacements are reported not in absolute terms, but with respect to the equilibrium configuration.

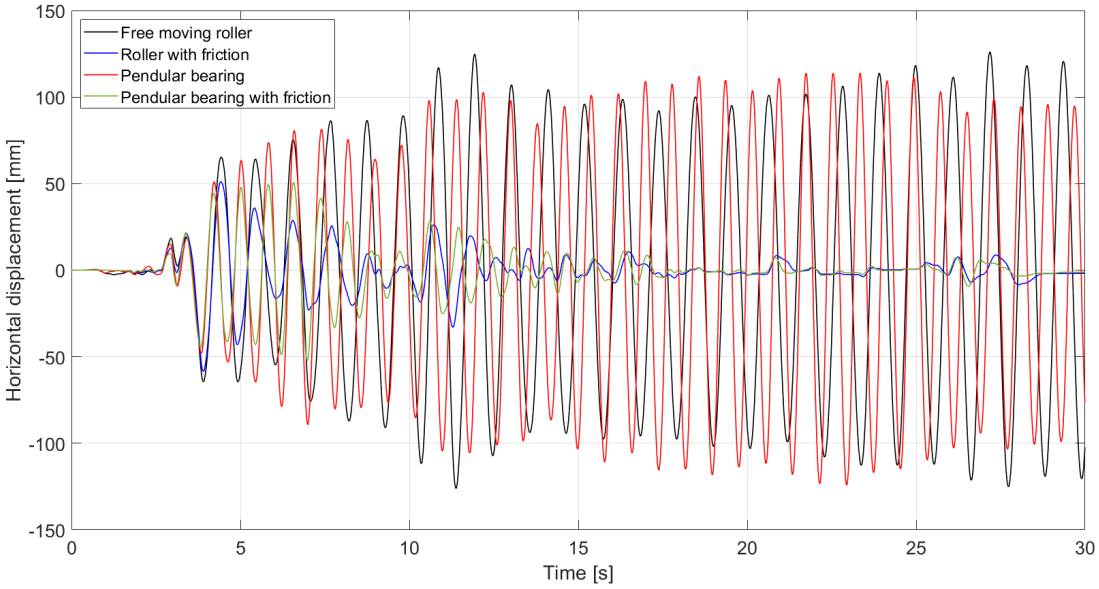

Figure 30: Comparison of the displacements of the support of the simple structure for the various boundary conditions for the considered seismic event - IPE 140 elements

The presence of a pendular bearing increases the stiffness of the structure quite significantly, as already discussed, hence the macro-periodicity of the red curve can be observed to have a larger frequency compared to that of the black one; however, they do not display significant differences in terms of displacements under seismic action, which is a consequence of the structure being rather stiff, with and without considering the pendulum effect, and its natural frequency of vibration having a value $f \approx 0.9Hz$ if an ideal roller as support is considered and $f \approx 1.2Hz$ when the pendular bearing is added. On the other hand, a real bridge, such as the Third Bridge over the Bosphorus, which will be discussed in the following chapter, has its principal modes of vibration characterized by a much smaller natural frequency, in the region of $f = 0.1 \div 0.2Hz$, causing the response to be different; therefore, the graph in Figure 31 displays the same results as the previous one in Figure 30, except for the fact that the

cross section of beam and column of the simple structure was changed from an IPE 140 to a full $40x40mm$ element, resulting in a frequency of vibration of $f = 0.18Hz$ when the support is an ideal roller. In this way, even though the values themselves will not be the same as those calculated later for the real bridge, this analysis will give a first idea of what to expect when a structure characterized by such value of natural frequency is subjected to the chosen earthquake action.

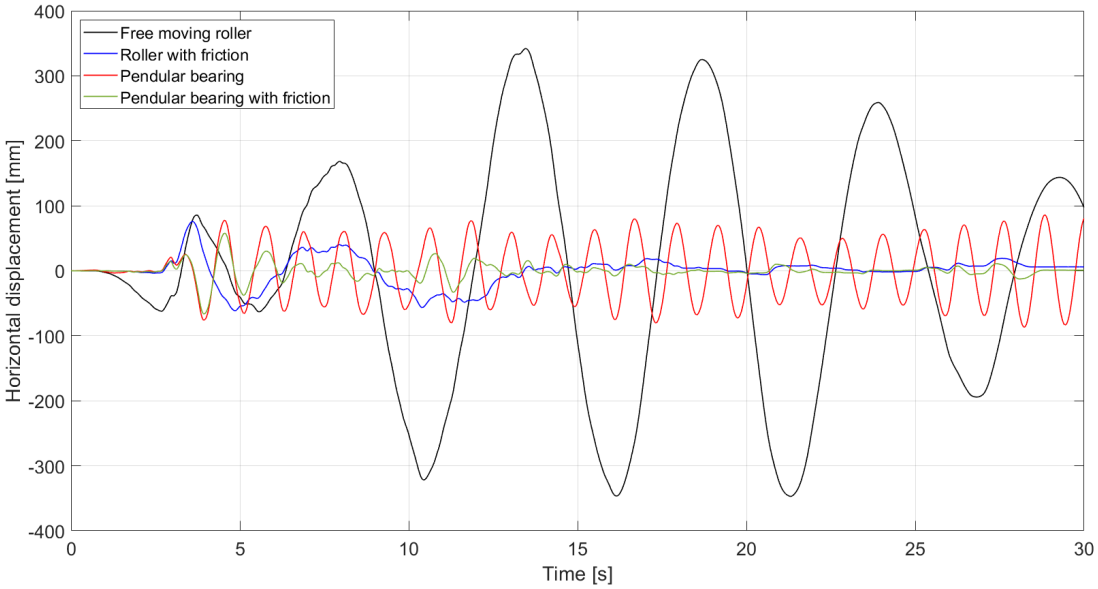

Figure 31: Comparison of the displacements of the support of the simple structure for the various boundary conditions for the considered seismic event - $40x40mm$ elements

Perhaps closer to what is expected, the case with freely moving support undergoes much larger displacements with respect to the initial equilibrium configuration; when the pendulum effect is added, the curve reaches quite smaller peak values and the increase in stiffness is evident by the tightening of the vibrations and their considerably larger frequency.

The results considering friction, on the other hand, both for IPE 140 and $40x40mm$ cross sectional elements, are much more similar to each other, with the green curve being of course much more stable around the horizontal axis; both scenarios are characterized by an initial shaking of the structure, corresponding to the most violent phase of the seismic action, followed by very small displacements due to the dissipation of energy granted by the friction effect.

Since the analyses were performed with no structural damping, the movement will continue indefinitely after the seismic event when friction is not accounted for. Given

that in reality some damping is always present this of course is not accurate, but it is clear that neglecting the friction effect of the support has a notable impact on the final result: when a frictional support is considered, the oscillations dissipate considerably more quickly than when only the pendulum effect is accounted for; moreover, the final equilibrium configuration which the structure tends towards is influenced by the presence and magnitude of the friction action as well.
The effect of friction is very evident also in the variation of velocity and acceleration of the support (see Figure 56 for the structure with IPE 140 elements and Figure 57 for the structure with solid $40x40mm$ elements in the Appendix), as it acts as a strong damping effect, causing the frequent onset of a sticking phase and slowing the oscillations down quite effectively.

3.2 Third Bosphorus Bridge

The Yavuz Sultan Selim Bridge, or Third Bridge over the Bosphorus, is a road and rail transport bridge spanning the Bosphorus Strait in Istanbul, Turkey. Opened in 2016, it has a total length of $2169m$ and is supported by two towers and eight piers on either side of the free span; each one of these supports was built with a pendular bearing, since the area is characterized by a relatively high seismic hazard.

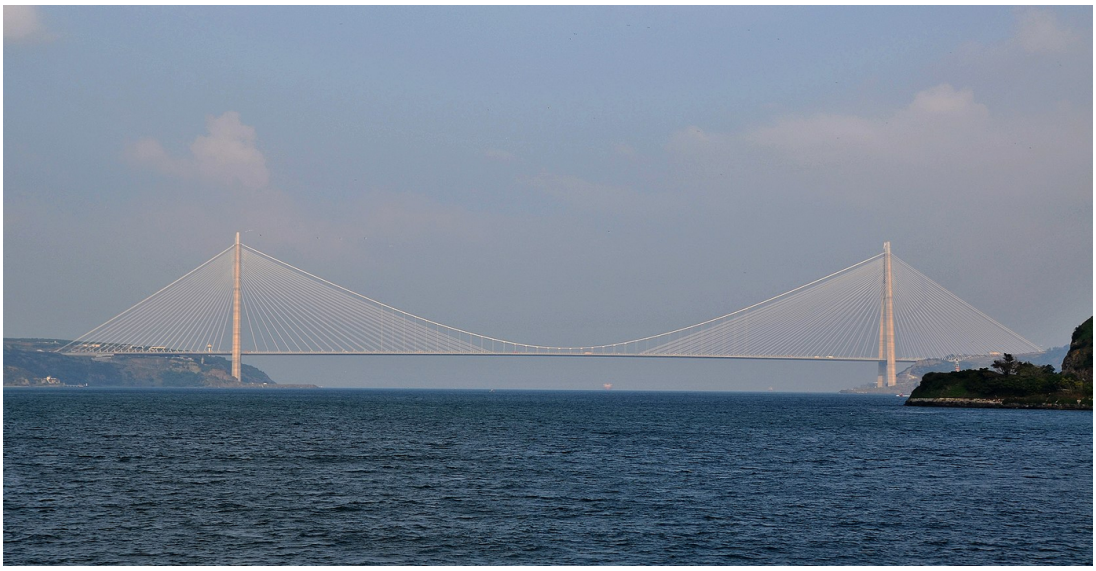

Figure 32: View from the south of the Third Bridge over the Bosphorus

This particular bridge is not very conventional, as it is both cable-stayed and suspended: the choice the cable-stayed option was developed based on the fact that using inclined cables gives the structure a greater stiffness compared to the suspended option, but the span was too large to allow for sufficiently short pylons, therefore both configurations were adopted; however, technically speaking, only the central part of the span is suspended. Moreover, the portions of the bridge at either side of the pylons, differently from the main span, are in concrete: the extra weight is functional to counterbalance the actions generated by vehicles and trains crossing the bridge, while for seismic calculations, for which only the dead weight is accounted for, it ends up resting on top of the piers and pylons, ensuring a greater stiffness and recalling force of the pendular bearings installed on them.

During the design of the bridge, the pendulum effect was accounted for in all cases, while the friction (conservatively taken with a coefficient of 5%) was included only in the various static analyses for train transit and neglected for the dynamic calculations under seismic action. This is due to the fact that the spring to model the friction, as described previously, has a nonlinear constitutive law, characterized by an initial very high stiffness and then a plateau after reaching the elastic limit: when performing a dynamic analysis there can be many numerical problems when the external action changes sign, especially if it is not uniform and periodic (as for an earthquake) and applied to a complex structure such as a large bridge, leading to the calculation being remarkably slower and not converging. For this reason, the friction effect was originally accounted for only for train transit because, due to the nature of the external solicitation, the analysis could be performed by assuming a static regime, but this is not an option during a seismic event, for which a dynamic analysis is required.

In order to study the effect of friction, therefore, a simplified model of the bridge was created on FineLg and calibrated so that it gives results similar to the real one, both when considering ideal rollers as supports and pendular bearings only; afterwards, friction-modelling springs were added and the same dynamic analyses performed on such simplified model, so that comparisons may be carried out.

3.3 Simplified model

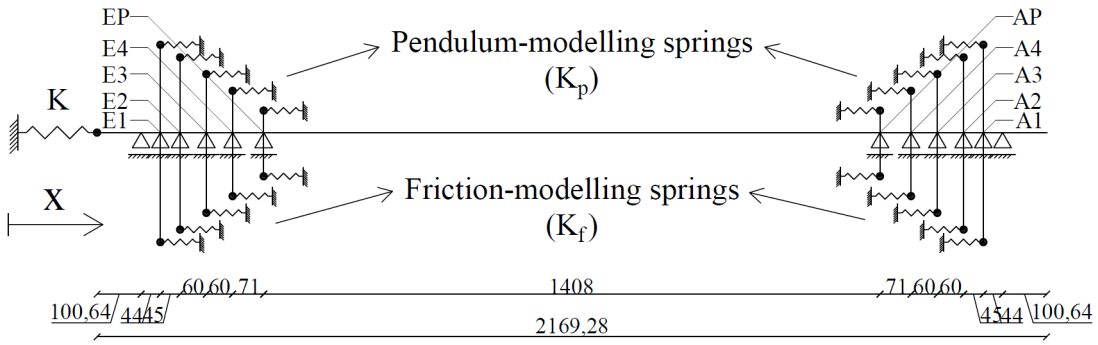

Figure 33: Simplified model of the bridge (measurements in meters)

In Figure 33, the model used to simplify the real bridge is illustrated: a simple steel beam was considered, with a length of $2169.28m$ and rollers placed where the abutments, piers and pylons are located in reality. Since the effect of friction and pendular bearings is of interest, any movement in the transversal out of plane direction was neglected and the same seismic action shown in Figure 29 along x was considered. To make the structure as similar as possible to the real one, the total mass was imposed equal and a spring was placed at one end of the beam, the stiffness of which was calibrated in order to have the same natural frequency of vibration in the longitudinal direction; moreover, structural Rayleigh damping was included, defined by the formula $C = \alpha M + \beta K$ and using coefficients calculated as $\alpha = 0.0578576$ and $\beta = 0.00932$ in both complete and simplified models.

Finally, just as previously discussed, both pendular bearings and friction can be modelled as springs (see Figures 4 and 5): to account for both effects at once, each roller (except for the abutments, which are not equipped with pendular bearings) is connected to two springs in parallel, one modelling the pendulum effect and the other the friction, with defining parameters which depend on the vertical force R_v acting on the support; specifically, as mentioned before, the stiffness of pendulum-modelling springs is equal to the vertical reaction divided by the radius of curvature of the support ($K_p = R_v/r$), while the friction-modelling springs have a very large initial stiffness (the value $K_f = 10^9 kN/m$ was chosen) and a plateau once the limit force, equal to the vertical reaction multiplied by the friction coefficient ($F_{el} = \phi R_v$), has been reached. Depending on the specific analysis to perform, each of these springs was either included in the model with its particular characteristics (detailed below) or deactivated,

thus controlling the behaviour of each support separately.
Given the great simplicity of the model, some important characteristics of the real structure cannot be accounted for; for instance, the end spring allows to calibrate the frequency of the structure, but only longitudinally and for one mode of vibration, which means that all the others with their relative frequencies are completely neglected. This translates in globally similar results, but any particular perturbation or oscillation in the behaviour cannot be forced to match the full model.
Nevertheless, the simplified model was calibrated considering the most important longitudinal mode of vibration of the complete bridge model, which was identified as the one characterized by the largest percentage of mass participating in the x direction. The value of such modal mass is the one which was attributed to the beam of the simplified model, considered uniformly distributed and equal to $M = 6.66 \cdot 10^7 kg$ for the first analyzed scenario, which is that of ideal rollers as supports (therefore with all springs modelling pendular bearings and friction effect deactivated); then, in order to have the same natural frequency, the modal stiffness had to be matched as well, hence the stiffness of the end spring was accordingly derived and set equal to $K = 52986.53 kN/m$.
Having thus defined the characteristics of the structure, in Figure 34 the resulting horizontal displacements with freely moving supports are reported, calculated in the midpoint of the deck and comparing real bridge and simplified model.

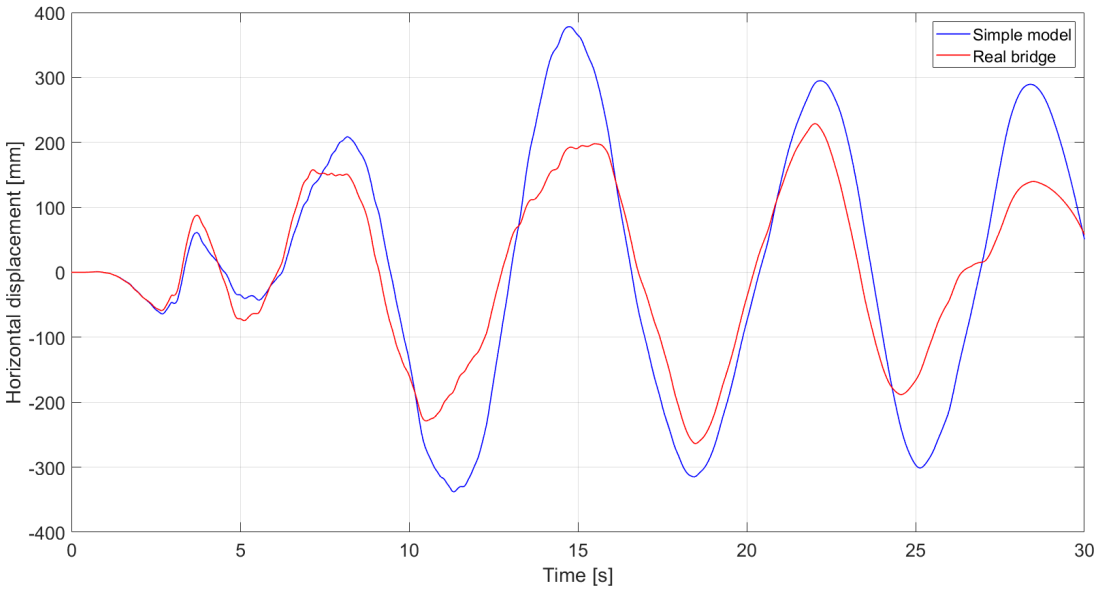

Figure 34: Comparison of the results of the two models - Freely moving supports

The outputs of the simplified model are rather close to the results obtained for the real structure, both in terms of values reached and of frequency of the oscillations; the same can be said for the variation of velocity and acceleration with time, shown in Figure 58 in the Appendix, which are even more similar, therefore the case with freely moving rollers as supports is well calibrated.

Subsequently, the pendulum effect was added in the model and taken into account by progressively activating the relative springs. However, the real bridge is a much more complex structure compared to the simplified model, characterized by many different modes of vibration, each with its modal mass and stiffness, which are related also to the cables and the pylons and in general are influenced by how the loads are distributed in the bridge; given that the simplified structure does not include such elements and the horizontal stiffness is governed by just one end spring, it is impossible to account for so many variables and, as mentioned before, the calibration of the model can match only the most important mode of vibration and its frequency. Because of this, it is clear that the results of the two models will not be perfectly matching, as was the case for the previous analysis (see Figure 34), but when the pendular bearings are added to the structure such difference becomes more prominent, as detailed afterwards.

To have a better tuning of the model and also more insight on their effect on the response of the structure, the pendular bearings were added progressively, starting from the outermost supports (E1 and A1) and then adding them two by two going inwards, until all piers and pylons are equipped with such bearings. Each time, the load distribution (therefore the modal mass) and overall stiffness of the structure change, therefore also the mass of the simplified model and the stiffness of the end spring were modified to match the frequency of the principal longitudinal mode of vibration. In order to match the frequencies, even the stiffness of the pendular bearings of the two pylons had to be taken smaller (specifically 25% of the real value), because their effect on the simplified model is much larger compared to the real bridge; on the other hand, the rest of the pendular bearings used on the piers were included with the same stiffness as the originals.

In Table 1, the values of support reactions R_v (derived from a static analysis of the real bridge under self weight only), radii of curvature r and pendular bearing stiffnesses K_p used in the simplified model are reported (note that the K_p for the pylons EP and AP is considered reduced in the model, as explained above); the friction coefficients ϕ and the elastic limits of the friction-modelling springs F_{el}, which will be added later, are

listed as well.

	R_v [kN]	r [m]	K_p [kN/m]	ϕ	F_{el} [kN]
E1	27909.96	10	2791.00	0.05	1395.50
E2	28864.99	5	5773.00	0.05	1443.25
E3	29302.23	3	9767.41	0.05	1465.11
E4	28200.96	2.25	12533.76	0.05	1410.05
EP	57510.38	2	7188.80 (25%)	0.05	2875.52
AP	57510.38	2	7188.80 (25%)	0.05	2875.52
A4	28306.26	2.25	12580.56	0.05	1415.31
A3	29167.43	3	9722.48	0.05	1458.37
A2	28898.93	5	5779.79	0.05	1444.95
A1	27897.84	10	2789.78	0.05	1394.89

Table 1: Data of the pendulum and friction modelling springs

Naturally, as previously discussed, the displacement of the structure influences the vertical reactions on the supports, which in turn change the stiffnesses and elastic limits of the springs, but the vertical forces on the rollers were assumed constant and so such differences were not accounted for.
The pendular bearings were therefore progressively added two by two in order to see their effect on the behaviour of the structure, starting with the piers E1 and A1 at the extremities of the bridge and proceeding inwards. In Table 2, the total mass of the simplified structure and the stiffness of the end spring for each of such analyses are reported, along with the resulting frequency of vibration.

	2 supports	4 supports	6 supports	8 supports	All supports
M [kg]	$6.36 \cdot 10^7$	$5.82 \cdot 10^7$	$4.07 \cdot 10^7$	$4.61 \cdot 10^7$	$3.26 \cdot 10^7$
K [kN/m]	46934.19	34205.54	51728.39	43335.88	6004.81
f [Hz]	0.145	0.149	0.234	0.240	0.253

Table 2: Longitudinal mass, spring stiffness and frequency of vibration of the simplified model for different numbers of pendular bearings included

In Figure 35, the results for pendular bearings on all supports are reported, comparing complete and simplified model.

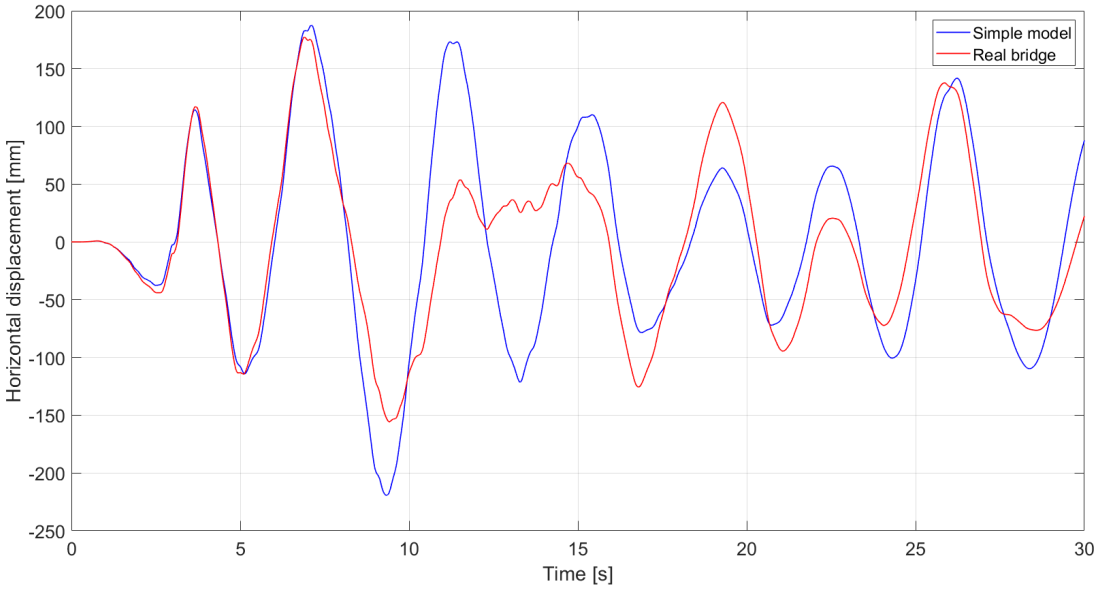

Figure 35: Comparison of the results of the two models - Pendular bearings only

The two models are shown to be in good agreement in this case as well, in terms of displacements but also of velocity and acceleration (shown in Figure 59 in the Appendix); therefore, the calibrated simplified model was used to assess the effect of friction, as detailed in the next chapter.

Moreover, given the differences between these results and those previously obtained for the case with freely moving supports, it is of interest to evaluate the changes in the outputs when different numbers of pendular bearings are accounted for: in Figure 36, the displacement variation calculated using the simplified model is reported for all the configurations that were analyzed, starting from freely moving supports and then adding the pendular bearings two by two, from the extremities inwards.

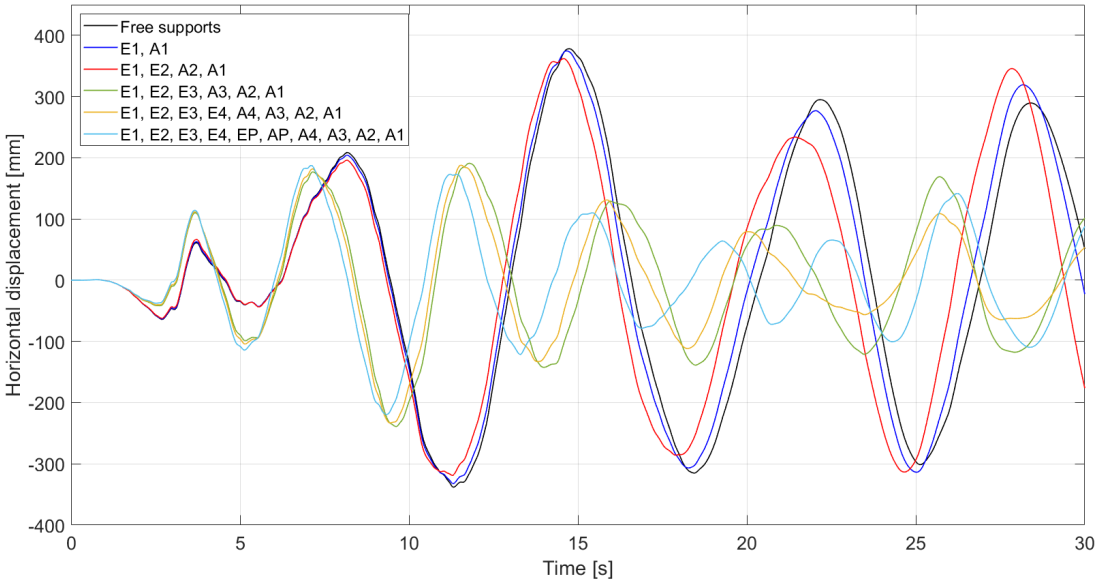

Figure 36: Horizontal displacements with different combinations of pendular bearings

As expected, the more pendular bearings are added to the structure, the more the displacements in absolute value are reduced; additionally, the movements are less violent and more controlled with more pendular bearings and both velocity and acceleration tend to go down in absolute value, as shown in Figure 60 in the Appendix.
The most apparent difference, however, is the stark increase in the frequency of the oscillations, particularly when going from four to six total pendular bearings on the supports, almost differentiating between two families of curves. The reason for a greater frequency is of course the larger stiffness of the structure, but such quite abrupt change is due to the other effect of pendular bearings, which is the increased modal mass (and therefore significance) of secondary modes of vibration: while at the beginning the first longitudinal mode is the most important one, defining the general shape of the response curve, and the successive ones are those causing the particular perturbations in the oscillations, when the pendular bearings are added all the frequencies are progressively increased; once the number of such supports is large enough, the second longitudinal mode of vibration becomes the most significant one, thus determining the macro-behaviour of the structure. The first mode of vibration is still important though, hence the difference between the two models, as only the frequency of the most significant mode can be matched.
Such phenomenon of increase of both natural frequency and modal mass of successive modes of vibration is evident by performing a Fourier transform of the time-

displacement curves, shown in Figure 37.

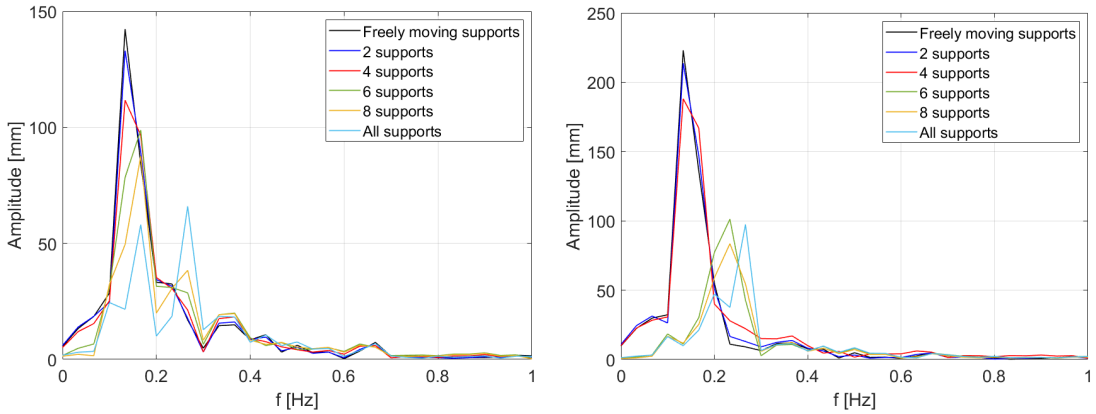

(a) Fourier transform of the complete model

(b) Fourier transform of the simplified model

Figure 37: Fourier transforms of the time-displacement curves of the two models for the various pendular bearing configurations

The peaks in the graphs above show the most prominent frequencies in the response of the structure: when no or few pendulum supports are included a single spike is visible, but as the pendular bearings increase in number not only the peaks move towards the right, but also the secondary modes of vibration become more important, increasing in amplitude and progressively leading to the development of a second spike. Given that, as already explained, the simplified model can match only one mode with its frequency, there is always one such peak in the Fourier transform, but the final results of displacement variation and oscillation frequency are quite accurately approximated.
Finally, as mentioned earlier, having thus realized and correctly calibrated a simplified model of the bridge, further analyses were conducted with it to assess the effect of friction on the behaviour of the structure. In order to define the mass and the stiffness of the end spring, a comparison with the complete model was necessary, for the various reasons previously mentioned, so that the frequency of vibration could be matched; with regards to the friction-modelling springs, on the other hand, such calibration is not necessary in order to obtain realistic results, since adding frictional supports will merely change the values of the displacements reached during the seismic event and not really affect the stiffness of the structure. This is shown in Figure 28 for instance, where adding the friction effect does not alter the natural period of vibration; therefore, the elastic limit for the friction-modelling springs was calculated as $F_{el} = \phi R_v$ (see Table 1).

The displacement in time was calculated first with purely frictional supports, then for the case with the combined action of friction and pendular bearings too; specifically, in the latter case the pendulum effect was considered always on all the supports, while friction was added progressively in the same fashion as the previous analysis.

3.4 Effect of the friction

Using the calibrated simplified model of the bridge, various analyses were carried out to evaluate the friction effect on the behaviour of the structure under the same seismic action.

First of all, the supports without pendular bearings have been considered with friction progressively, starting with the piers at the extremities (E1 and A1), then adding two more at the next analysis, and so on until all support are modelled considering the friction, but not the pendulum effect; the results of such calculations are reported in the graph in Figure 38. Since, as previously pointed out, the friction does not change the stiffness of the structure but only lowers its displacements, the characteristics in terms of total mass and stiffness of the end spring for this analysis were considered the same as those of the scenario with no pendular bearings and only ideal rollers as supports, given that the load distribution and natural period of vibration are the same.

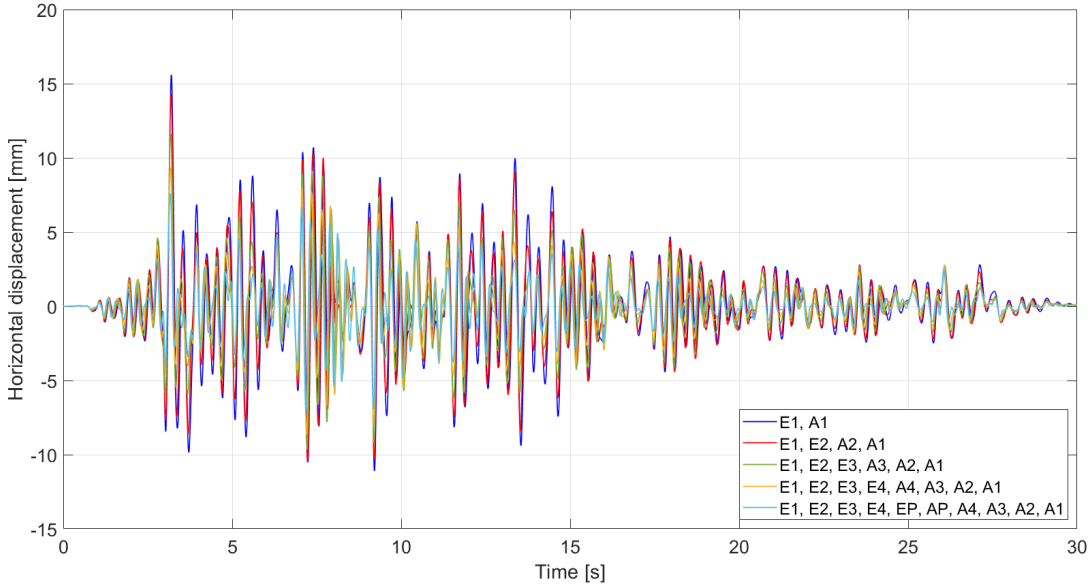

Figure 38: Displacements with friction effect on different numbers of supports

The more the supports modelled considering friction, the more the displacements are reduced in absolute value, as is perfectly reasonable, and the same observation can be made from the analysis of the variations of velocity and acceleration of the deck midpoint, displayed in Figure 61 in the Appendix; moreover, the frequency of the oscillations is now dictated not by the natural period of the structure itself, but by that of the earthquake.

What is quite striking is the difference between these results and those obtained previously without considering the friction effect, which were characterized by considerably larger oscillations, several times larger in fact; moreover, as mentioned before, these analyses were performed considering structural damping, therefore with time the oscillations would naturally die out, but when friction is considered the displacements are not only controlled very effectively, but they also dissipate much more quickly.

Subsequently, the supports all equipped with pendular bearings have been considered with friction progressively in the same way as above, starting with the piers at the extremities (E1 and A1), then adding the frictional behaviour to the two adjacent ones for the next analysis, and so on until all support are modelled with both friction and pendulum effect; the results of such calculations are reported in the graph in Figure 39. For the same reasons as before, the total mass and stiffness of the end spring for this analysis match those relative to the scenario with pendular bearings on all the supports.

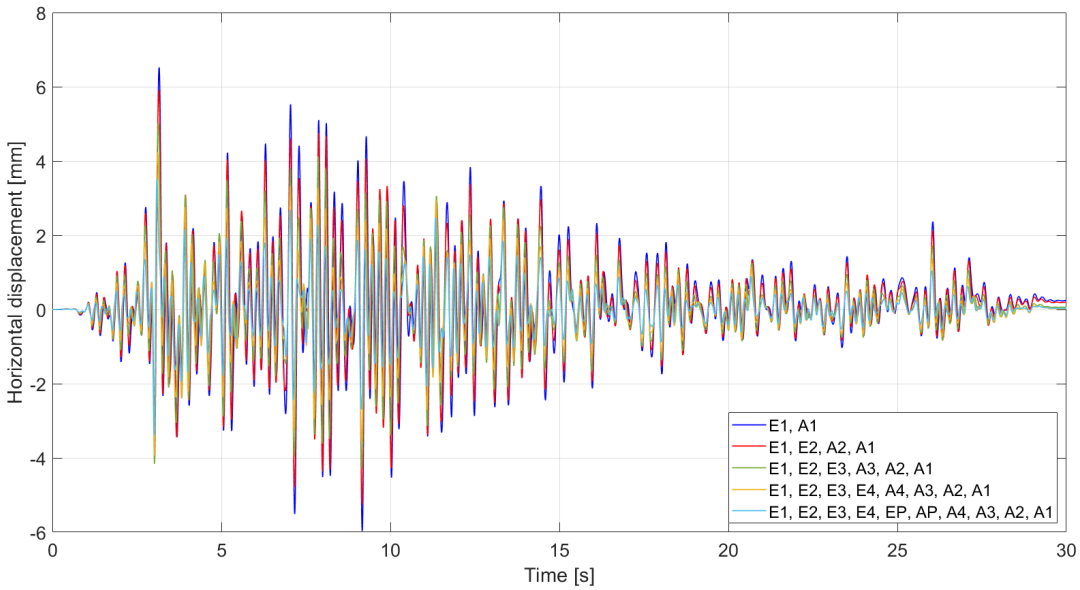

Figure 39: Displacements with friction effect on different numbers of supports equipped with pendular bearings

The same conclusions as for the previous analyses can be drawn here: the structure undergoes much smaller displacements compared to the pendular bearing only case and roughly two times smaller than those displayed in Figure 38 above, and in the last part of the earthquake event, when the ground acceleration is less violent, the bridge settles in an equilibrium configuration with some residual displacement. This is due to the fact that the friction contrasts any movement in any direction, and when the seismic action is reduced there comes a point where the recalling elastic force of the pylons and the pendular bearings equates the maximum frictional force which can be mobilized, resulting in the structure stopping its motion. As for the previous analyses, the variations of velocity and acceleration were calculated and are reported in Figure 62 in the Appendix, from which the same observations can be made.

Compared to the simple structure studied in the first part of this work, the Third Bosphorus Bridge shows a much more significant movement reduction when the effect of friction is included in the analysis: for instance, during the first part of the seismic action, whilst the smaller and less stiff structure oscillates reaching values of displacements comparable to those registered without the effect of friction (see Figure 31), the Third Bosphorus Bridge is always strongly influenced by it and undergoes tiny movements; this is of course related to it being supported on many more points, each contributing to increasing the limit friction force and very efficiently so, since the structure is starkly larger and heavier. However, both display a very quick dissipation of energy and reach displacements close to zero, with and without the contribution of pendular bearings: this behaviour shows that additional dynamic effects are present, a more detailed explanation of which is presented in the next chapter.

3.5 Comparison of the results

In order to better evaluate the effect on the results of pendular bearings and friction applied on all the supports, in Figure 40 a comparison between the displacements for the various cases (obtained using the simplified model) is reported, while velocity and acceleration variations are shown in Figure 63 in the Appendix.

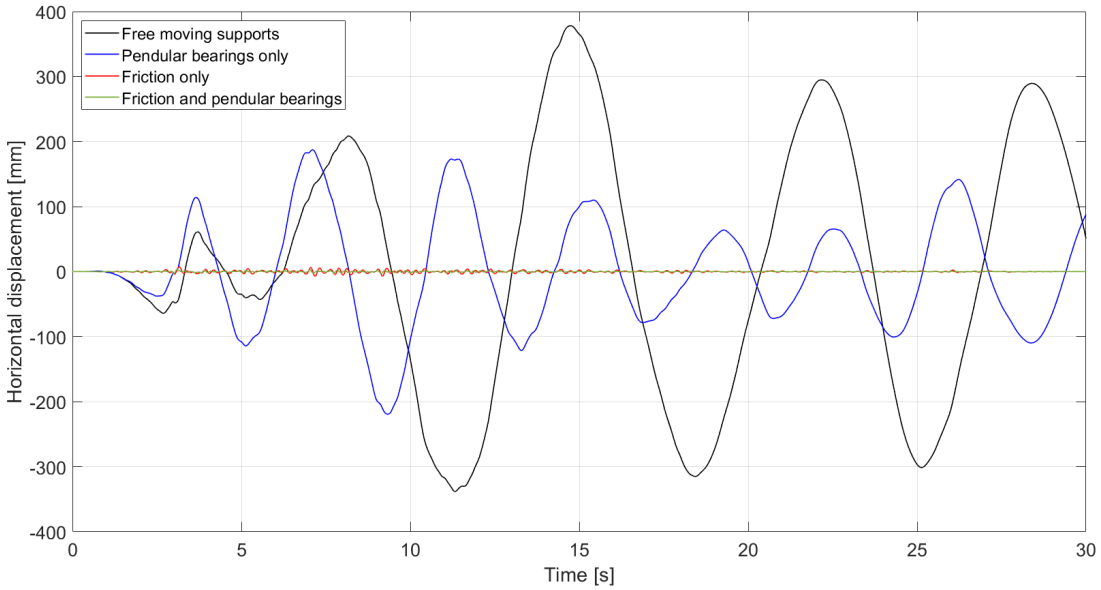

Figure 40: Comparison of the displacements for the various cases studied

While the complete absence of friction is not physically possible, the blue curve clearly shows the effect of the pendular bearings compared to the ideal case described by the black one: they reduce the displacements of the structure quite noticeably and increase both the stiffness (compared to the friction-less roller case) and the importance of secondary modes of vibration characterized by a larger natural frequency.
As previously mentioned, the frictional behaviour of the supports is very challenging to model, especially in a dynamic way, due to it being inherently nonlinear, therefore it is often neglected in such analyses, as for the Third Bridge over the Bosphorus; nevertheless, even a friction coefficient as small as 5% can make a huge difference, not only in reducing the displacements but also in the introduction of a very strong damping effect, capable of controlling the initial vibrations very quickly and leading the structure to an equilibrium configuration.
Such a strong contribution of the friction on the behaviour of the structure is caused mainly by two factors, the first one being the intensity of the earthquake: the seismic

action considered is not exceptionally severe, and the friction force is sometimes sufficient to oppose the movement, especially in the latter part of the event. However, this is not the case at first, when the earthquake does cause the supports to reach the friction limit and movement starts; nevertheless, the displacements are still very small and this is linked to the second defining factor, which is related to the period of vibration of both the bridge and the seismic action.

The bridge with no pendular bearings and considering its supports to be ideal rollers has a natural period $T \approx 7s$, which goes down to $T \approx 4s$ when the pendulum effect is considered; even if certainly not regular, the earthquake is a ground acceleration oscillating with a period $T = 0.2 \div 0.3s$, which is considerably smaller compared to the structure. This causes the supports to move back and forth and alternate between stick and slip phases very quickly, not giving the bridge enough time to adjust to the new configuration, therefore the displacements are greatly reduced even when the friction force is overcome.

Some analyses were conducted neglecting the frictional effect to show important results, such as the pendulum effect, but in reality friction is of course always present in some measure and possibly even twice or three times stronger than what considered until now; given the great importance that it has on the behaviour of a structure with the characteristics of the Third Bosphorus Bridge in terms of mass and stiffness, the contribution of the pendular bearings on the evolution of displacements under the action of a regular earthquake is rather negligible. In fact, this happens even for stronger seismic actions, as the driving factor is the frequency: to have a better comparison, the same calculations were performed under a more severe earthquake as well and both the accelerogram and the resulting displacements are shown in Figure 41, while the outputs for velocity and acceleration are displayed in Figure 64 in the Appendix.

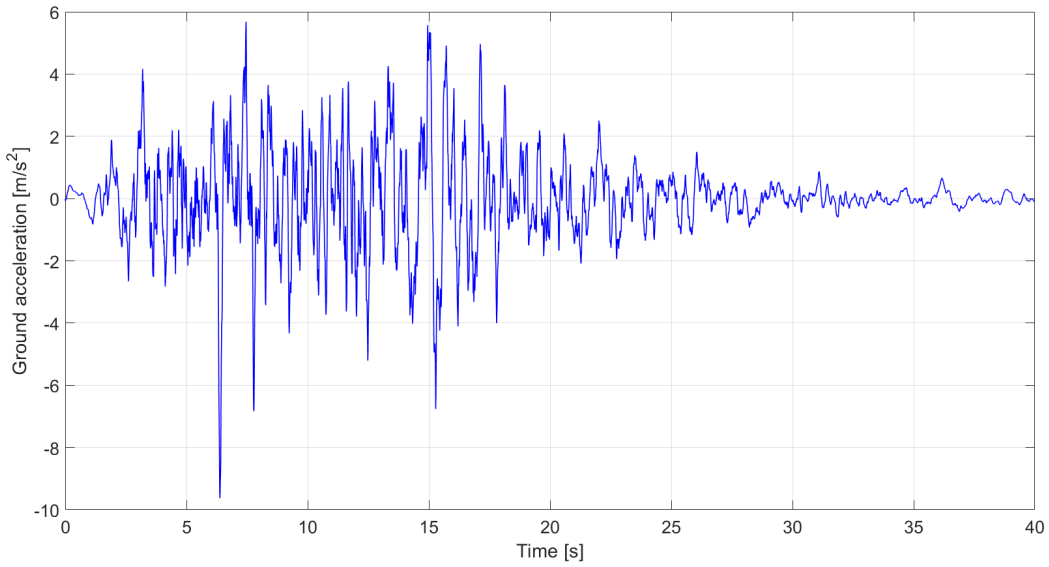

(a) Chosen ground acceleration of a stronger earthquake

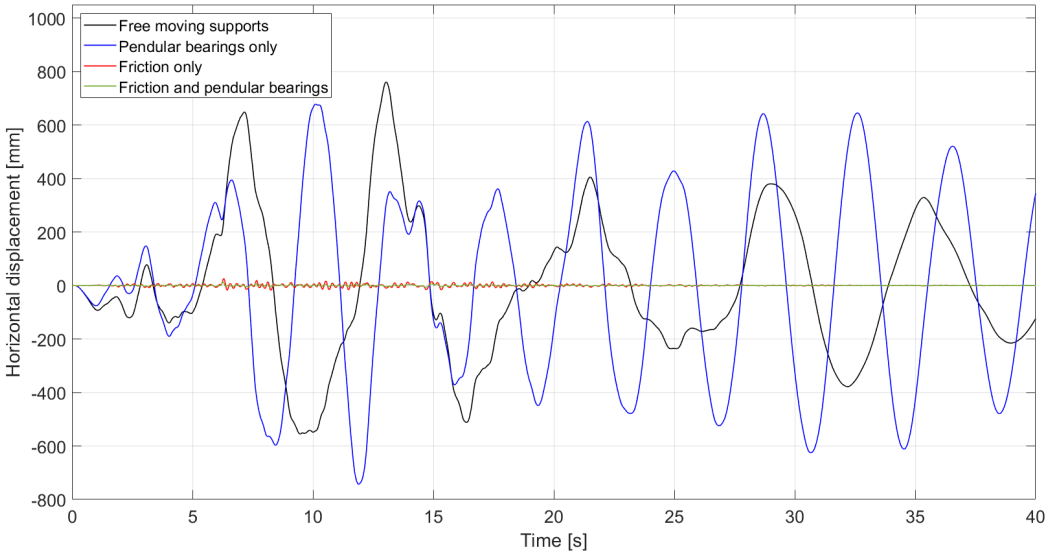

(b) Comparison of the displacements for all the scenarios

Figure 41: Accelerogram and final displacement results for a more severe seismic action

The seismic action is considerably stronger than the one previously considered, which results in noticeably larger displacements in absolute value; even though the same applies for the cases accounting for friction, it is apparent that the reduction in the amplitude of the oscillations is still very large, as previously observed, due to the great importance that the difference in frequency has on the final behaviour.

This of course is not to say that pendular bearings have no use at all: firstly, the Third Bosphorus Bridge is used also for railway transit, therefore it is subjected to quite significant traffic loads. Such external actions are very different in terms of duration and frequency compared to a seismic event, and in fact they were originally modelled as static forces in the design phase of the structure; as a result, no dynamic effects take place and the longitudinal displacement depends entirely on the magnitude of the applied load, for which the pendulum effect of the supports does contribute quite significantly, as was accordingly calculated.
Secondly, while the friction can provide damping and movement control in its own right, it has a rather undesirable side effect, which is the permanence of residual displacements after a given event, causing the structure to be unable to return to its original equilibrium configuration. The implementation of pendular bearings, on the other hand, can help to counter this: since any movement in the horizontal direction causes also uplift of the structure as it slides along the curved surface of the support, an elastic recalling force is always present and it will tend to bring the bridge back to its original position without the need for any external intervention.
Finally, what is important to keep in mind is that, even though over the course of this work they were compared to the ideal case of rollers with no inherent stiffness, in reality the pendular bearings would be installed as substitutes to some other kind of support, such as pot bearings or elastomeric bearings with neoprene pads, which would have a completely different behaviour; in fact, compared to these other kinds of bearings, the pendulum supports would actually decrease the overall stiffness of the structure and allow more movements, not the other way around, in order to decouple the pylons and the deck, provide to the latter a longer period of vibration and thus lessen the stresses on the bridge caused by the ground shaking of the earthquake. If the structure was equipped with alternative types of bearings, it would have quite a larger stiffness and natural frequency, so much so that it could be so close to that of the seismic action to greatly reduce the effectiveness of friction, for the same reasons as explained above, and actually result in more violent oscillations compared to the scenarios presented previously.
In light of this, the pendular bearings installed on the supports can help in the redistribution of loads and in taking a part of the efforts, to the benefit of the other parts of the bridge, such as pylons and cables; this is quite effectively visualized by monitoring the force in the various springs, especially the end spring.

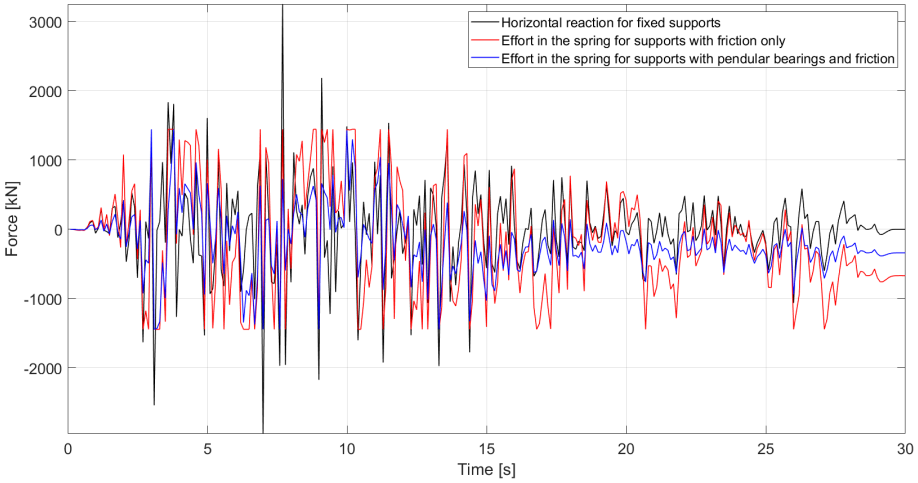

(a) Support E2

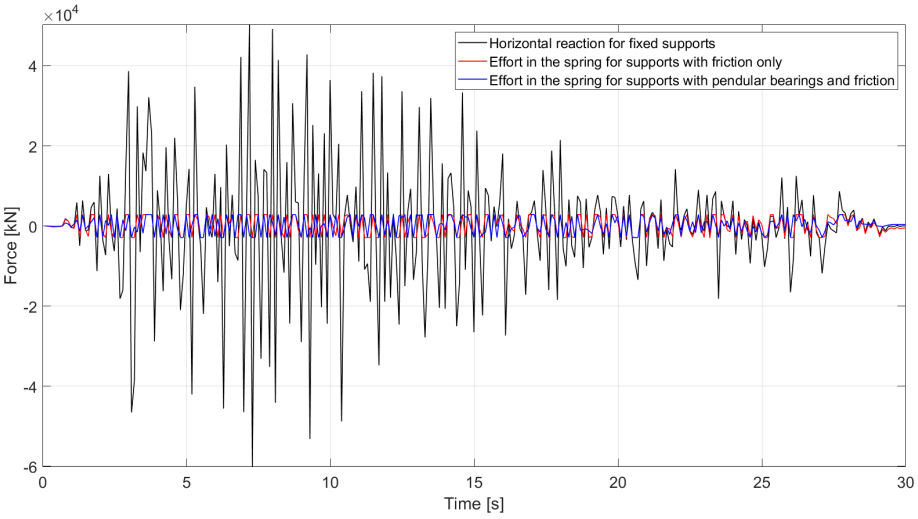

(b) Support EP

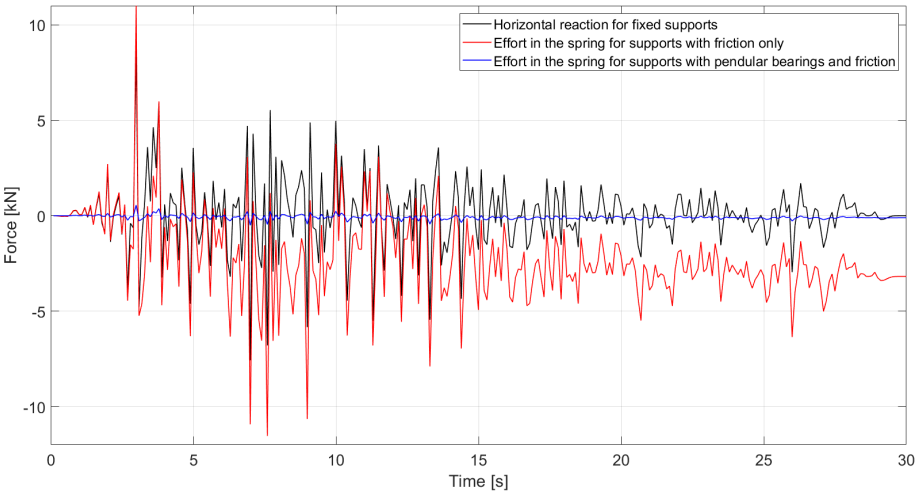

(c) End spring

Figure 42: Effort in some support springs and in the end spring of the model, comparing three different scenarios

In Figure 42, the evolution of the efforts in some of the springs is shown for the cases of supports with friction only and with both friction and pendulum effect, compared to the case of fully fixed support as well, which can give an idea of a scenario in which a much stiffer bearing is used.
Clearly, the fully fixed supports is just a limit case to compare the other scenarios to and it would not be very feasible in reality, as evidently the bridge, not being able to undergo displacements, would suffer tensions in the deck during the earthquake and, as shown in the graphs above, the piers and pylons would be subjected to quite larger forces in order to ensure no movements; moreover, any thermal action would result in very high stresses due to the impossibility of the deck to expand.
When the supports are allowed to move but are modelled with friction, on the other hand, they provide some resistance up to their specific limit force; hence, the horizontal reaction imparted by the supports, and therefore the resulting stress transferred to pylons and piers, is limited with respect to the previous scenario.
Given that the recalling force of pendular bearings is proportional to the displacement, the difference between blue and red curves for the individual supports is not too large, depending on the specific one under examination, due to the fact that the movements of the bridge are very small, as detailed previously; however, the end spring, which represents the longitudinal stiffness provided by all those parts of the structure which were not included in the simplified model (specifically piers, pylons and cables), does display quite a significant difference between these two cases, as the stresses are greatly reduced in absolute value. Therefore, these results show that the introduction of pendular bearings has a noticeable impact on the global distribution of loads in the structure: thanks to their decoupling of the supports and the deck itself, they provide a substantial effect of shock absorption, which is of critical importance during seismic events.

4 Conclusions

The object of this work was to perform a general study of the behaviour of structures under the action of forces variable in time, during earthquake events for instance, which constitute a critical and greatly important scenario in the field of modern Civil Engineering. Specifically, the work was centered around pendular bearings, which are a type of support used as shock absorbers and often implemented for non regular structures potentially susceptible to the effect of seismic actions, such as large bridges. Given the numerical challenges related to the inclusion of friction between the moving parts of such objects, since their behaviour becomes nonlinear, it is often neglected when performing dynamic analyses; however, as was shown in the course of this work, the frictional effect does indeed play a very important part in the global response of the structure and can affect the results quite considerably.

The problem was preliminarily analyzed through calculations performed on a simple academic structure, fixed to the ground and equipped with a roller; such roller was firstly considered as an ideal support with no horizontal resistance, but afterwards both the friction and pendulum effect were added, comparing an analytical model with a software model created using FineLg. Moreover, the first analyses were carried out statically, followed by dynamic calculations as well, where the external horizontal force was applied varying with time in a sinusoidal fashion and with different periods of oscillation. What was found was that, compared to the ideal slider scenario, the pendulum effect increases the stiffness of the structure quite effectively and is responsible for a large reduction of displacements, both statically and dynamically, while friction, considered with a coefficient $\phi = 5\%$, had a less important contribution in that regard; however, it causes the structure to stop moving for a period of time whenever the direction of motion is switched, creating a stick-slip behaviour.

Afterwards, a seismic analysis was performed as well using the analytical model, through which another significant role of friction was demonstrated, which is a strong damping effect: the oscillations are controlled very effectively at the beginning of the earthquake and then almost die out, with the displacements retaining very small values throughout the remaining part of the seismic event. However, the study of such a simple structure is useful only to a certain extent, therefore a more realistic case was considered.

The second part of this work was centered around the calibration of a simplified model

of a real structure, the Third Bridge over the Bosphorus located in Turkey, so that it could be used to perform nonlinear dynamic calculations aimed at better assessing the effect of friction on the behaviour during an earthquake and comparing it to the pendular bearing only case, which was the configuration considered during the design of the actual bridge under seismic action.
The simplified model was realized using a simple steel beam, as long as the real deck, on a total of twelve sliding supports, which correspond to the two abutments, the eight piers and the two pylons; given that any horizontal displacement is accompanied also by a vertical uplift, the pendular bearings were installed on all supports except for the two abutments. The stiffness provided by the pylons and cables was modelled using a single spring on one end of the beam, while the pendulum effect and friction were accounted for on each support using two springs in parallel: the resulting behaviour is that of an equivalent spring with a bilinear constitutive law and kinematic hardening.
The results show that adding pendular bearings increases both the stiffness and the relevance of secondary modes of vibration characterized by a shorter natural period, hence the displacements in absolute value decrease quite significantly compared to the ideal roller scenario. The friction effect, on the other hand, changes the output dramatically, as the oscillations almost drop to zero: the reason for this was identified as being the difference between the natural frequencies of structure and earthquake, which leads the seismic force to change so rapidly that its effect on the bridge is very tiny, with and without pendular bearings.
Nevertheless, this particular type of supports is in reality not implemented to substitute ideal sliders: compared to more traditional solutions, pendular bearings actually decouple deck and pylons and decrease the stiffness and frequency of vibration of the structure, creating a large difference in natural period between bridge and seismic action. Moreover, allowing the deck quite a lot of movement compared to other solutions, they help with load distribution and shock absorption, lowering the stresses in other elements of the bridge, such as the pylons and the cables; finally, the elastic recalling force they provide helps the structure to automatically center itself after a movement from its equilibrium position, which is useful as friction tends to act to opposite effect.
In view of what was developed, pendular bearings constitute a very effective solution for bridges under seismic action, as they decouple the supports and the deck and provide excellent load distribution and shock absorption; in such a scenario, friction can indeed play a crucial role, making its inclusion in the model extremely important.

Bibliography

Greisch (2014) *Actions - Seism*. Northern Marmara motorway (including 3rd Bosphorus Bridge) construction, operation and transfer of section Odayeri - Paşaköy (including 3rd Bosphorus Bridge) through BOT model - Design report

Greisch (2014) *Analysis results - Service life - Seismic analysis*. Northern Marmara motorway (including 3rd Bosphorus Bridge) construction, operation and transfer of section Odayeri - Paşaköy (including 3rd Bosphorus Bridge) through BOT model - Design report

Greisch (2016) *Pendular bearings - Longitudinal displacements with friction (UIC trains)*. Northern Marmara motorway (including 3rd Bosphorus Bridge) construction, operation and transfer of section Odayeri - Paşaköy (including 3rd Bosphorus Bridge) through BOT model - Technical report

Abdel Seed F. K. et al. (2013) *Dynamic Non - Linear Behaviour of Cable Stayed Bridges Under Seismic Loadings*. JES. Journal of Engineering Sciences

Almazán J. L., De la Llera C., Inaudi J. A. (1998) *Modelling aspects of structures isolated with the frictional pendulum system*. Earthquake Engineering Structural Dynamics

Castaldo P., Palazzo B., Della Vecchia P. (2015) *Seismic reliability of base-isolated structures with friction pendulum bearings*. Engineering Structures

Castiglioni C. et al. (2018) *Earthquake-Induced pallet sliding in industrial racking systems*. Politecnico di Milano, Department of Architecture, Built Environment and Construction Engineering, Milan, Italy

Denoël V. (2001) *Calcul sismique des ouvrages d'art*. Master Thesis, ULg

Denoël V., Degée H. (2005) *Cas particulier d'étude analytique de l'élément à frottement*. Internal report 2005-1, Department M&S

Denoël V., Degée H. (2006) *An investigation on the sliding of pallets on storage racks subjected to earthquake*. Proceedings of the 7th National Congres on Theoretical and Applied Mechanics

Denoël V., Degée H. (2007) *Numerical modelling of storage racks subjected to earthquake*. Proceedings of COMPDYN 07, Conference on Computational Dynamics

Denoël V., Degée H., Castiglioni C. (2008) *Seismic Behaviour of Storage racks made of Thin-Walled Steel members*. Proceedings of the VII European Conference on Structural Dynamics, Eurodyn 2008, Southampton, UK

Drozdov Yu. N., Nadein V. A., Puchkov V. N. (2007) *Influence of Earthquake Parameters on Tribological Behavior of Frictional Pendulum Bearings (Seismic Dampers)*. Probl. Mashinostr. Nadezh. Mashin

Eröz M., DesRoches R. (2008) *Bridge seismic response as a function of the Friction Pendulum System (FPS) modeling assumptions*. Engineering Structures

Fagà E., Ceresa P., Nascimbene R., Moratti M., Pavese A. (2015) *Modelling curved surface sliding bearings with bilinear constitutive law: effects on the response of seismically isolated buildings*. Materials and Structures

FineLg (2021) *User's Manual*. Greisch Info – Department ArGEnCo – ULg

Henriques J., Morelli F., Vandoren B., Salvatore W., Degée H. (2016) *Efficiency of seismic isolation on industrial plants - case study of a gas tank*. Proceedings of the VII European Congress on Computational Methods in Applied Sciences and Engineering, M. Papadrakakis, V. Papadopoulos, G. Stefanou, V. Plevris (Editors), Crete Island, Greece

Karoumi R. (1999) *Some modeling aspects in the nonlinear finite element analysis of cable supported bridges*. Computers & Structures

Karoumi R. (2000) *Modeling of Cable Stayed Bridges for Analysis of Traffic Induced Vibrations*. Proceedings of IMAC-XVIII, Conference on Structural Dynamics

Keri L. R., Chopra A. K. (2003) *Estimating the seismic displacement of friction pendulum isolators based on non-linear response history analysis*. National Science Foundation

Kumar M., Whittaker A. S., Constantinou M. C. (2014) *Characterizing friction in sliding isolation bearings*. Earthquake Engineering Structural Dynamics

Mazza F., Sisinno S. (2017) *Nonlinear dynamic behavior of base-isolated buildings with the friction pendulum system subjected to near-fault earthquakes*. Mechanics Based Design of Structures and Machines

Mokha A., Constantinou M. C., Reinhorn A. M., Zayas V. A. (1991) *Experimental Study of Friction-Pendulum Isolation System*. Journal of Structural Engineering

Suren C., Cai C. (2004) *Coupled vibration control with tuned mass damper for long-span bridges*. Journal of Sound and Vibration

Thai H., Seung-Eock K. (2011) *Nonlinear static and dynamic analysis of cable structures*. Finite elements in analysis and design

Wang Y., Chung L., Liao W. (1998) *Seismic response analysis of bridges isolated with friction pendulum bearings*. Earthquake Engineering Structural Dynamics

Wang Y., Teng M., Chung K. (2001) *Seismic isolation of rigid cylindrical tanks using friction pendulum bearings*. Earthquake Engineering Structural Dynamics

Warn G. P., Whittaker A. S. (2004) *Performance estimates in seismically isolated bridge structures*. Engineering Structures

Yang F. (1996) *Vibrations of cable-stayed bridges under moving vehicles*. Ph. D. Thesis, ULg

Appendix

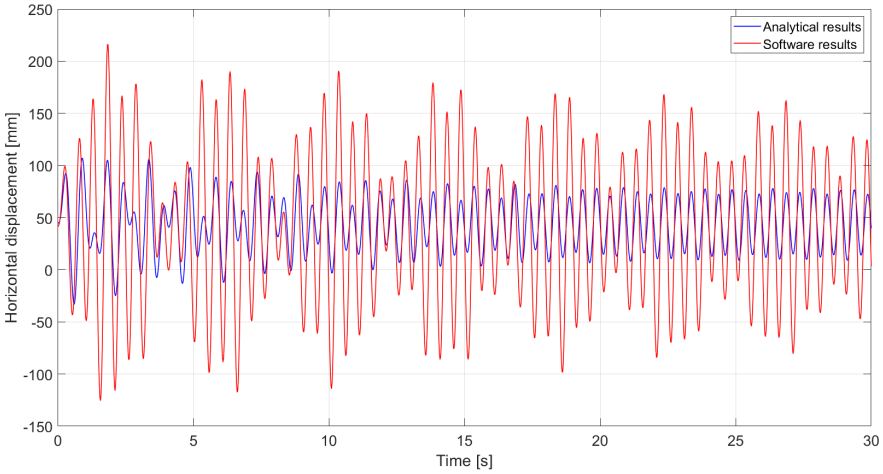

(a) Displacement variation

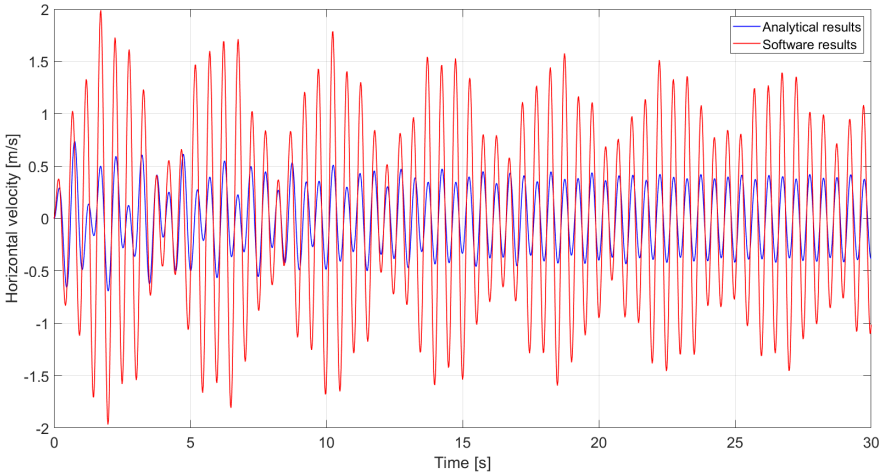

(b) Velocity variation

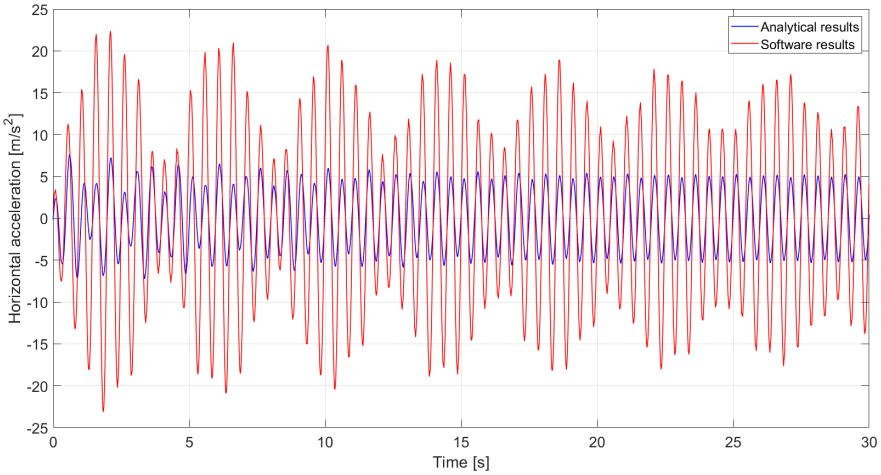

(c) Acceleration variation

Figure 43: Variation of displacement, velocity and acceleration at the moving support for a period of the applied force T = 0.5s - Friction and pendular bearing

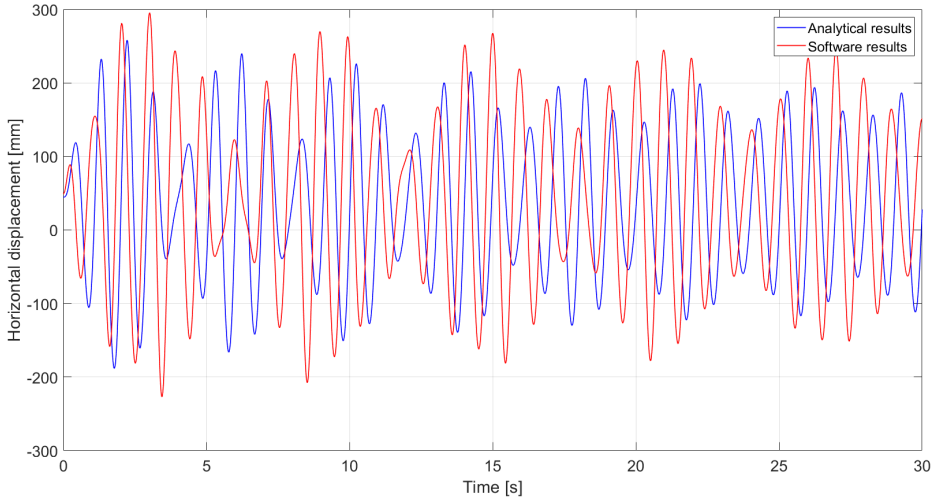

(a) Displacement variation

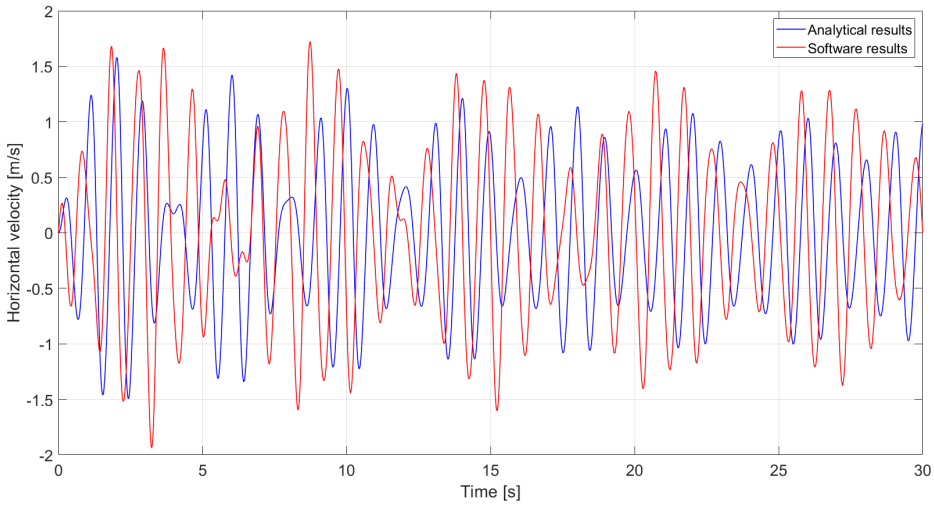

(b) Velocity variation

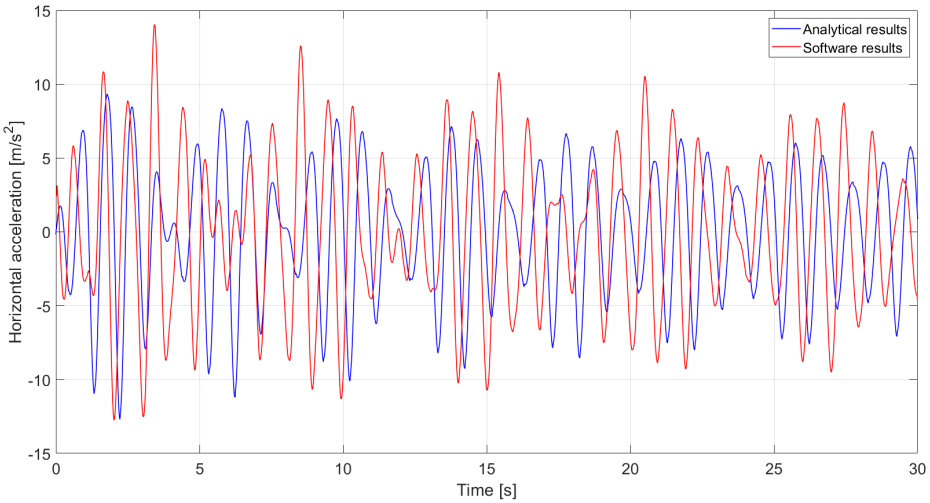

(c) Acceleration variation

Figure 44: Variation of displacement, velocity and acceleration at the moving support for a period of the applied force T = 1s - Friction and pendular bearing

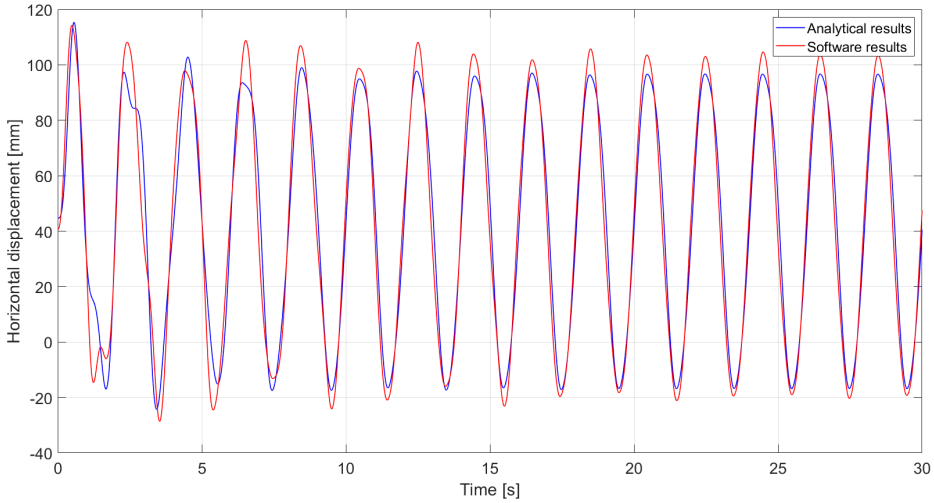

(a) Displacement variation

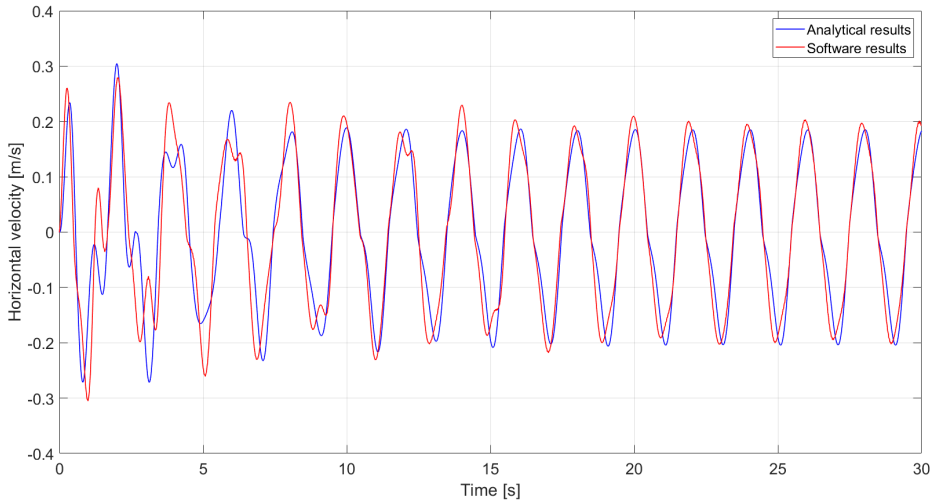

(b) Velocity variation

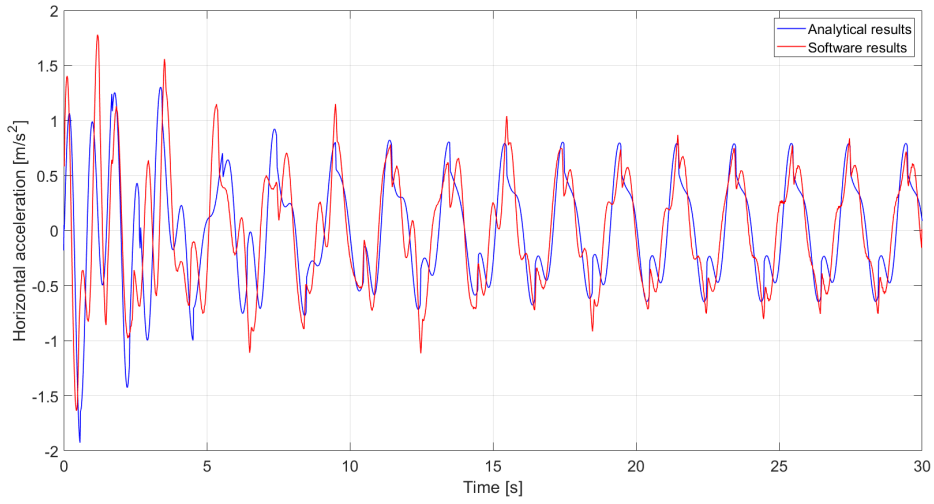

(c) Acceleration variation

Figure 45: Variation of displacement, velocity and acceleration at the moving support for a period of the applied force T = 2s - Friction and pendular bearing

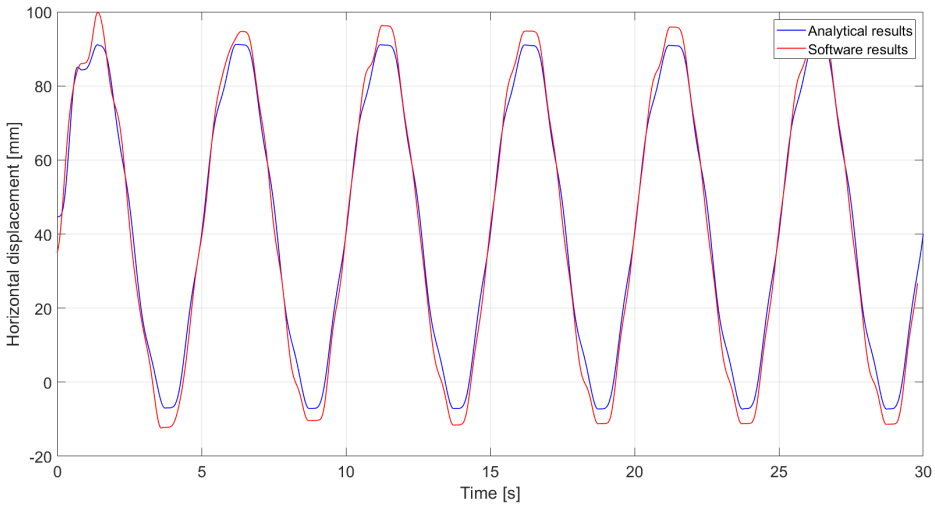

(a) Displacement variation

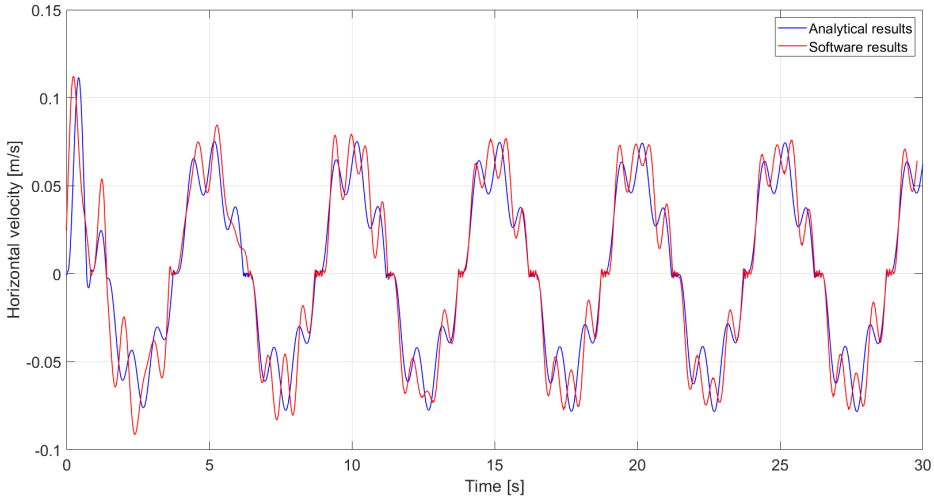

(b) Velocity variation

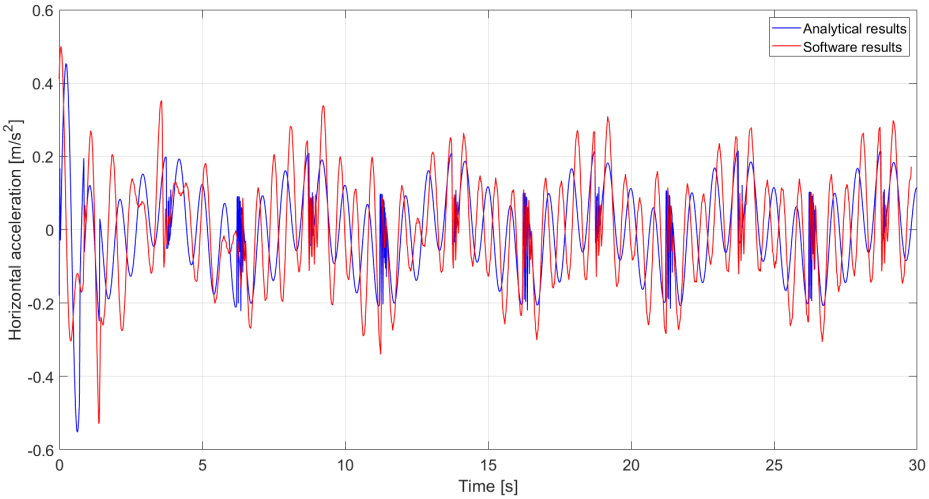

(c) Acceleration variation

Figure 46: Variation of displacement, velocity and acceleration at the moving support for a period of the applied force T = 5s - Friction and pendular bearing

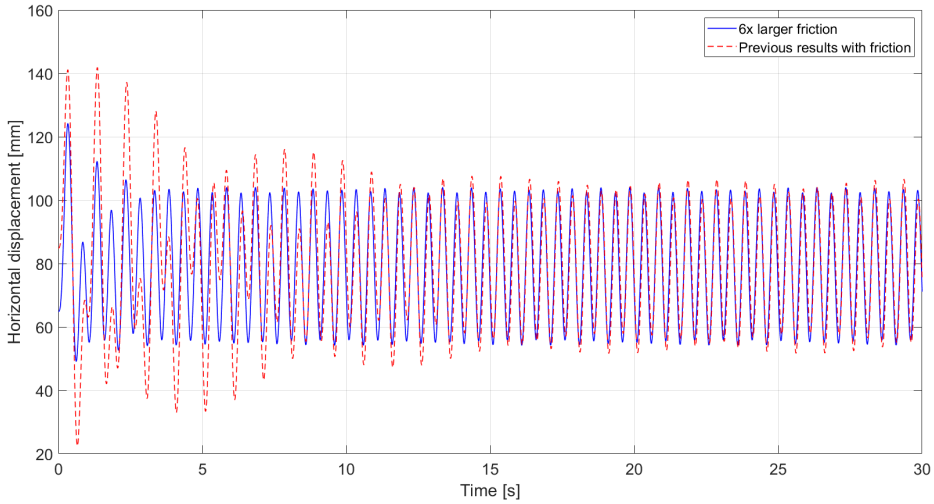

(a) Displacement variation

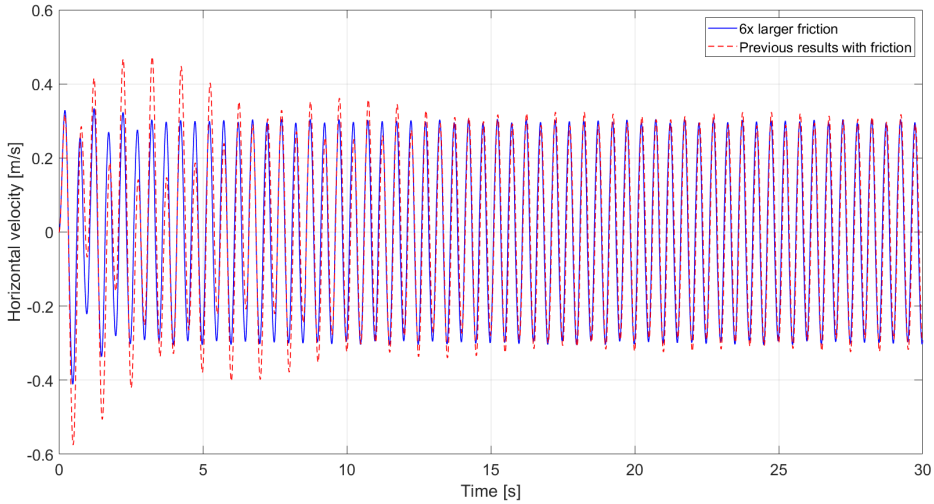

(b) Velocity variation

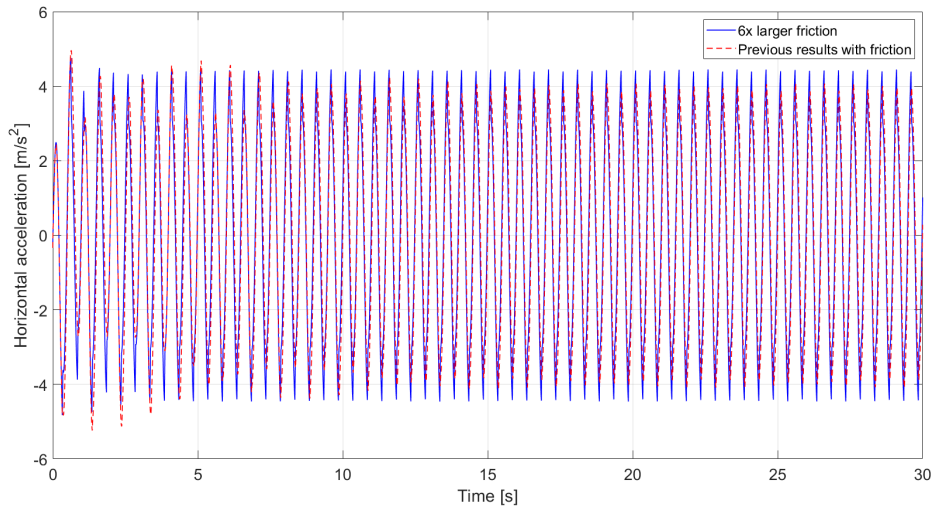

(c) Acceleration variation

Figure 47: Comparison of displacement, velocity and acceleration variations at the moving support for a period of the applied force T = 0.5s - Friction only

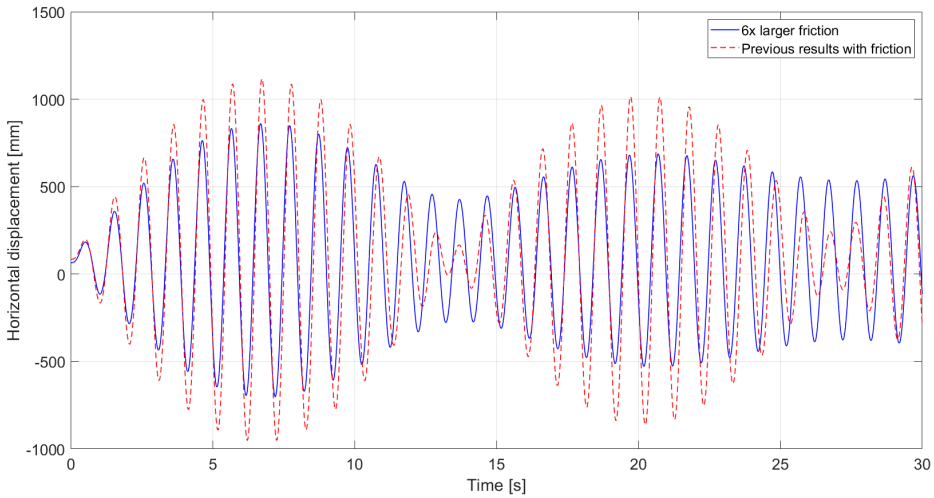

(a) Displacement variation

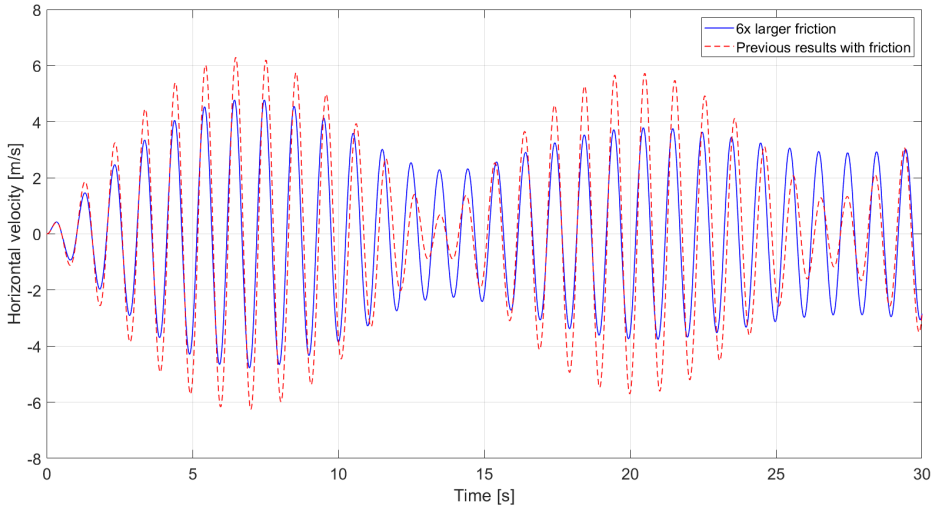

(b) Velocity variation

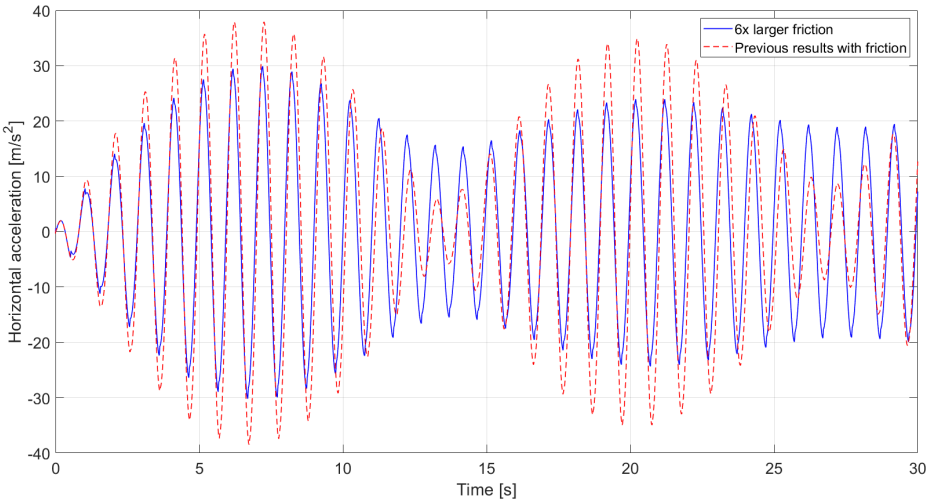

(c) Acceleration variation

Figure 48: Comparison of displacement, velocity and acceleration variations at the moving support for a period of the applied force T = 1s - Friction only

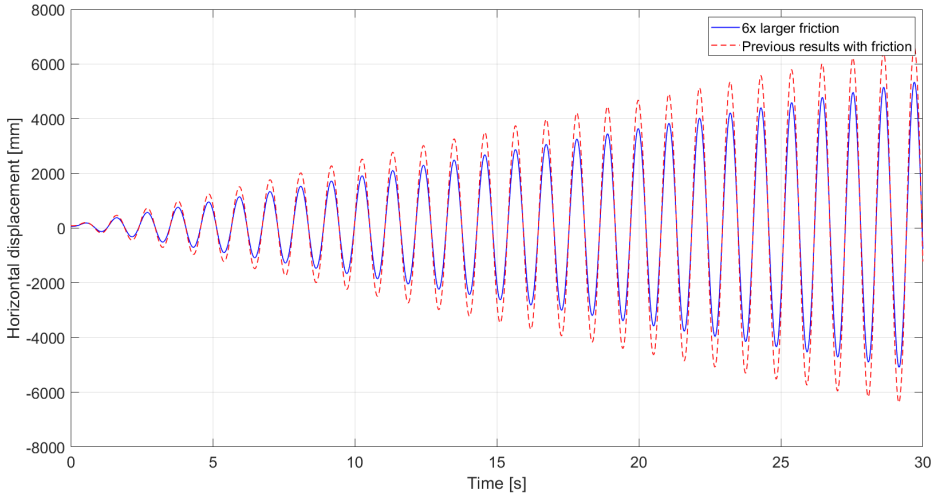

(a) Displacement variation

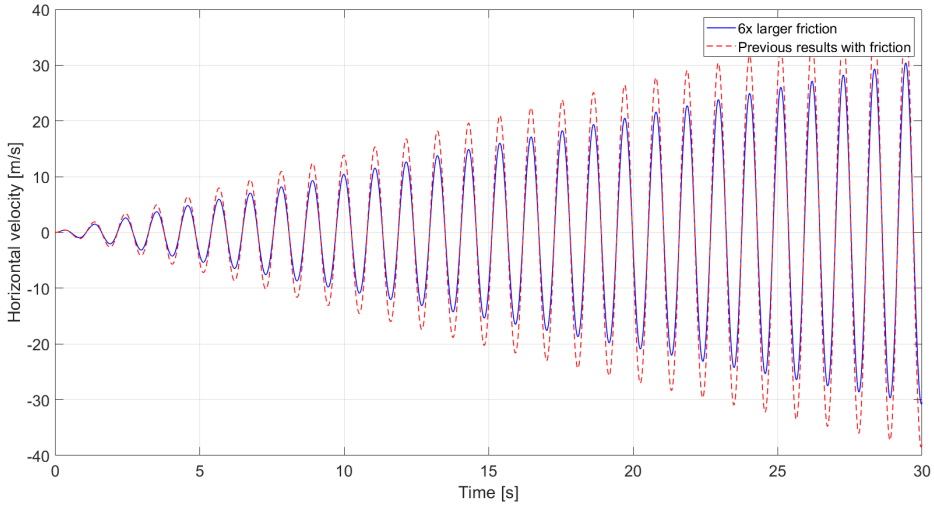

(b) Velocity variation

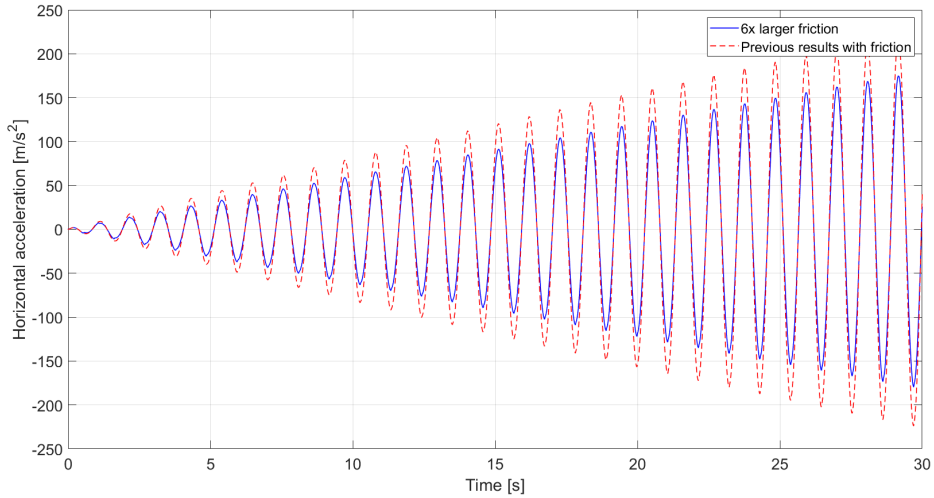

(c) Acceleration variation

Figure 49: Comparison of displacement, velocity and acceleration variations at the moving support for a period of the applied force T = 1.08s - Friction only

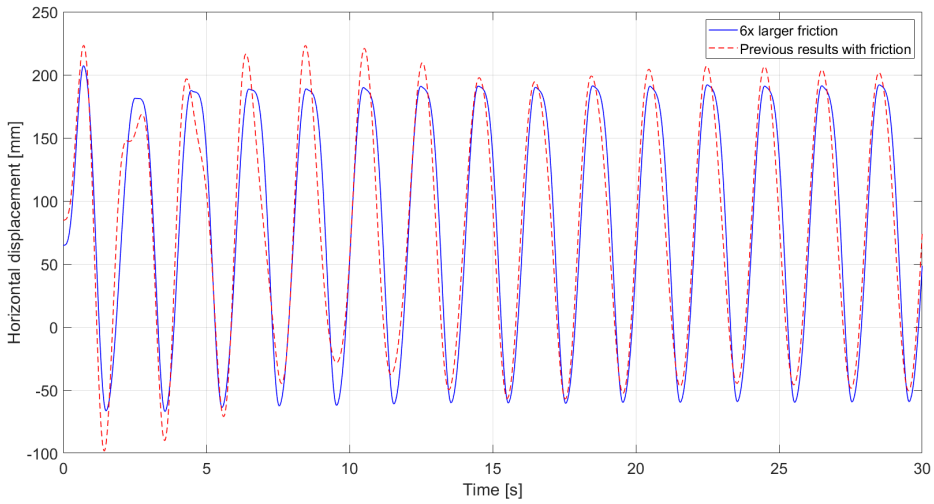

(a) Displacement variation

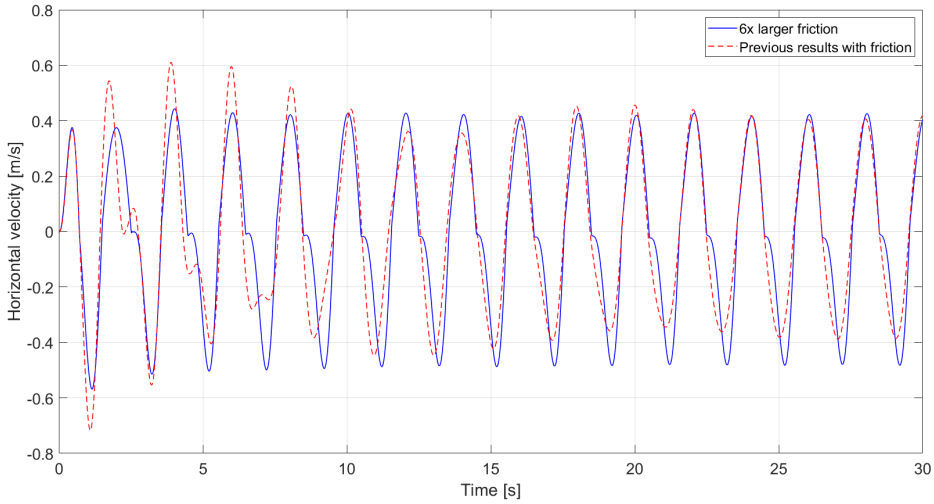

(b) Velocity variation

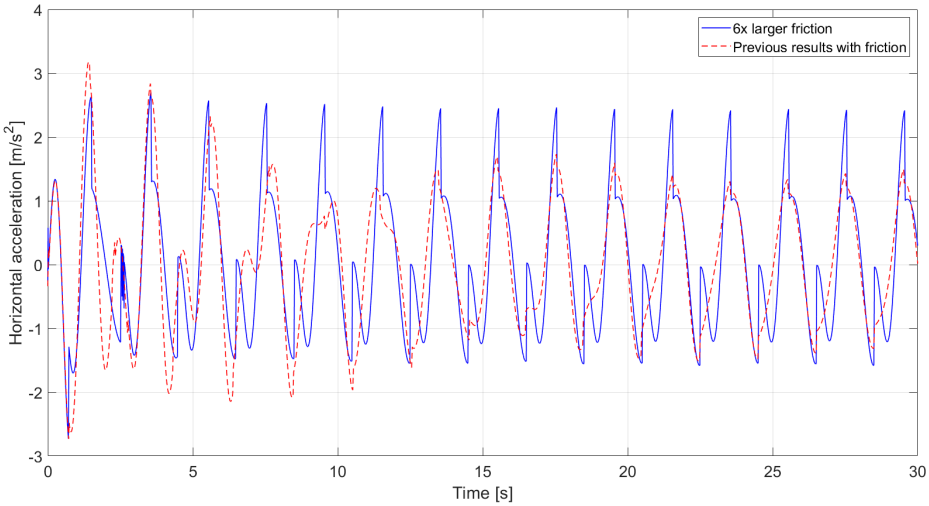

(c) Acceleration variation

Figure 50: Comparison of displacement, velocity and acceleration variations at the moving support for a period of the applied force T = 2s - Friction only

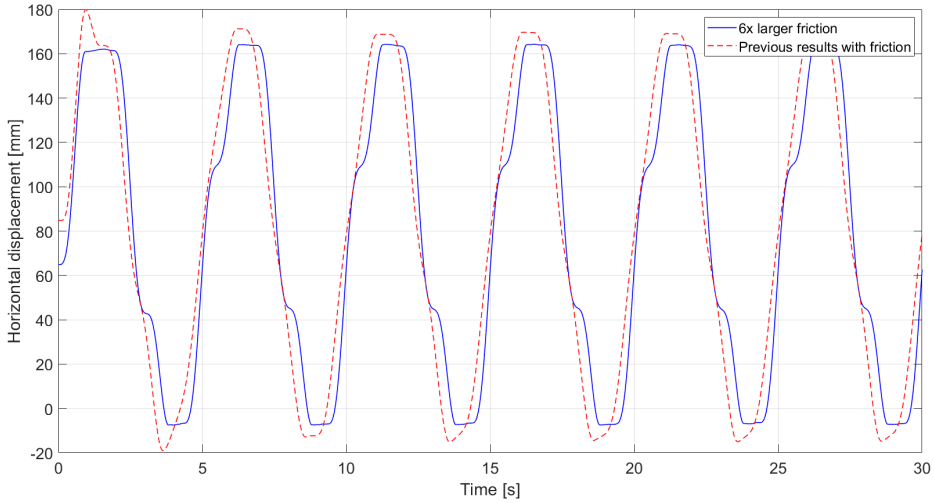

(a) Displacement variation

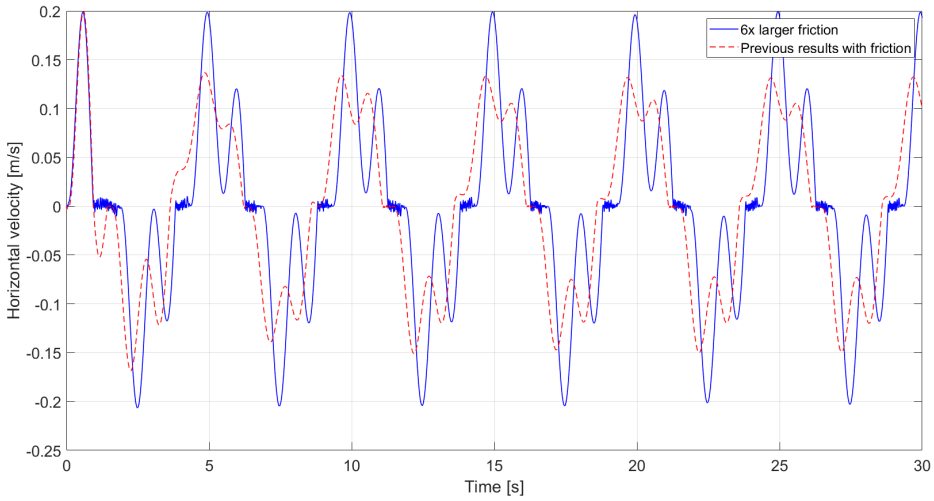

(b) Velocity variation

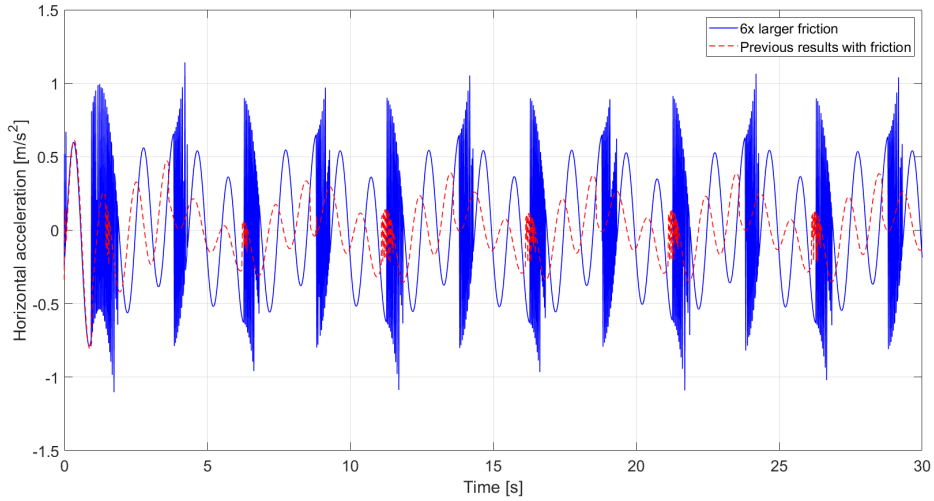

(c) Acceleration variation

Figure 51: Comparison of displacement, velocity and acceleration variations at the moving support for a period of the applied force T = 5s - Friction only

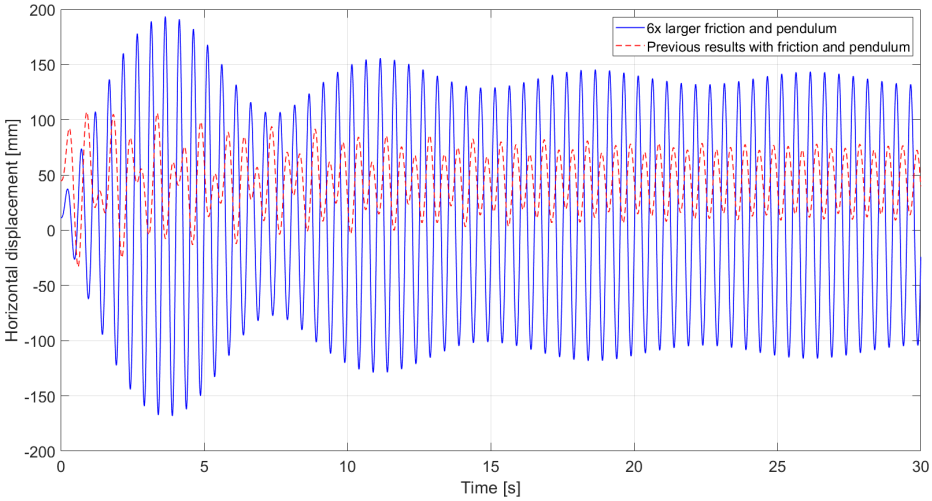

(a) Displacement variation

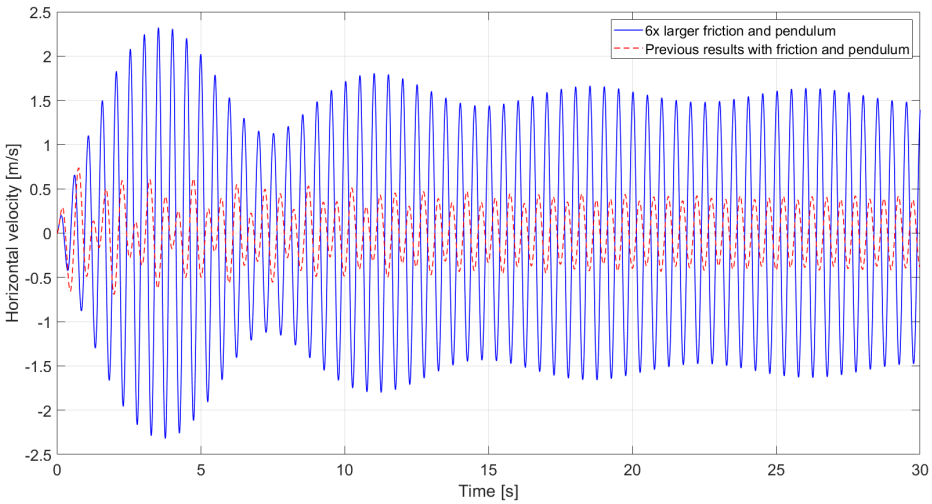

(b) Velocity variation

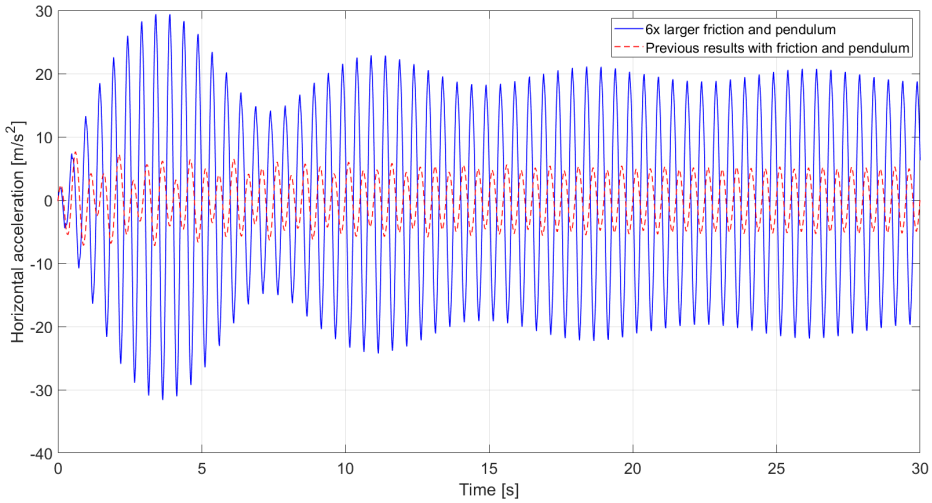

(c) Acceleration variation

Figure 52: Comparison of displacement, velocity and acceleration at the moving support for a period of the applied force T = 0.5s - Friction and pendular bearing

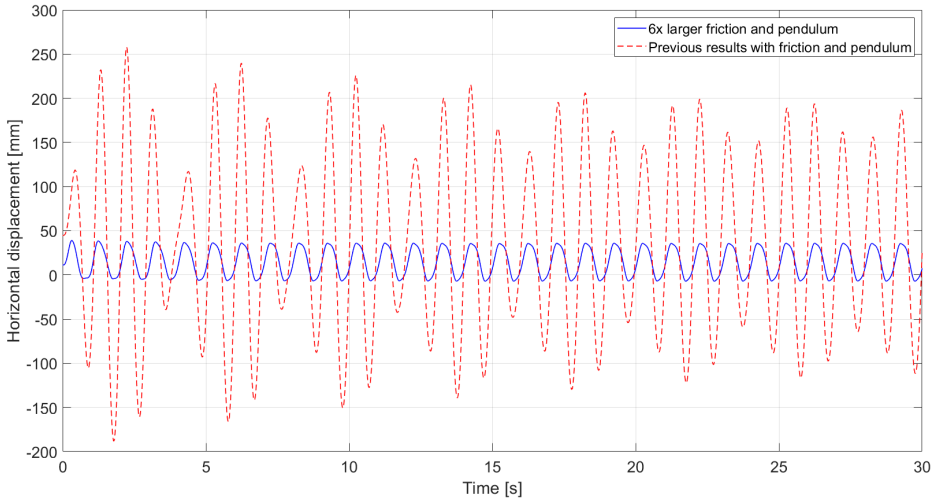

(a) Displacement variation

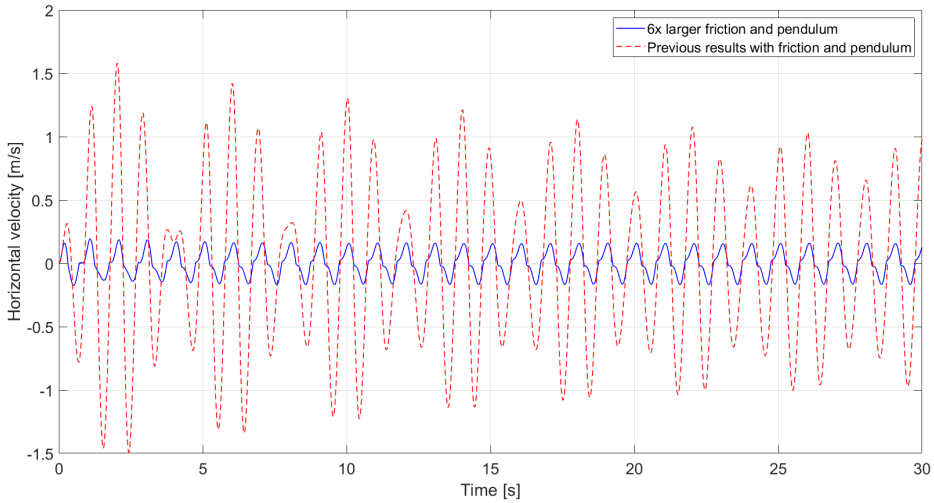

(b) Velocity variation

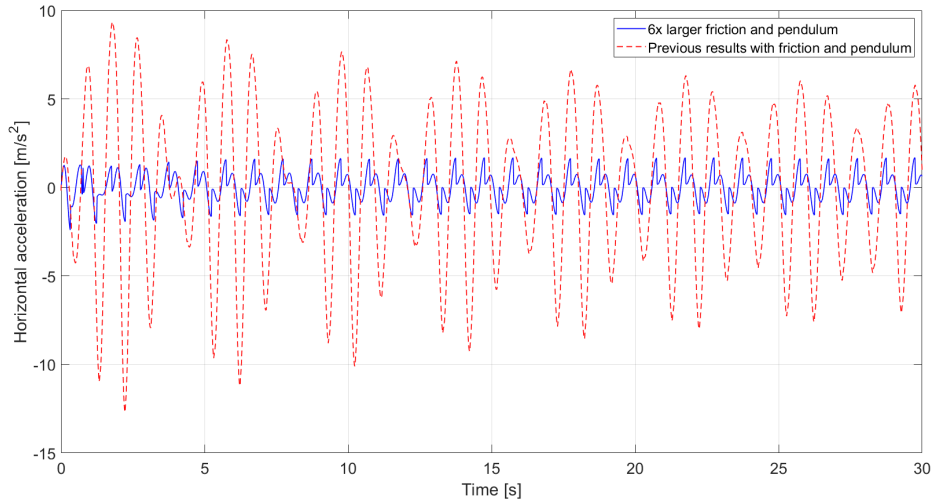

(c) Acceleration variation

Figure 53: Comparison of displacement, velocity and acceleration variations at the moving support for a period of the applied force T = 1s - Friction and pendular bearing

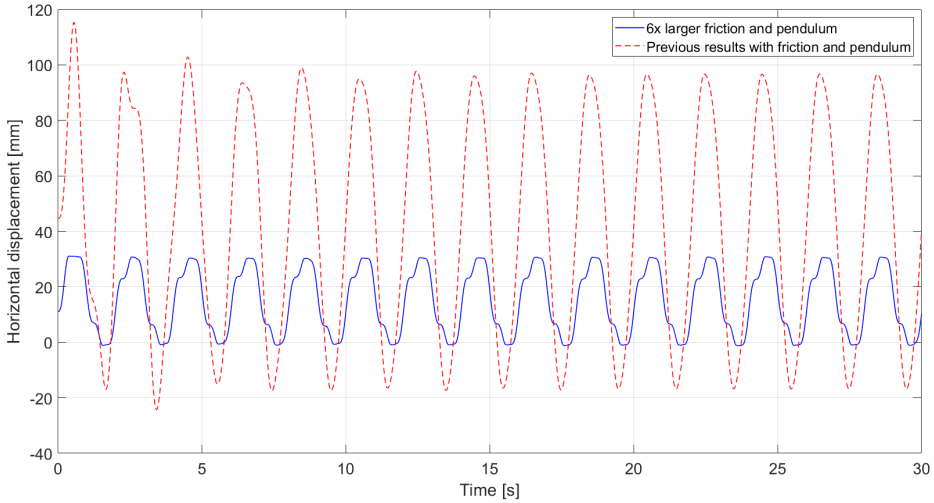

(a) Displacement variation

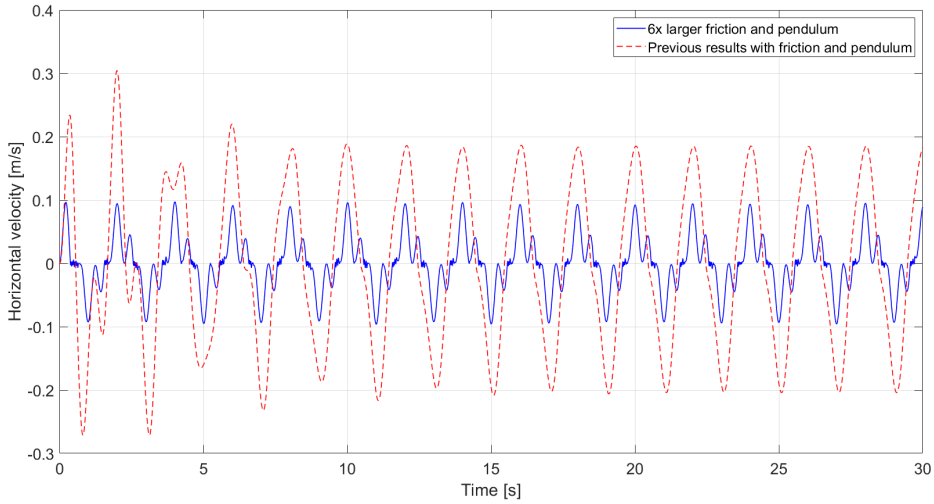

(b) Velocity variation

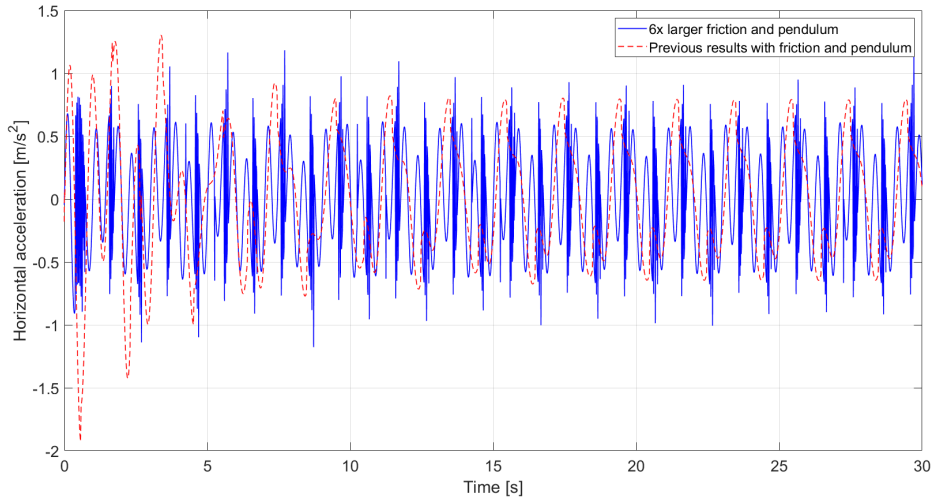

(c) Acceleration variation

Figure 54: Comparison of displacement, velocity and acceleration variations at the moving support for a period of the applied force T = 2s - Friction and pendular bearing

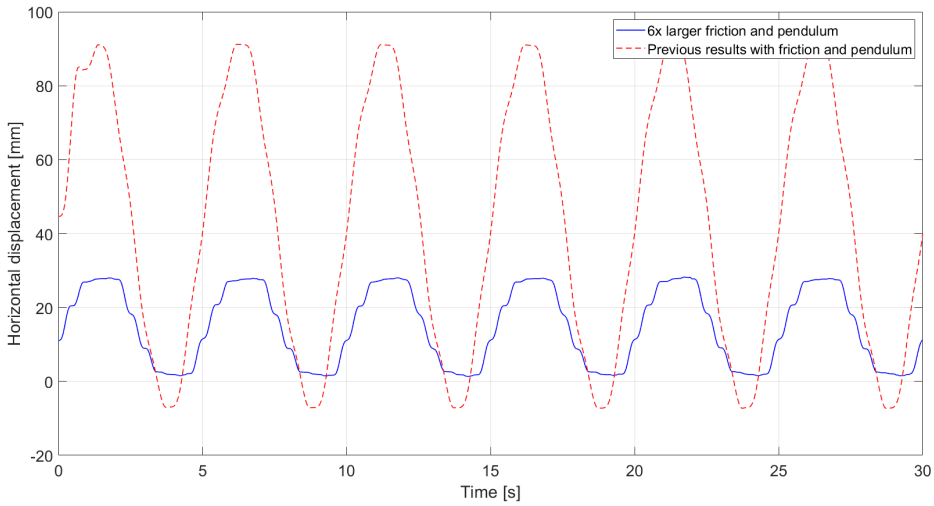

(a) Displacement variation

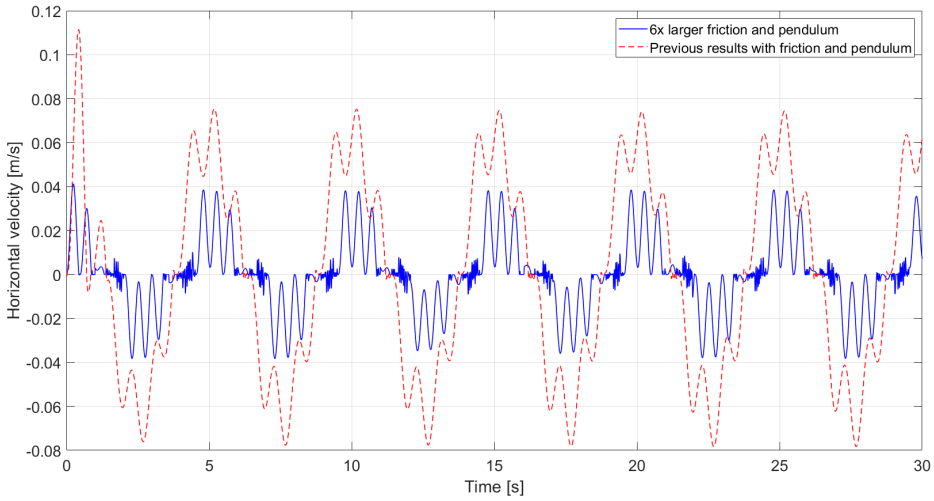

(b) Velocity variation

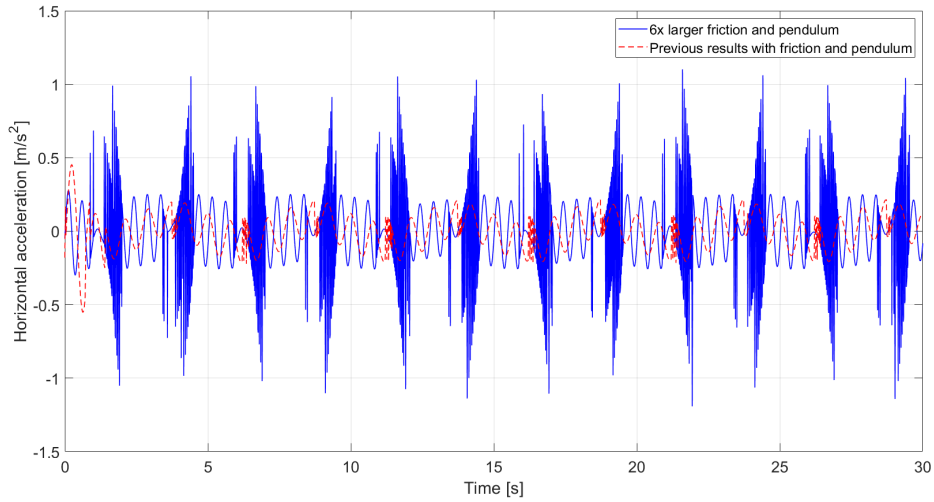

(c) Acceleration variation

Figure 55: Comparison of displacement, velocity and acceleration variations at the moving support for a period of the applied force T = 5s - Friction and pendular bearing

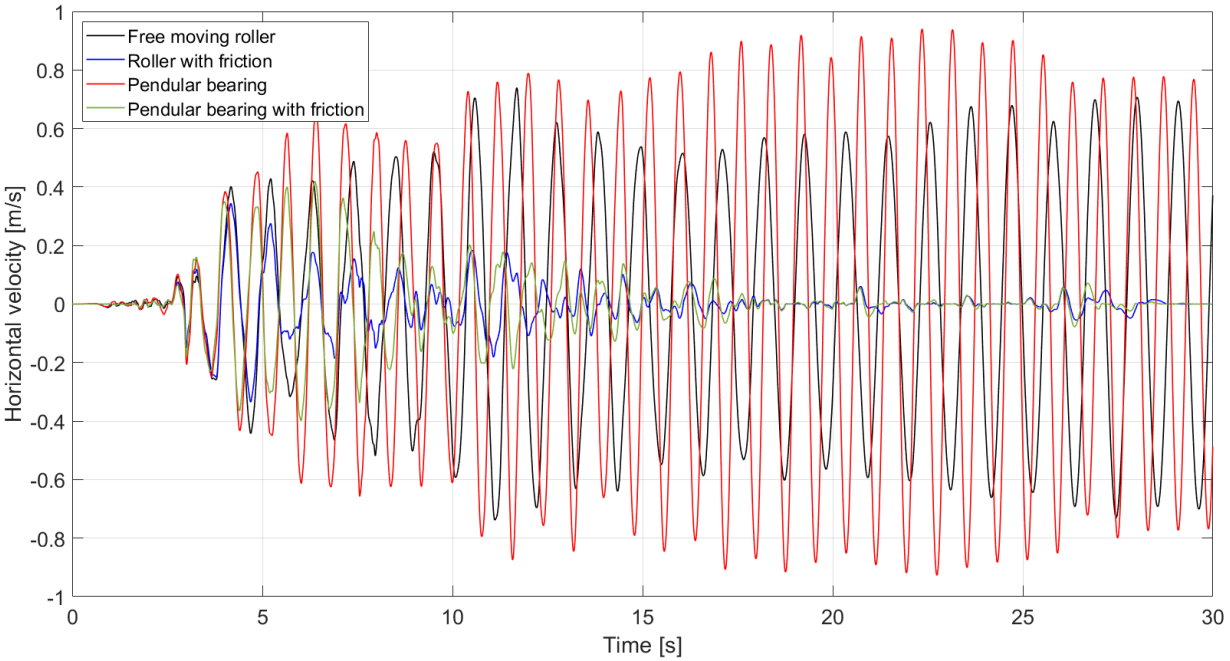

(a) Velocity variation

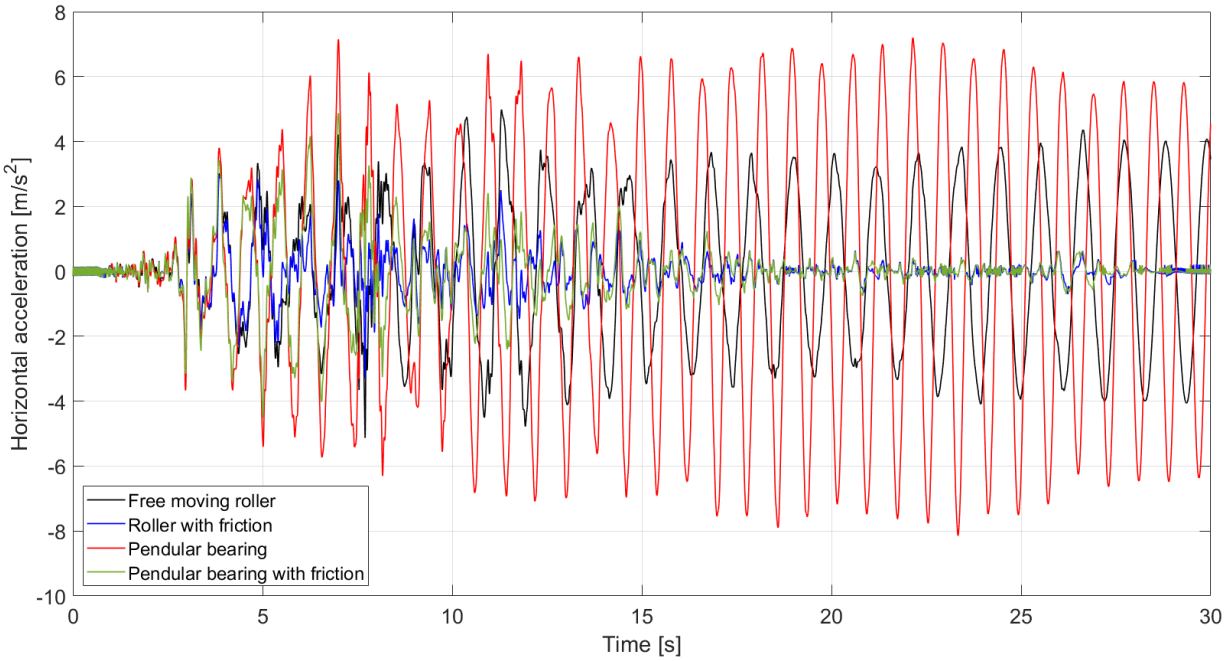

(b) Acceleration variation

Figure 56: Velocity and acceleration variations at the moving support of the simple structure under seismic solicitation - IPE 140 elements

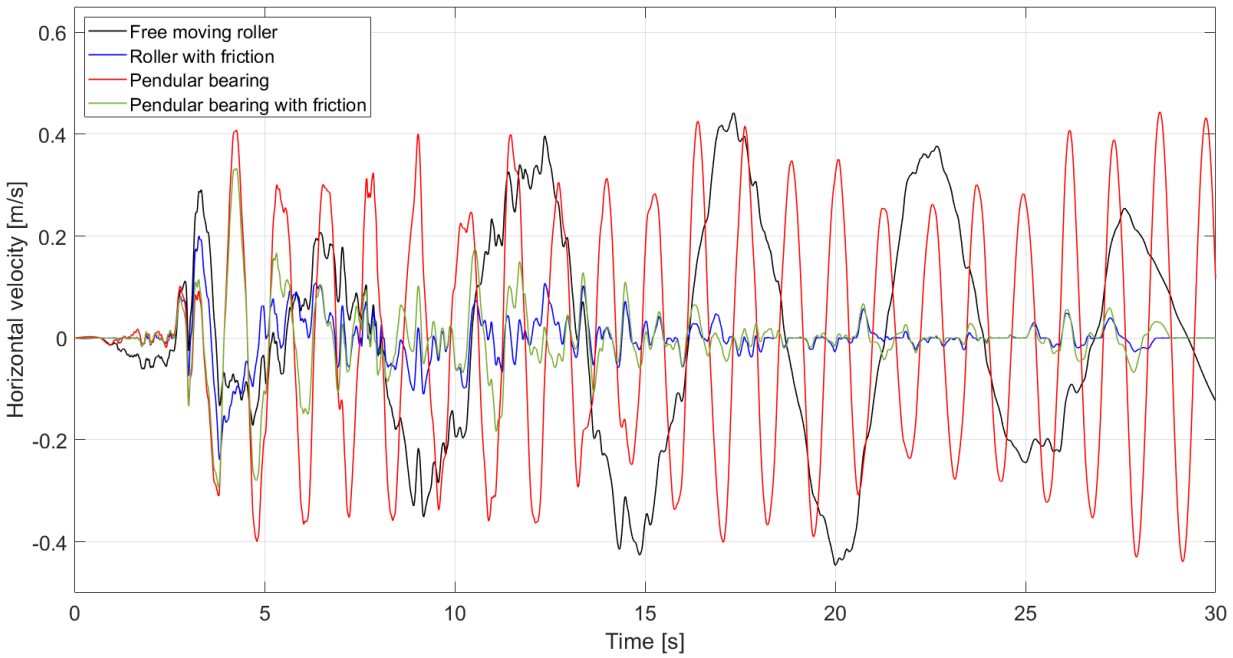

(a) Velocity variation

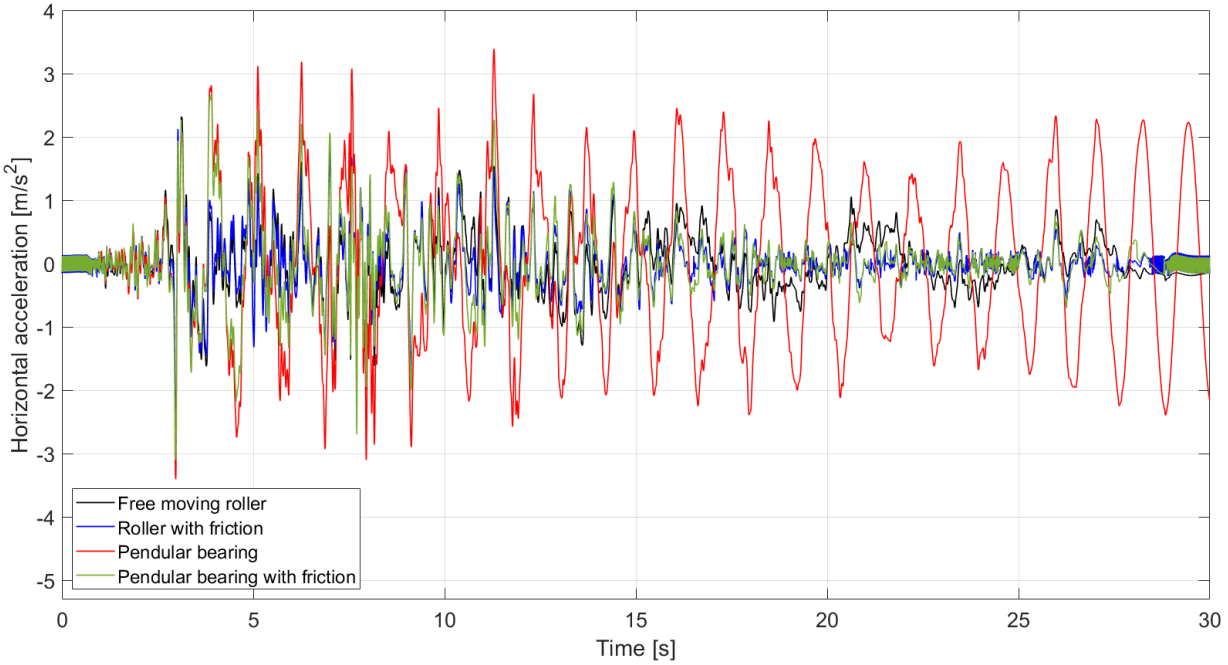

(b) Acceleration variation

Figure 57: Velocity and acceleration variations at the moving support of the simple structure under seismic solicitation - 40x40mm elements

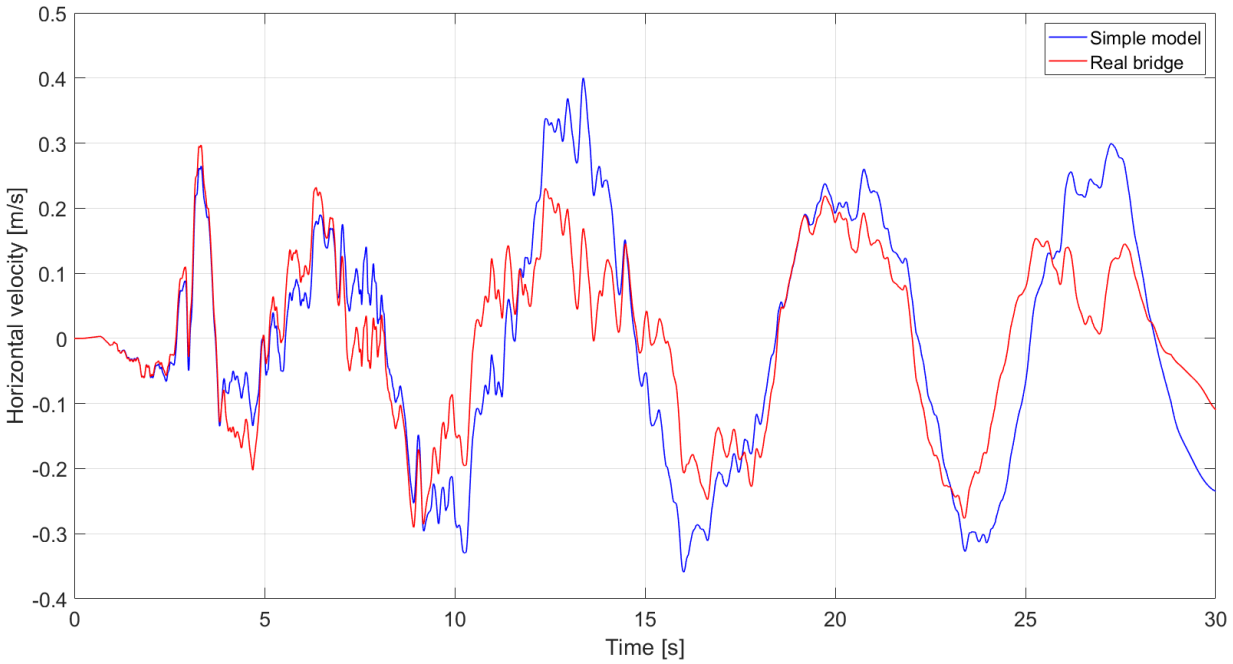

(a) Velocity variation

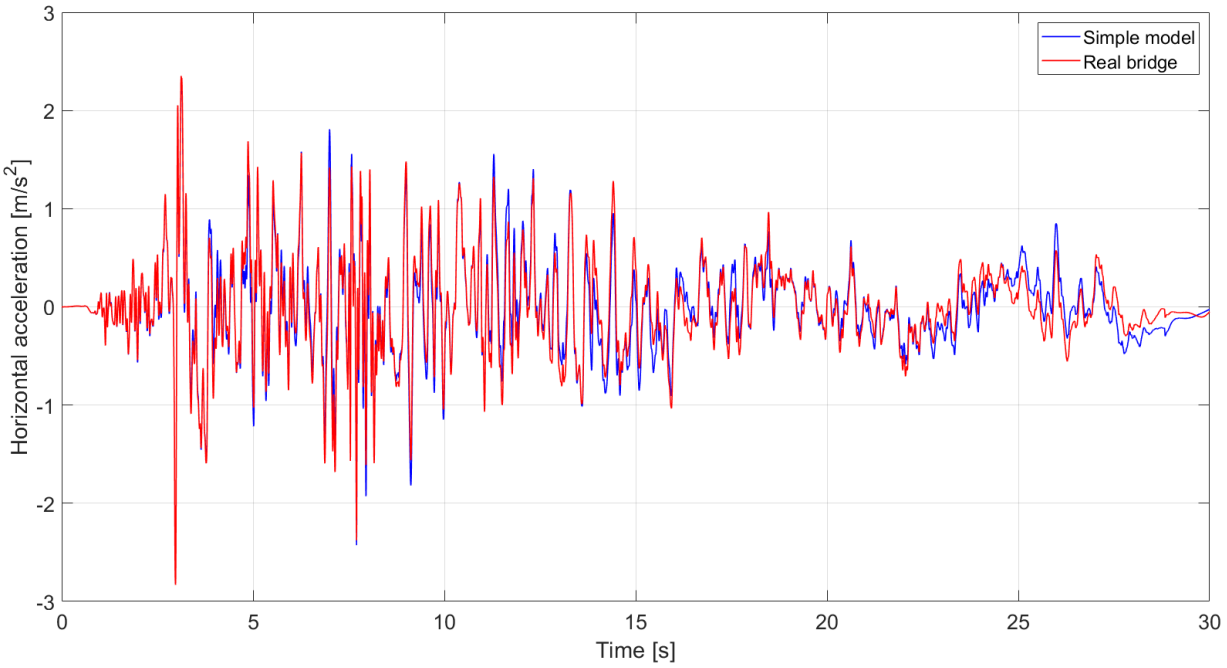

(b) Acceleration variation

Figure 58: Comparison of velocity and acceleration variations between the two bridge models - Freely moving supports

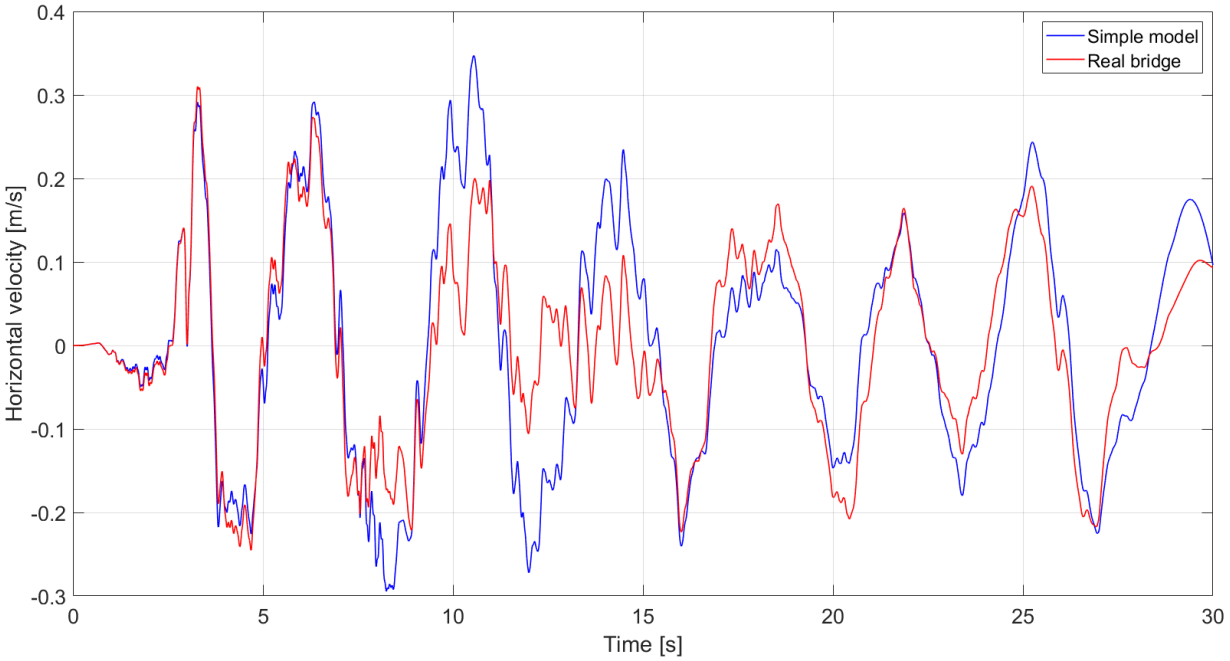

(a) Velocity variation

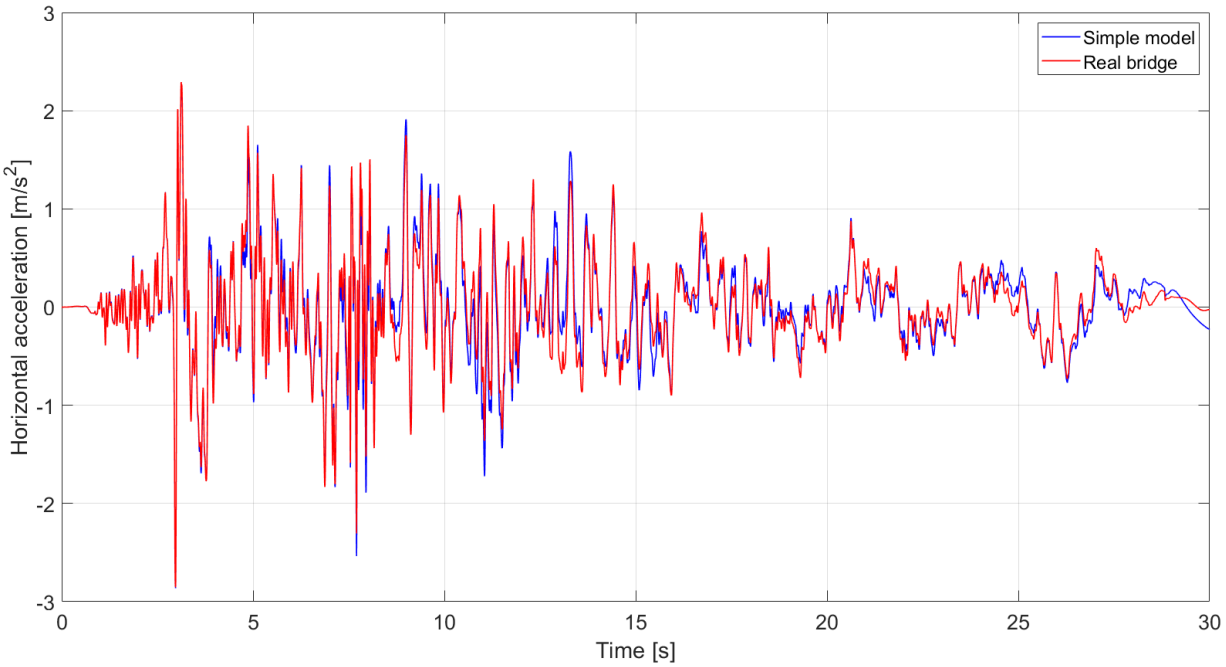

(b) Acceleration variation

Figure 59: Comparison of velocity and acceleration variations between the two bridge models - Pendular bearings only

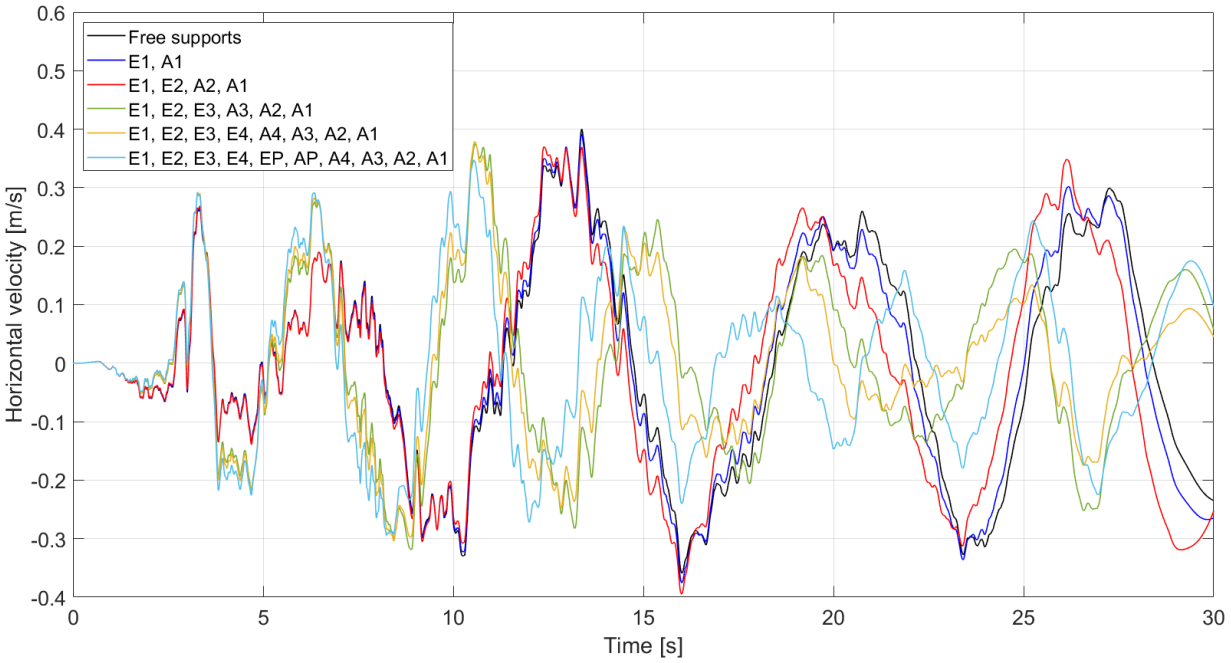

(a) Velocity variation

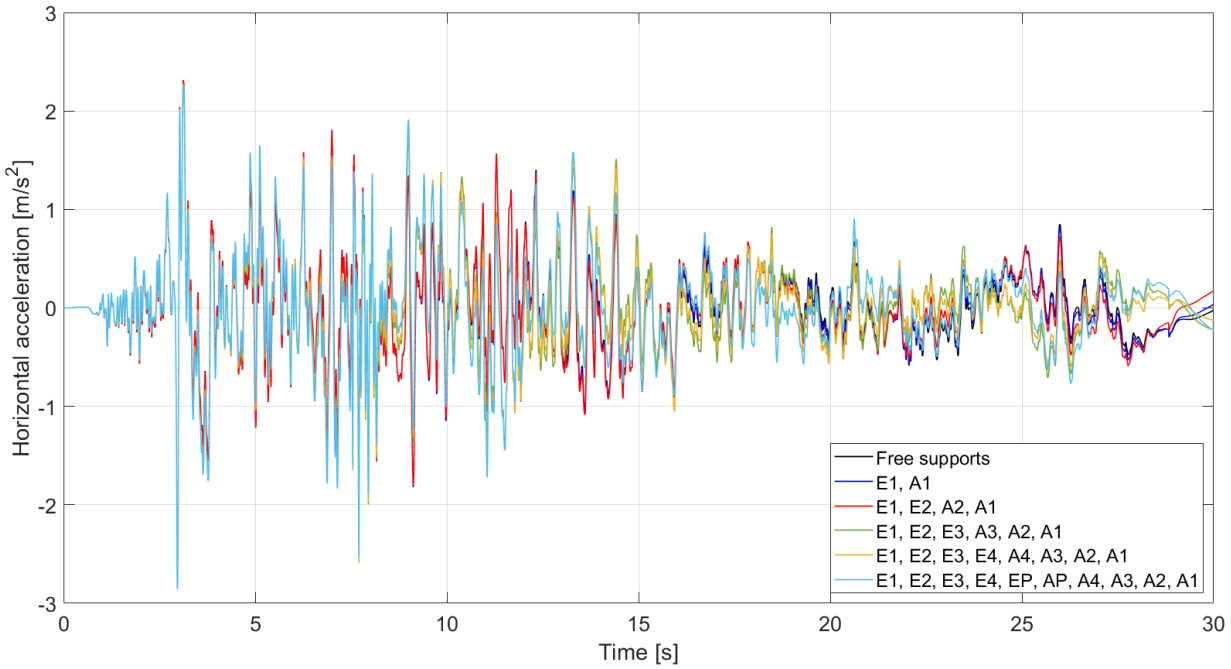

(b) Acceleration variation

Figure 60: Horizontal velocity and acceleration with different combinations of pendular bearings

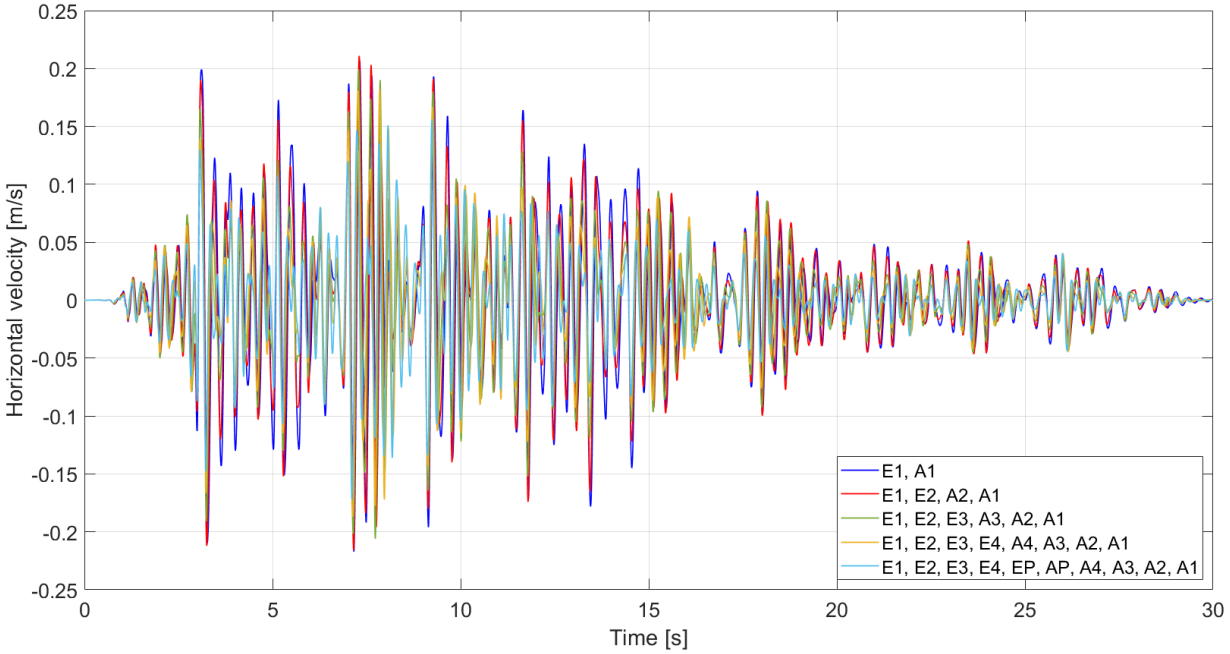

(a) Velocity variation

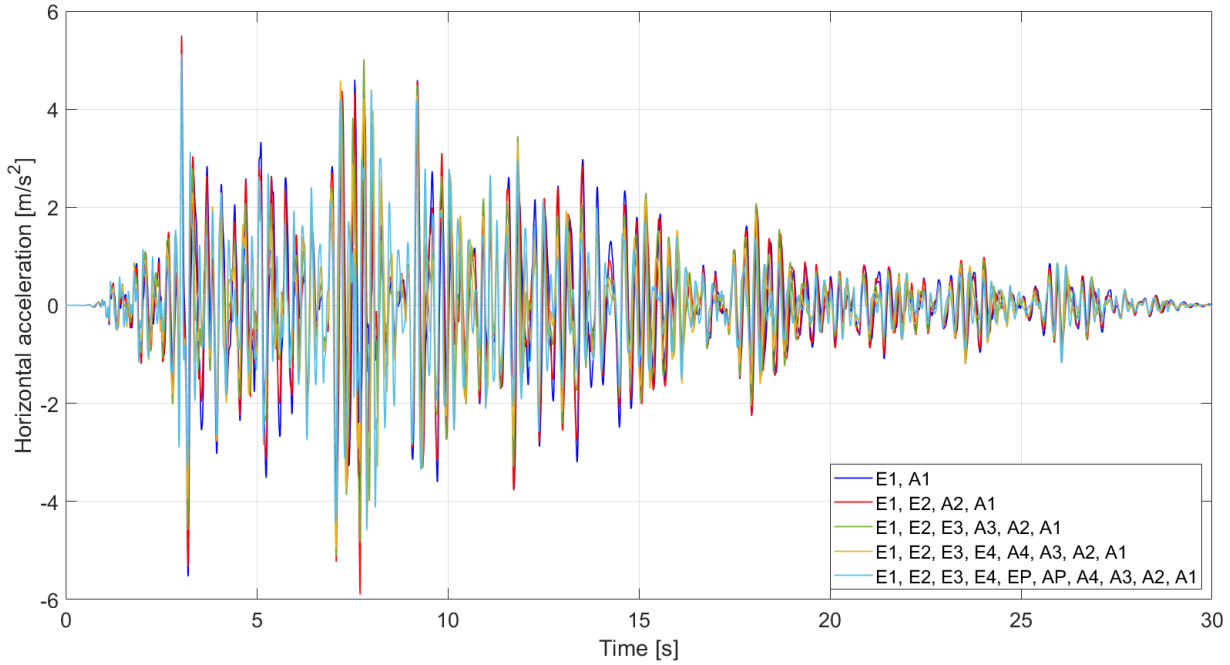

(b) Acceleration variation

Figure 61: Horizontal velocity and acceleration with different combinations of frictional supports

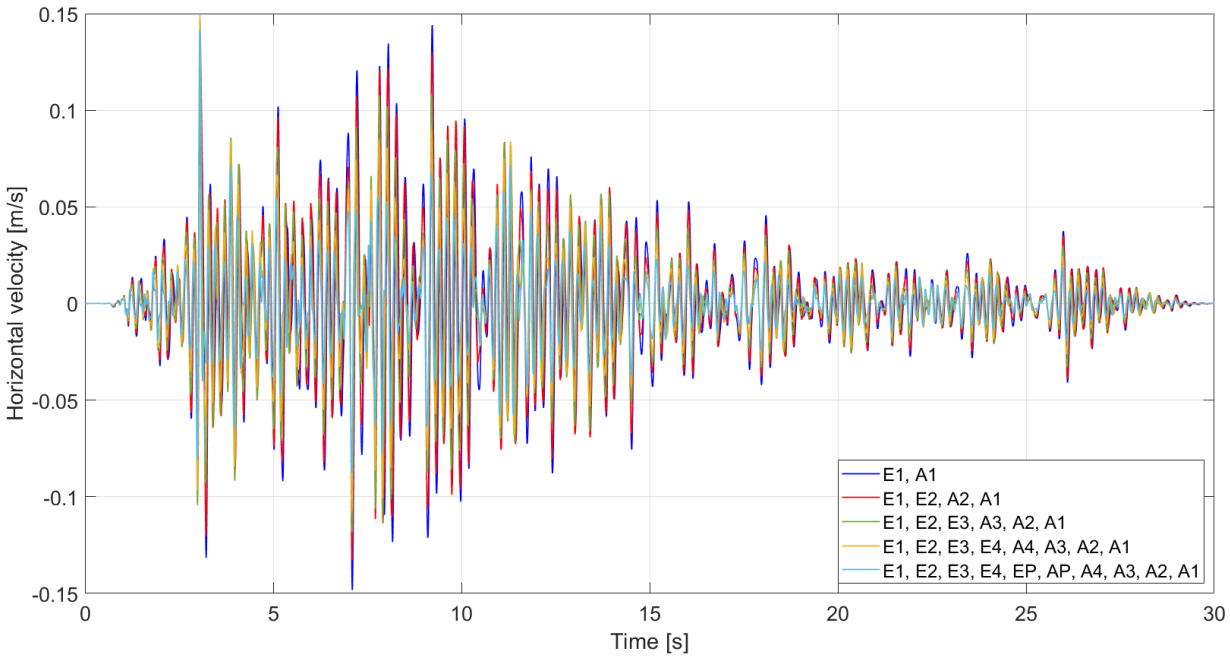

(a) Velocity variation

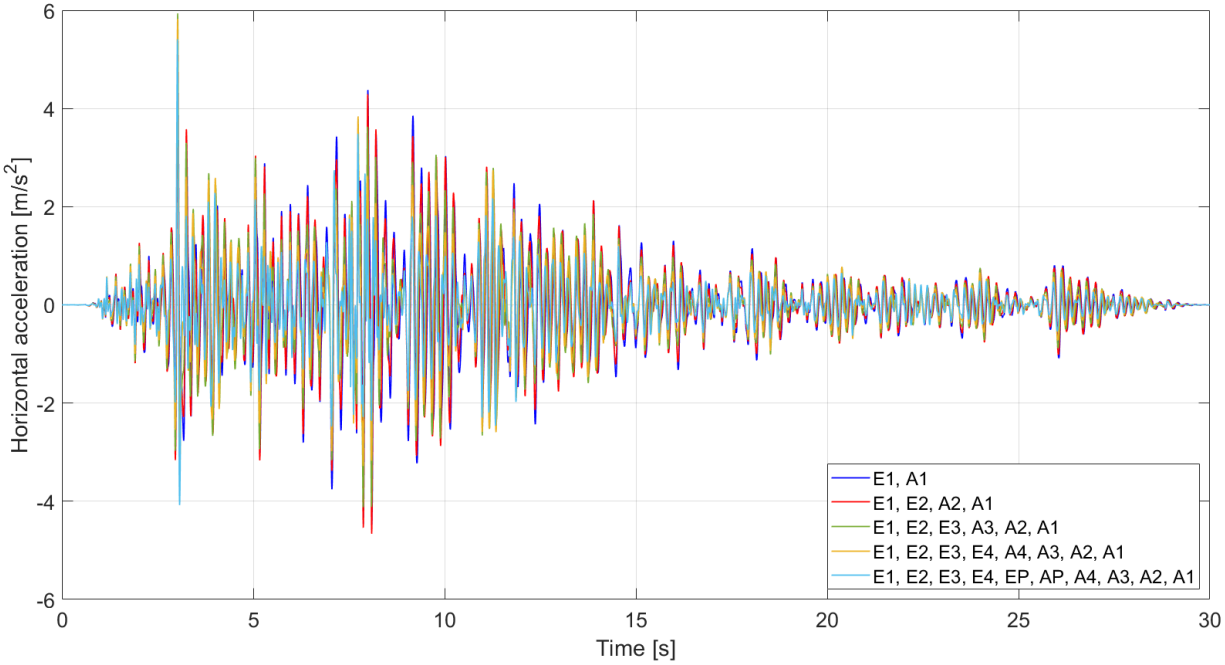

(b) Acceleration variation

Figure 62: Horizontal velocity and acceleration with friction effect on different combinations of supports equipped with pendular bearings

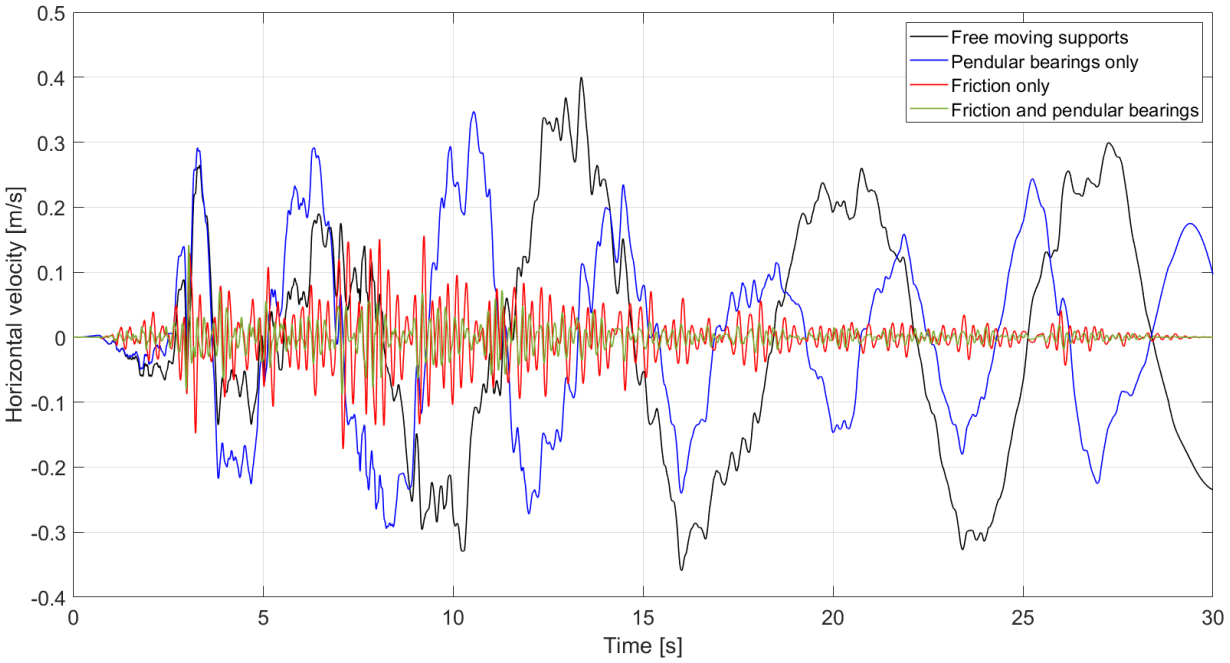

(a) Velocity variation

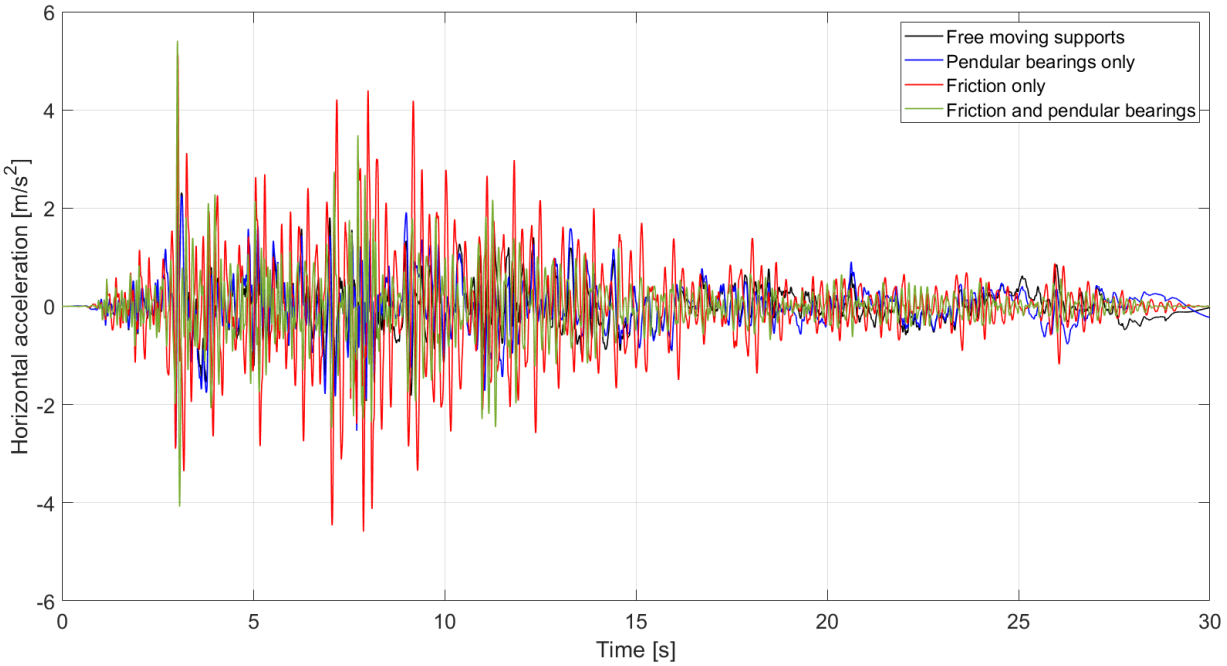

(b) Acceleration variation

Figure 63: Comparison of horizontal velocity and acceleration for the various cases studied

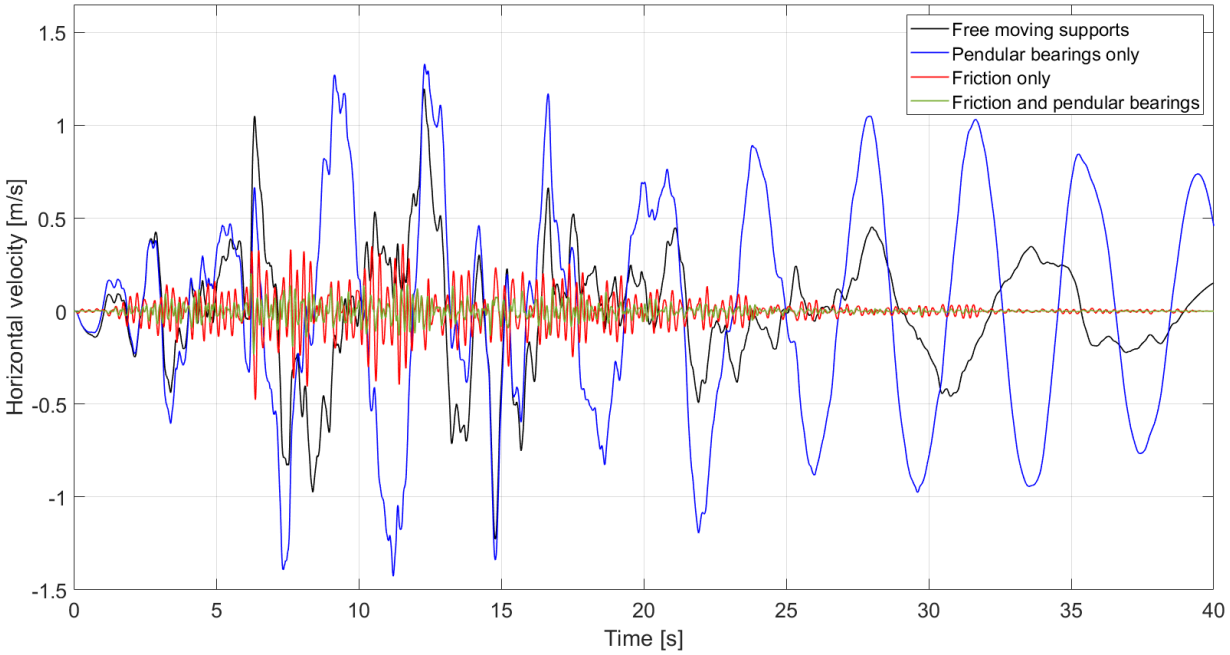

(a) Velocity variation

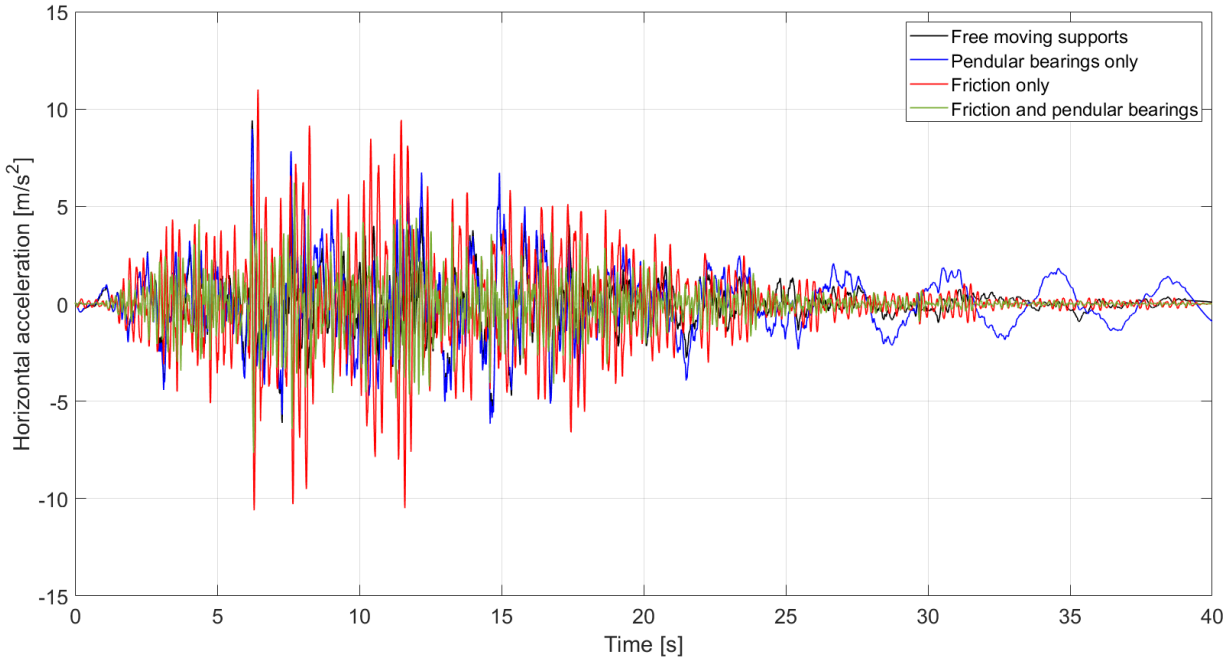

(b) Acceleration variation

Figure 64: Comparison of horizontal velocity and acceleration under a stronger earthquake for the various cases studied